5-2018

Mechanisms of Fluconazole-based Aneuploidy in *Cryptococcus neoformans*

Damiana Altamirano
Clemson University, damiana@g.clemson.edu

MECHANISMS OF FLUCONAZOLE-BASED ANEUPLOIDY IN *CRYPTOCOCCUS NEOFORMANS*

A Dissertation
Presented to
the Graduate School of
Clemson University

In Partial Fulfillment
of the Requirements for the Degree
Doctor of Philosophy
Genetics

---

by
Damiana Sophia Altamirano
May 2018

Accepted by:
Dr. Lukasz Kozubowski, Committee Chair
Dr. Julia Frugoli
Dr. Meredith Morris
Dr. Michael Sehorn

ABSTRACT

Cryptococcus neoformans is an opportunistic fungal pathogen that primarily infects the immunocompromised. It is responsible for approximately 180,000 deaths per year in individuals with HIV. Fluconazole (FLC) is a fungistatic drug widely used to treat cryptococcosis and prevent recurrence. *C. neoformans* exhibits an intrinsic heteroresistance to FLC, which is an emerging barrier to effective treatment especially in resource-limited regions where FLC is often the only therapy available. Previous studies have demonstrated that *C. neoformans* cells confer resistance to FLC through aneuploid formation. The mechanisms underlying aneuploid formation during FLC treatment are unknown.

This dissertation characterizes the effects of the initial exposure to FLC, which is critical to development of aneuploidy and resistance in *C. neoformans*. It highlights the unique mitotic cycle of *C. neoformans*, providing evidence that the ploidy increase during FLC treatment is likely due to the progression of nuclear division despite inhibition of cellular growth. It shows FLC inhibits budding and cytokinesis, producing cells with aberrant morphologies that exhibit increased ploidy levels. Furthermore, through cell sorting and microdissection analysis it highlights the role of multibudded cells or “multimeras” in promoting proliferation during FLC therapy. It provides support that FLC produces a widespread increase in ploidy from which aneuploids could then potentially be selected.

Additionally, this dissertation further characterizes the phenomenon of heteroresistance through single cell and colony level analyses. Filipin staining

displays the unequal depletion of ergosterol between individual cells within a population, highlighting the heterogeneous response within a population to FLC. It further explores the heterogeneity of FLC-treated cells within a population through colony size analysis. Interestingly, factors that influence slower growth promote the proliferation of resistant cells and also the proliferation of cells we refer to as “survivors.” Survivors are characterized by their ability to form small colonies on FLC, while not exhibiting the fitness tradeoff seen in resistant cells. It provides a thorough analysis of the response of *C. neoformans* to FLC and proposes a model that summarizes the factors that contribute to growth during FLC treatment.

DEDICATION

To my family: Mom, Dad, Tom, James, Arlo, and Richard Parker. I love you all!

ACKNOWLEDGMENTS

First, I would like to thank my advisor, Dr. Lukasz Kozubowski, for his mentorship. Since rotating in his lab, I have enjoyed learning from someone so genuinely interested in science and in the success of his students. His constant curiosity is contagious, and it has been an honor to be his first graduate student. I am especially grateful for the time he has patiently spent helping me become a better scientist and a better thinker. His endless supply of baby doughnuts, windmill cookies, and orange juice has also been greatly appreciated. I would also like to thank my committee members: Dr. Julia Frugoli, Dr. Meredith Morris, and Dr. Michael Sehorn for their help in and out of lab. The time and interest they have invested in me has helped advance my career and for that I am truly thankful.

In addition to my mentors, I would like to thank Charles Simmons, Diana Fang, and Namrata Paladugu whose hard work has directly contributed to this research. I also am eternally grateful for the opportunity to work alongside friends who have listened to me complain, made me laugh, and always reminded me that everything is going to be alright. Finally, I would like to thank my family and friends from afar for their love, support, and refreshing perspectives – thanks for dealing with all of my phone calls!

TABLE OF CONTENTS

Table of Contents (Continued)

LIST OF TABLES

LIST OF FIGURES

List of Figures (Continued)

CHAPTER ONE

LITERATURE REVIEW

A portion of this review was previously published – **Altamirano, S, Chandrasekaran, S., Kozubowski, L.** 2017. Mechanisms of Cytokinesis in Basidiomycetous Yeasts. Fungal Biol Rev **2**:73—87.

CRYPTOCOCCUS NEOFORMANS: A BASIDIOMYCETEOUS, HUMAN PATHOGEN

The Mitotic Cycle and Cytokinesis of the Yeast Form of *C. neoformans*

Cryptococcus neoformans is a member of Agaricomycotina in the second largest fungal phylum, Basidiomycota. It can undergo both asexual and sexual reproduction. Sexual reproduction occurs through a bipolar mating system (mating type a and alpha). During the sexual cycle, mating results in dikaryotic hyphae formation. The basidium is then formed where nuclei fusion and meiosis occurs. After meiosis, mitotic divisions occur that result in spore formation that bud from the basidium surface producing four spore chains (1). Despite is ability to form hyphae, C. *neoformans* is predominantly a haploid yeast that reproduces asexually via budding, and it is the yeast form that causes infection (2). The mitotic cycle and cytokinesis in *C. neoformans* remain largely unexplored. The mechanisms of mitosis and cytokinesis in yeast are largely based on the more thoroughly studied budding yeast, *Saccharomyces cerevisiae*, and the fission yeast, *Schizosaccharomyces pombe*. Both of these model yeasts are ascomycetes that likely exhibit similarities and differences in cell division compared to the basidiomycete, *C. neoformans*. In addition to potentially highlighting new therapeutic targets against cryptococcosis, studying the cell cycle of the yeast form of *C. neoformans* may be critical in better understanding the evolution of the mechanisms of mitosis and cytokinesis.

During mitosis, a mother cell undergoes nuclear division and gives rise to a

genetically identical daughter cell. Mitosis is a highly-regulated process that ensures accurate and equal chromosome segregation between the daughter and mother cell. Kinetochores play a crucial role in chromosome segregation by linking centromeres to spindle microtubules, which then pull sister chromatids to separate cellular poles. The kinetochore consists of trilaminar plates referred to as the inner, middle, and outer layers that surround the centromeric DNA. The architecture of kinetochores is thought to be conserved from yeast to animals (3). A recent study in *C. neoformans* identified six putative kinetochore homologs corresponding to each of the three layers, suggesting that the kinetochore architecture is also conserved in *C. neoformans*. Time-lapse microscopy utilizing the Mif2 inner layer homologue, the Mis12/Mtw1 middle layer homologue, and the Dad1 outer layer homologue showed that prior to mitosis, kinetochores in *C. neoformans* undergo a step-wide assembly. Utilizing a strain expressing fluorescently-labelled tubulin and fluorescently-labelled homologue of CENP-A, Cse4, to visualize the centromeres, the microtubule-kinetochore attachment was also established to only occur during mitosis (4, Figure 1.1). The kinetochore dynamics of *C. neoformans* appear to more closely resemble metazoans than other yeast. In metazoans, kinetochores also assemble in a step-wise manner and the kinetochore-microtubule attachment does not persist throughout mitosis, whereas the kinetochores of *S. cerevisiae* are fully-assembled and remain attached to microtubules throughout the cell cycle, except a brief reassembly during replication (5–8).

The kinetochore-microtubule attachment takes place only during mitosis in metazoans due to the fact that the microtubule organizing centers localize outside the nuclear envelope. A complete breakdown of the nuclear envelope, known as open mitosis, has to occur to allow the attachment of kinetochores with microtubules (9). In contrast, *S. cerevisiae* undergoes a closed mitosis, where the nuclear envelope remains intact. Closed mitosis allows spindle pole bodies (SPBs), the equivalent of the microtubule organizing centers in yeast, to remain attached to the nuclear envelope and in constant contact with kinetochores (10). Consistent with metazoan-like dynamics of the kinetochores, *C. neoformans* undergoes an intermediate type of cell division known as semi-open mitosis, where the nuclear envelope partially breaks open during mitosis (4, Figure 1.1). An additional strikingly distinct feature of mitosis in *C. neoformans* is the translocation of all of the chromatin to the daughter cell where the spindle is formed. Segregation of chromosomes then proceeds in the direction from the bud into the mother cell (4, Figure 1.1). The seemingly energy-inefficient process of nuclear division in the daughter cell does not occur in ascomycetes, but it appears to be characteristic of other basidiomycetes (4, 11).

Cytokinesis is the final step in the cell cycle that results in two physically separate cytoplasms of the dividing cells. How cytokinesis is activated in *C. neoformans* is presently unknown. Given the unique nuclear division of *C. neoformans*, mechanisms of entry into cytokinesis may also demonstrate a significant divergence. In *S. cerevisiae*, the entry to cytokinesis is regulated

through the signaling dependent on the Polo kinase and a network of proteins collectively known as the Mitotic Exit Network (MEN) (12–15). MEN signaling initiates during late anaphase at the SPB where the GTPase, Tem1, stimulates the kinase, Cdc15, to activate the Mob1-Dbf2 kinase complex. Mob1-Dbf2 in turn promotes the release of the protein phosphatase, Cdc14, from the nucleolus. Cdc14 reverses phosphorylation of a number of Cdk1 targets, leading to mitotic exit and cytokinesis (16, 17). It is puzzling how a signaling based on Cdc14 release from the nucleolus would operate in *C. neoformans* given that the nucleolus disintegration initiates before the spindle assembles (4). Furthermore, a spindle position checkpoint could not operate in *C. neoformans* if the Cdc14 were released from nucleolus and signaled to start cytokinesis before metaphase (18). One possibility is that Cdc14-based signaling similar to MEN is not conserved in *C. neoformans*. On the other hand, *C. neoformans* contains a homologue of the Cdc14 phosphatase and other typical MEN components (Table 1.1). Cdc14-like phosphatases are likely critical for the mitotic exit control in metazoans and may localize to the nucleolus (19, 20). Therefore, the Cdc14 homologue may act in the mitotic exit network in *C. neoformans* via mechanisms similar to that occurring in metazoans.

An important component in the process of cytokinesis, conserved in fungi and metazoans, is the actomyosin ring (AMR). The AMR is composed of myosin II (heavy, light, and regulatory chains) and filamentous actin (F-actin) (21). Non-muscle myosin II is the essential motor that drives actin-based cytokinesis (22).

The antiparallel filaments of actin in the AMR undergo a continuous cycle of nucleation, polymerization, and depolymerization (23). In *C. neoformans*, Myo1, the myosin II heavy chain, localizes to the bud neck and constricts similarly to the *S. cerevisiae* homologue (24). The F-actin localization and dynamics in *C. neoformans* appear similar to *S. cerevisiae* (25). While tropomyosins have not been thoroughly described in basidiomycetes, *C. neoformans* mutants lacking formin or tropomyosin homologues exhibit defects in cytokinesis (26). Thus, it is likely that the AMR in *C. neoformans* would have a similar architecture to the AMR in ascomycetes.

In fungi, an important part of cytokinesis is the formation of the future cell wall between the mother and the daughter cell. In *C. neoformans*, similar to ascomycetous yeasts, an initial cell wall is produced in the form of a primary septum and subsequently two secondary septa are formed on each side of the primary septum (27). The fungal septum is made of a cell wall-like material that ultimately forms a physical barrier separating the cytoplasm (28). To allow final cell separation, the primary septum is degraded and the secondary septa serve as new wall between the dividing cells.

In model yeasts the AMR constriction is coincidental with the formation of the primary septum (29). The primary septum grows centripetally inward as the AMR closes. Whether the AMR drives the septum formation directly remains unclear. A study by Proctor et al. proposed that in *S. pombe* the essential contribution to cytokinesis of myosin and F-actin is restricted to only an initial part

of the constriction process (30). Thus, the major force in cytokinesis is likely attributed to the assembly of cell wall polymers in the growing septum; the AMR plays only a minor role. Other studies suggest that the optimal AMR constriction and primary septum formation are interdependent; AMR guides septum formation, while septum formation stabilizes AMR constriction (23, 31–34). Given that all fungal cells have cell walls and form septa during cytokinesis it is likely that the mechanism of the constriction of the AMR and its relative contribution to cytokinesis are conserved in most fungi, including *C. neoformans*.

The final daughter cell detachment in fungi is accomplished by the concerted action of hydrolytic enzymes that degrade the thin layer of the primary septum and is controlled by a highly conserved morphogenesis-related pathway (MOR) also known as the RAM (regulation of Ace2 and morphogenesis) pathway (35, 36). In *S. cerevisiae*, the Ace2 transcription factor accumulates specifically in the daughter nucleus and promotes hydrolysis of the septum from the daughter side (37). Interestingly no clear homologues of Ace2 are present in the *C. neoformans* genome. This suggests an alternative mechanism for positioning the activity of the hydrolytic enzymes specifically on the daughter side. Surprisingly, none of the endochitinases encoded by the *C. neoformans* genome are necessary for vegetative growth consistent with an absence of the bud scar in this yeast (38, 39). As *C. neoformans* may not have an enzyme that specifically hydrolyzes chitosan, an alternative mechanism for daughter cell separation that is based on the increased flexibility and solubility of the chitosan has been proposed (39).

Epidemiology and Virulence of *C. neoformans*

C. neoformans is an opportunistic, fungal pathogen that can cause meningitis primarily in immunocompromised individuals. It is the leading mycotic killer of individuals with HIV-1. According to recent reports, approximately 220,000 HIV-related cryptococcal cases occur annually, resulting in 181,000 deaths. The majority of cases occur in sub-Sahara Africa where the burden of cryptococcal infection is especially high due to the increased prevalence of HIV and the limited availability of both anti-retroviral therapy and antifungal drugs (40).

C. neoformans is a globally distributed pathogen that is commonly found in sources of decaying material, such as tree hollows, soil, and pigeon guano (41). Despite its ability to colonize humans and non-human hosts, human-to human transmission does not occur and zoonotic transmission is rare (42). The primary method of transmission is through inhalation of spores or desiccated yeast cells from the environment (41). C. *neoformans* is an opportunistic pathogen that takes advantage of the attenuated immune state of its host while also displaying virulent phenotypes that promote pathogenicity.

In healthy individuals, infection results in a state of latency that rarely leads to disease. However, in immunocompromised individuals, latent infections are likely to advance into disease. Disease is primarily associated with dissemination into the central nervous system, marked by fungemia and/or meningitis. Pneumonia and skin lesions are also symptoms characteristic of disease (43). The ability of *C. neoformans* to cause disease primarily in patients with compromised

immune system highlights the importance of the host immune response in preventing cryptococcosis. Studies have shown the critical role of the CD4 T-cell mediated response in controlling cryptococcal infection (44). Phagocytosis by macrophages and dendritic cells is a key element of the immune system that is crucial in controlling initial cryptococcal infection. Depletion of alveolar macrophages and dendritic cells results in increased rates of cryptococcal dissemination, while neutrophils and B cells alone cannot control infection and may instead increase damage to the host (45, 46).

In addition to taking advantage of the weakened immune system of the host, *C. neoformans* displays virulence factors that allow it to further evade host immune recognition. Often referred to as the “sugar-coated killer”, the protective polysaccharide capsule of *C. neoformans* has been shown to be important in promoting infection (47). Mutants that fail to produce capsule exhibit a significantly attenuated virulence in murine model of cryptococcosis (48). The polysaccharide capsule protects the cell from phagocytosis. Capsular enlargement and increased capsular matrix density decrease the deposition of complements or antibodies, reducing immune system recognition and phagocytosis (49). Melanization is another prominent virulence factor that allows for evasion of the immune system in *C. neoformans* (50). Melanized cells occur during infection and display reduced levels of phagocytosis, which is likely due to surface charge effects (51). Additionally, melanin synthesis contributes to increased resistance to oxygen and nitrogen related stresses, as well as antifungals (52). Metabolic pathways leading

to capsule formation and melanin production have been a subject of intense studies, with the primary goal of finding new drug targets and development of vaccines preventing cryptococcosis (53–55).

Several studies have also highlighted the significant role of *C. neoformans*'s genome plasticity in promoting pathogenicity (56). During infection, *C. neoformans* is able to produce aneuploid and polyploid cells that likely act as sources of adaptive phenotypic change during infection. *In vitro* and *in vivo* studies have shown that aneuploid formation is responsible for resistance to the commonly used azole drug, fluconazole (57, 58). Polyploid cells isolated from the lung, known as titan cells, have been shown to be protected from the host's immune response due to their enlarged size and cell surface alterations (59–61). Titan cells and titan daughter cells also exhibit increased stress resistance, suggesting these cells are critical for host adaptation during infection (62). Despite evidence that the genomic plasticity is critical in promoting survival of yeast cells during infection, little is known about the mechanisms underlying aneuploid and polyploid formation in *C. neoformans*. The mechanism of aneuploid formation during fluconazole treatment is the major subject of this thesis and will be further discussed in subsequent chapters.

Diagnosis and Treatment of Cryptococcosis

Diagnostic methods of cryptococcosis include typical serological and histopathological techniques. Histopathology analysis often involves staining to

identify virulence factors such as capsule formation and melanization (63). The most common diagnostic method is the detection of cryptococcal antigen in serum or cerebrospinal fluid using latex agglutination or enzyme immunoassay (64). In resource-limited countries these techniques are not always readily accessible. Intriguingly, a lateral flow assay has recently been implemented that allows rapid, more sensitive detection and is cost effective (65, 66).

Treatment of cryptococcosis is limited to the following three drugs: amphotericin B (AmpB), flucytosine (5FC), and fluconazole (FLC) (63). Treatment strategies for cryptococcal infection are based on the severity and site of infection. During mild to moderate pulmonary infections, FLC is the preferred method of treatment. FLC inhibits the conversion of lanosterol to C-14-demethyl-lanosterol in the ergosterol synthesis pathway through binding to the cytochrome P-450 enzyme, 14-alpha-demethylase, which is encoded by ERG11 (67). FLC is fungal-specific, resulting in low toxicity levels and is widely available (68). Treatment for more severe pulmonary infections and infections of the central nervous system consists of a combination therapy of ampB and 5FC. FLC is then administered as maintenance therapy (63). AmpB is a fungicidal polyene that binds to ergosterol. It is thought to act as a “sterol sponge” that binds and removes ergosterol from the membrane (69). 5FC intercalates into fungal RNA, blocking protein synthesis and inhibits DNA synthesis through the inhibition of thymidylate synthetase (70). Both ampB and 5FC exhibit increased levels of toxicity compared to FLC and are not widely available due to relatively high cost.

Cost, availability, and toxicity are all major drawbacks of ampB and 5FC therapy. In sub-Saharan Africa, where the majority of HIV-related cryptococcal cases occur, 5FC is unregistered and the facilities to safely administer ampB are often not available (71). These challenges often leave FLC as the primary method of treatment in resource-limited countries. FLC is also the preferred drug to administer as a form of maintenance therapy. In patients with HIV, prophylactic therapy may be lifelong, so the reduced toxicity and cost of FLC make it an ideal candidate (72). Despite the advantages of FLC, the widespread use of FLC as a primary method of treatment in resource-limited countries and in maintenance therapy has led to the increasing problem of FLC resistance (73).

While several other antifungal drugs are available, their ability to treat *C. neoformans* is not effective or remains to be fully elucidated. The newest class of antifungals, the echinocandins, are not recommended due to their inability to treat cryptococcosis. Echinocandins are effective *in vitro*, but are likely not effective *in vivo* likely due to the increased chitin levels of *C. neoformans* cells *in vivo* (74–77). Other azoles, such as itraconazole, voriconazole, posaconazole, and isavuconazole have shown to be effective *in vitro*, but there has been limited assessment of their clinical use. Itraconazole, voriconazole, and posaconazole exhibit poor penetration of the central nervous system. Interestingly, isavuconazole showed adequate central nervous system penetration and may be advantageous in treating invasive cryptococcal infections, especially considering the reduced adverse effects of isavuconazole compared to ampB. Further clinical

studies are needed to further assess the efficacy of isavuconazole (78). Until new therapies are developed and proven effective, strategies to reduce resistance to currently administered antifungals are necessary.

FLUCONAZOLE RESISTANCE

The Effects of FLC

As mentioned above, FLC is a cytochrome P450 inhibitor. It targets the cytochrome P450 demethylase encoded by *ERG11*, which is involved in the oxidative metabolism of lanosterol in the ergosterol synthesis pathway (67). Ergosterol is a sterol found in fungal cellular membranes that is similar to mammalian cholesterol and is important in membrane dynamics, including but not limited to membrane fluidity, determination of membrane thickness, and endocytosis. It can be found in the membranes of all membrane-bound organelles, with the plasma membrane containing the highest percentage of ergosterol (79). The fungistatic effects of FLC on fungal cells are primarily attributed to changes in membrane structure and function due to ergosterol depletion and the buildup of toxic sterol precursors (80).

Ergosterol has been shown to be important in V-ATPase activity and vacuolar acidification (81). Zhang et al. showed that FLC affects proper V-ATPase activity, which could potentially contribute to the inhibitory effects of FLC through disruption of multiple downstream cellular processes (81). FLC treatment also results in the accumulation of methylated sterols, especially 14-methyl-3,6, diols. Deletion strains of *C. albicans* that are unable to synthesize 14-methyl-3,6 diol

have been shown to be resistant to FLC, suggesting that toxic sterol intermediates play a role in the antifungal activity of FLC (82). Additional studies in *S. cerevisiae* have shown that the replacement of ergosterol with methylated sterols affects the membrane rigidity and fluidity (83). FLC also likely leads to growth inhibition through production of endogenous reactive oxygen species (84). Proteomic analysis in *C. albicans* also highlighted the increased abundance of proteins associated with cell wall integrity during FLC treatment, suggesting FLC also induces cell wall stress (85).

The effects of FLC have not been specifically investigated in *C. neoformans*, but they are likely similar to the effects described above. Intriguingly, sterol-rich domains in fungal plasma membranes, which include ergosterol, may also play a key role in cellular polarity and cytokinesis (86). Furthermore, a study in *C. albicans* showed the initial effects of FLC lead to cytokinesis defects, which may contribute to the formation of resistant aneuploids (87). In *C. neoformans*, cells have also been shown to confer resistance to FLC through aneuploidy, and it would be of particular interest to explore whether the initial effects of FLC on *C. neoformans* cells could potentially lead to cellular growth defects that could lead to resistant aneuploids.

Aneuploidy During FLC Treatment in *C. neoformans*

The molecular mechanisms underlying how *C. neoformans* cells evade the effects of FLC and become resistant have not been well characterized. In another

pathogenic species, *Candida,* the mechanisms have been more thoroughly studied and have been shown to emerge through mutations that result in drug target overexpression, drug target modification, sterol synthesis modification, or increased drug efflux (88). In addition to mutations, aneuploidy has also been shown to produce FLC resistant cells through key gene duplications (89–93).

In *C. neoformans*, aneuploid formation is thought to be the primary mechanism of FLC resistance. Studies have shown that resistant populations of C*. neoformans* cells exhibit disomy of certain whole chromosomes that are beneficial for FLC resistance (57). Disomy of chromosome 1 is typically the first duplication seen during FLC resistance, but additional chromosomal duplications are associated with higher levels of resistance. Under higher FLC concentrations, resistant cells have been shown to contain disomies of up to four chromosomes (chromosome 1, 4, 10 and 14) (57). *ERG11*, the target of FLC, and *AFR1*, a gene that encodes the ATP-binding cassette (ABC) transporter efflux pump, are both located on chromosome 1 and have been shown to directly determine FLC resistance in *C. neoformans* (57). A study investigated the role of *ERG11* in conferring resistance by inserting a copy of the *ERG11* gene onto chromosome 3, which resulted in increased FLC resistance without duplication of chromosome 1 (57). The importance of *AFR1* in FLC resistance has been shown through the reduced resistance of its deletion strain (57).

Disomy of chromosome 4 is the second most common disomy observed in FLC resistant cells. Three genes important in ER maintenance, *SEY1*, *GLO3*, and

GSC2, are located on chromosome 4 and have been shown to be important in FLC resistance (94). In addition to the genes located on chromosome 4, *YOP1*, located on chromosome 7, is an ER-curvature maintenance protein shown to interact with *SEY1* and play a role in FLC resistance (94). These ER-associated genes likely increase the fitness of cells during FLC treatment by reducing the effects of FLC on the ER (94).

Mechanisms of Aneuploid Formation

The increased fitness of aneuploids observed during FLC exposure is intriguing. Aneuploidy is characterized by an imbalanced chromosome state, which is generally thought to be detrimental to the fitness of a cell. There are several mechanisms to ensure proper cell division and prevent aneuploid formation (95). When aneuploidy does arise, it is typically poorly tolerated due to its detrimental consequences (57, 96). It has been estimated that aneuploidy only occurs approximately once in 5×10^5 cell divisions in yeast (97). Notably, this rate increases to approximately 0.3-0.6% in *C. neoformans* during FLC treatment (57). This increase in aneuploidy during drug treatment highlights the potential advantage of aneuploidy at a population level as a source of adaptive phenotypic change (98). Although aneuploid formation has been shown to be important in conferring resistance in *C. neoformans*, the mechanisms underlying aneuploid formation during FLC treatment have not been thoroughly investigated.

Although it has not been shown whether aneuploids are produced or selected during FLC treatment, aneuploid formation generally involves defects in mitosis or cytokinesis, which may arise due to FLC-triggered ergosterol depletion. Whole chromosomal aneuploidy typically develops through chromosome missegregation after DNA replication. More specifically, it has been shown to arise through the following defects: spindle assembly checkpoint defects, improper microtubule-kinetochore attachment, cohesion errors, supernumerary centrosomes, tetraploid formation, and telomeric defects (99).

Interestingly, a recent study in the ascomycete, *Candida albicans*, showed that aneuploidy may arise during FLC treatment through a tetraploid intermediate state. It showed that C. *albicans* cells become aneuploid in response to FLC by producing a tetraploid cell, which then undergoes subsequent DNA missegregation to form aneuploid cells. A tetraploid cell is formed through a delay in budding and a failure in cytokinesis, which produces a three-budded or “trimera” cell. Trimeras continue to undergo nuclear division to produce cells with two nuclei. Binucleate cells undergo a mitotic collapse followed by successful cell separation or cytokinesis, resulting in a tetraploid cell (87). Tetraploidy has previously been described to produce aneuploids due to the formation of extra centrosomes, which then result in multipolar spindles and subsequent chromosome missegregation (99). It is important to note that there are several unique differences in the cell cycle of *C. albicans* compared to *C. neoformans*. *C. neoformans* is predominantly a haploid, while *C. albicans* is a diploid yeast. Additionally, as mentioned earlier,

C. neoformans undergoes a unique mitosis, whereas *C. albicans* undergoes a closed mitosis similar to other ascomycetes. Lastly, aneuploids that arise during FLC treatment in *C. neoformans* primarily consist of whole chromosome duplications, whereas the aneuploidy in *C. albicans* FLC-resistant cells typically refers to the addition of an isochromosome of the left arm of chromosome 5 (91, 92). Therefore, the process of aneuploid formation during FLC treatment in *C. neoformans* may differ from that described in *C. albicans*.

FLC Heteroresistance in *C. neoformans*

The Kwon-Chung lab has characterized the aneuploid-based resistance to FLC in *C. neoformans* as heteroresistance. Mondon et al. first described the phenomenon of FLC heteroresistance in *C. neoformans* through the characterization of two clinical isolates, one from a non-AIDS patient never treated with FLC and one from an AIDS patient that exhibited recurrent cryptococcal meningitis (100). This study used the term heteroresistance to describe the wide array of susceptibilities seen in a clonal population of cells during FLC treatment (100). Additional *in vitro* and *in vivo* studies showed that heteroresistance is an intrinsic feature of *C. neoformans* that promotes virulence and more thoroughly defined the phenomenon of heteroresistance to include three characteristics (Figure 1.2). The first major characteristic of heteroresistance is the ability to isolate a homogenous population of resistant cells after one sub cloning, while a uniform population of susceptible cells cannot be isolated. The second characteristic is the potential of FLC-treated

cells to adapt in a step-wise manner to increasing levels of FLC, resulting in higher levels of heteroresistance. The last characteristic of heteroresistance is the ability of cells that have acquired increased levels of heteroresistance to revert back to their original susceptibility and MIC level when passaged several times in drug-free media (58, 101, Figure 1.2).

These initial studies on heteroresistance provide a good framework for further elucidation of the mechanisms responsible for the development of FLC resistance in *C. neoformans*. Hypothetically, the phenomenon of heteroresistance described above is a form of bet hedging, where clonal cells exhibit phenotypic heterogeneity that allows for the population to better adapt to stress (102, 103). How exactly the differences between individual cells in a clonal population could predispose them to become resistant aneuploids during FLC treatment still remains elusive.

Phenotypic Heterogeneity in *C. neoformans*

Phenotypic or non-genetic heterogeneity refers to the diversity within an isogenic population of cells that does not have a genetic basis (104). This underlying heterogeneity has been shown to play a critical role in acquisition of drug resistance in several microbial pathogens, highlighting the diversity in drug response between individual cells that is often overlooked (104, 105). It plays a significant role in drug resistance by allowing a subpopulation of cells to grow in conditions that are inhibitory to the majority of cells. Increased survival due to

phenotypic heterogeneity is typically non-heritable, so it is often referred to as a type of transient resistance. A prominent example of transient resistance has been described in bacteria as persistence, which arises due to a subpopulation of slow-growing cells that are able to better survive the stress of the drug (106, 107). Although persistence may potentially promote resistance, it differs from resistance in the fact that a clonal population of cells exhibiting increased proliferation during antibiotic treatment cannot be isolated. Instead, the persistent cells will display the same initial heterogeneous response to the antibiotic treatment (106, 107). Persistence leads to recurrence, and it has shown to occur in multiple human pathogens, including fungi (109). FLC heteroresistance in *C. neoformans* seems to be a chimera between persistence and resistance. During FLC treatment in *C. neoformans*, the isolation of a clonal population of resistant cells is possible, due to the fact that aneuploidy is heritable. However, the isolation of a clonal population of susceptible cells is not possible, suggesting there is an underlying source of phenotypic heterogeneity within the population.

Phenotypic heterogeneity and its role in FLC heteroresistance has not been addressed in *C. neoformans*. In clonal single-celled organisms, phenotypic heterogeneity is largely attributed to gene expression “noise” or differential gene expression, which arises during cellular processes, such as the developmental processes of cell cycle progression and cellular ageing (110, 111). Cells within a clonal population are asynchronous and express different gene profiles dependent on their cell cycle stage (112). Additionally, asymmetrical cell division between

mother and daughter cells also results in increased diversity, and, interestingly, even bacterial cells that undergo symmetrical division have been shown to undergo replicative aging (105, 113). Replicative aging leads to unequal segregation of cellular components, producing age-dependent heterogeneity within a genetically-clonal population (102, 114). The cell cycle stage and cell age are two potential sources of phenotypic heterogeneity in *C. neoformans* that likely contribute to the heterogeneous response to FLC. Interestingly, dormant cells that appear to be metabolically similar to the previously described persistent cells have been shown to occur in *in vivo* infections of *C. neoformans* (115, 116). Through single-cell flow cytometry analysis, cells isolated from different host niches showed a subpopulation of cells thought to be dormant cells due to their low-stress response phenotype. How dormant cells of *C. neoformans* respond to FLC has not been investigated. A correlation between replicative age and FLC resistance has been previously described in *C. neoformans*. Bouklas et al. utilized magnetic labeling to isolate older populations of cell (cells that had undergone 15 divisions) and showed that older cells exhibit an overall increase in stress resistance, including FLC resistance (117). This increased resistance is thought to be due to the increase in cell wall size in older cells, which could potentially reduce FLC penetration (117). Older cells may also exhibit increased FLC resistance due to their increased exposure to reactive oxygen species, which could contribute to aneuploid formation (84). It would be of particular interest to see how dormant cells and older cells contribute to the heterogeneous response to FLC in *C. neoformans*.

A better understanding of how phenotypic heterogeneity affects FLC heteroresistance in *C. neoformans* could potentially lead to better therapeutic approaches to prevent FLC resistance and reoccurrence. In addition to exploring the intrinsic sources of phenotypic heterogeneity that potentially lead to FLC heteroresistance, a better characterization of the effects of extrinsic sources on heteroresistance should also be investigated. Environmental changes contribute to overall changes in gene expression which affect drug response. For example, temperature growth has shown to affect biofilm susceptibility to antifungals in *C. neoformans* (118). Additional extrinsic factors, such as: nutrient availability, population density, and oxidative stress, have all also been shown to promote persistence and probably also play a role in FLC heteroresistance (109).

SUMMARY

In conclusion, *C. neoformans* is a basidiomycete, human pathogen that is commonly treated using FLC. Previous studies have shown that *C. neoformans* cells are able to become resistant to FLC by undergoing aneuploid formation (57, 58). The mechanisms underlying aneuploid formation during FLC treatment remain unknown in *C. neoformans*. Additionally, FLC is a fungistatic drug that may potentially allow for survival of certain cells without acquiring resistance, similar to the occurrence of persistence commonly seen in bacterial populations (106-109). The research in the following two chapters will investigate the mechanisms of fluconazole-based aneuploidy in *C. neoformans* and characterize the

heterogeneous response to FLC on a single cell and colony level. A better understanding of the complex response of *C. neoformans* cells to FLC may contribute to improved therapeutic approaches.

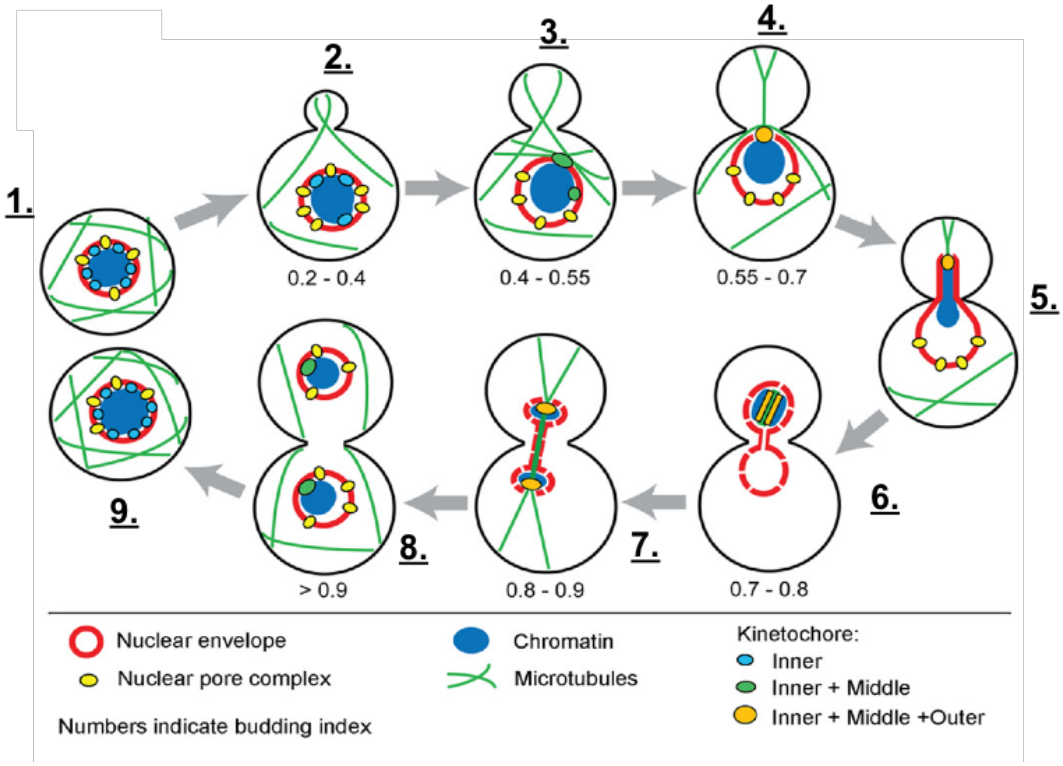

Figure 1.1. *C. neoformans* undergoes a unique mitotic cycle compared to ascomycetes. 1-9: In non-dividing cells, centromeres are not clustered and are positioned at the nuclear periphery. 2-4: Prior to mitosis, centromeres cluster concomitant with a step-wise assembly of the kinetochores. 5: *C. neoformans* undergoes a semi-open mitosis and chromatin moves from the mother cell to the daughter cell. 6-7: Division occurs and half the chromatin moves back to the mother cell. Figure adapted from (4).

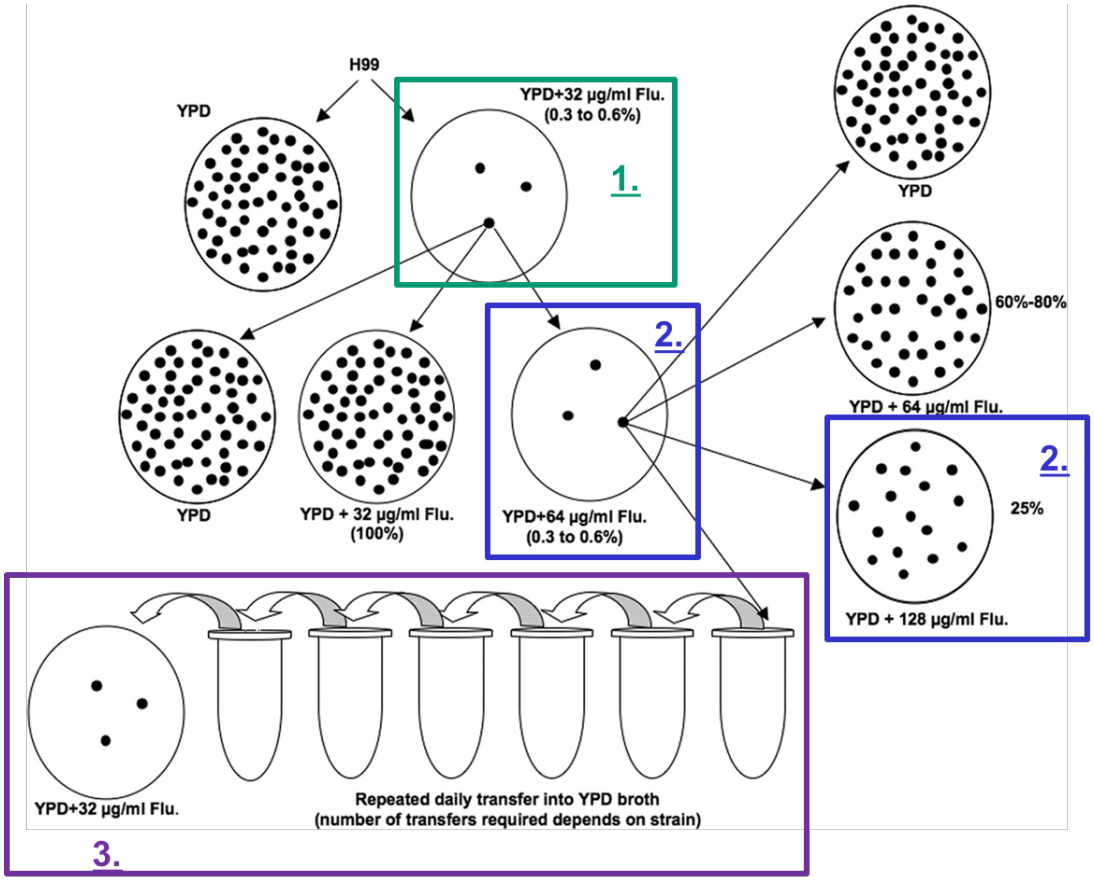

Figure 1.2. *C. neoformans* cells display heteroresistance to fluconazole. 1: The level of heteroresistance refers to the concentration of FLC where the majority of cells are susceptible, but a few subpopulations are viable. 2: These subpopulations are able to adapt in a step-wise manner to increasing levels of FLC concentrations. 3: Cells revert back to their original level of susceptibility when passaged into drug-free media. Model adapted from (101).

S. c	S. p	C. n (CNAG #)	E-value	U. m. (UMAG #)	E-value	Function in *S. cerevisiae*	References
Tem1	Spg1	05513	3.00E-83	11050	1.00E-78	GTP-binding protein	U: (Straube, Weber et al. 2005)
Cdc15	Cdc7	06845	5.00E-58	00721	2.00E-59	protein kinase of MEN	
Mob1	Mob1	05541	9.00E-58	04352	2.00E-64	component of MEN	U: (Sartorel and Perez-Martin 2012)
Cdc14	Clp1/ Flp1	00498	1.00E-83	06187	7.00E-90	protein phosphatase	
Sps1	Sid1	03290	6.00E-83	05543	9.00E-80	protein serine/threonine kinase	U: (Sandrock, Bohmer et al. 2006)
Dbf2	Sid2	02194	2.00E-157	03446	1.00E-151	protein serine/threonine kinase	
Myo1	Myo2 Myp2	01536	0.00E+00	03286	0.00E+00	type II myosin heavy chain	C: (Aboobakar, Wang et al. 2011)
Mlc1	Cdc4	00808	1.00E-29	11848	3.00E-36	myosin light chain	U: (Bohmer, Ripp et al. 2009)
Act1	Act1	00483	0.00E+00	11232	0.00E+00	actin	
Iqg1	Rng2	03763	2.00E-24	10730	3.00E-30	IQGAP-related protein	
Bni1	Cdc12	04815	7.00E-22	12254	4.00E-32	formin	C: (Chang, Lamichhane et al. 2012) U: (Freitag, Lanver et al. 2011)
Bnr1	Fus1	-	-	01141	1.00E-09	formin	U: (Freitag, Lanver et al. 2011)
Tpm1	Cdc8	05701	3.00E-18	11985	2.00E-21	tropomyosin	C: (Chang, Lamichhane et al. 2012)
Tpm2	Cdc8	05701	2.00E-16	11985	6.00E-24	tropomyosin	
Pfy1	Cdc3	00584	1.00E-24	10832	4.00E-32	profilin	
Cdc42	Cdc42	05348	1.00E-117	00295	2.00E-122	small rho-like GTPase	C: (Ballou, Nichols et al. 2009)

							U: (Bohmer, Bohmer et al. 2008)
Bud4	Mid2	06902	2.00E-08	UMAG12265	1.00E-56*	anillin-like protein	
Hof1	Cdc15, Imp2	06740	6.00E-12	00168	8.00E-09	F-bar protein	
Bni5	-	01051	3.40E+00	-	-	septin-Myo1 linker	
Chs1	Chs1	07499	0.00E+00	10117	0.00E+00	chitin synthase	C: (Banks, Specht et al. 2005) U: (Weber, Assmann et al. 2006)
Chs2	Chs2	03326	0.00E+00	04290	0.00E+00	chitin synthase	
Chs3	-	05581	0.00E+00	10277	0.00E+00	chitin synthase	
Chs4	Cfh1	07636	9.00E-83	10641	1.00E-69	activator of Chs3p	
Fks1 (Gsc1)	Bgs4	06508	0.00E+00	01639	0.00E+00	subunit of 1,3-beta-D-glucan synthase	
Fks2 (Gsc2)	Bgs4	06508	0.00E+00	01639	0.00E+00	subunit of 1,3-beta-D-glucan synthase	
Rho1	Rho5	03315	3.00E-102	05734	8.00E-107	GTP-binding protein	
Myo2	Myo52	06971	0.00E+00	04555	0.00E+00	type V myosin heavy chain	U: (Weber, Gruber et al. 2003)
Inn1	Fic1	03422	3.00E-04	06398	8.00E-47*	C2 domain protein	C: (Aboobakar, Wang et al. 2011)
Cyk3	Cyk3	-	-	-	-	SH3 domain protein	
Cbk1	Orb6	03567	0.00E+00	04956	0.00E+00	protein serine/threonine kinase of RAM	U: (Sartorel and Perez-Martin 2012) C: (Walton, Heitman et al. 2006)
Ssd1	Sts5	03345	1.00E-129	01220	1.00E-158	translational repressor	
Mob2	Mob2	05794	4.00E-66	12135	1.00E-62	activator of Cbk1p kinase in RAM	U: (Sartorel and Perez-Martin 2012)

Kic1	Nak1	00405	5.00E-83	11396	2.00E-96	protein kinase of the PAK/Ste20 family	C: (Walton, Heitman et al. 2006)
Tao3	Mor2	03622	2.00E-147	10098	1.00E-154	RAM component	
Sog2	Sog2	03918	7.00E-14	02656	1.00E-15	RAM component	
Cdc3	Spn1	05925	3.00E-146	10503	5.00E-150	septin	C: (Kozubowski and Heitman 2009) U: (Alvarez-Tabares and Perez-Martin 2010)
Cdc10	Spn2	01373	4.00E-135	10644	4.00E-122	septin	
Cdc11	Spn3	02196	5.00E-112	03449	2.00E-104	septin	
Cdc12	Spn6	01740	3.00E-141	03599	4.00E-152	septin	
Exo84	Exo84	04339	3.00E-24	04147	9.00E-20	exocyst complex component	
Eng1 (Dse4)	Eng2	-	-	-	-	daughter cell-specific secreted protein	

- The E-value based on similarity to the *C. neoformans* homologue.
- References refer to either C. neoformans (marked as C:) or U. maydis (U:)

Table 1.1. List of homologues in cytokinesis *C. neoformans* var. *grubii* H99 (C.n.), *U. maydis* 521 (U.m.), and *S. pombe* 972h (S.p.) genomes were probed for similarity against *S. cerevisiae* S288c (S.c.) using FungiDB (http://fungidb.org/fungidb/). Recorded E-values were products of protein BLAST results from FungiDB. Function and protein sequences were retrieved from SGD (http://www.yeastgenome.org). Taken from **Altamirano, S, Chandrasekaran, S., Kozubowski, L.** 2017. Mechanisms of Cytokinesis in Basidiomycetous Yeasts. Fungal Biol Rev **2**:73—87.

REFERENCES

1. **Kozubowski L, Heitman J.** 2012. Profiling a killer, the development of Cryptococcus neoformans. FEMS Microbiol Rev.

2. **Lin X. 2009.** Cryptococcus neoformans: Morphogenesis, infection, and evolution. Infect Genet Evol.

3. **Kitagawa, Hieter.** 2001. Evolutionary conservation between budding yeast and human kinetochores. Nat Rev Mol Cell Biol **2**:678–687.

4. **Kozubowski L, Yadav V, Chatterjee G, Sridhar S, Yamaguchi M, Kawamoto S, Bose I, Heitman J, Sanyal K.** 2013. Ordered kinetochore assembly in the human-pathogenic basidiomycetous yeast Cryptococcus neoformans. MBio **4**.

5. **Kitamura E, Tanaka K, Kitamura Y, Tanaka TU.** 2007. Kinetochore microtubule interaction during S phase in Saccharomyces cerevisiae. Genes Dev **21**:3319–30.

6. **Anderson M, Haase J, Yeh E, Bloom K. 2009.** Function and Assembly of DNA Looping, Clustering, and Microtubule Attachment Complexes within a Eukaryotic Kinetochore. Mol Biol Cell **20**:4131–4139.

7. **Duan Z, Andronescu M, Schutz K, McIlwain S, Kim YJ, Lee C, Shendure J, Fields S, Blau CA, Noble WS.** 2010. A three-dimensional model of the yeast genome. Nature **465**:363–367.

8. **Roy B, Varshney N, Yadav V, Sanyal K.** 2013. The process of kinetochore assembly in yeasts. FEMS Microbiol Lett.

9. **McDonald KL, O'Toole ET, Mastronarde DN, McIntosh JR.** 1992. Kinetochore microtubules in PTK cells. J Cell Biol **118**:369–383.

10. **Byers B, Goetsch L.** 1975. Behavior of spindles and spindle plaques in the cell cycle and conjugation of Saccharomyces cerevisiae. J Bacteriol **124**:511–523.

11. **Gladfelter A, Berman J.** 2009. Dancing genomes: Fungal nuclear positioning. Nat Rev Microbiol.

12. **Lee SE, Frenz LM, Wells NJ, Johnson AL, Johnston LH.** 2001. Order of function of the budding-yeast mitotic exit-network proteins Tem1, Cdc15, Mob1, Dbf2, and Cdc5. Curr Biol **11**:784–788.

13. **Lee SE, Jensen S, Frenz LM, Johnson AL, Fesquet D, Johnston LH.** 2001. The Bub2-dependent mitotic pathway in yeast acts every cell cycle and regulates cytokinesis. J Cell Sci **114**:2345–54.

14. **Petronczki M, Lénárt P, Peters JM.** 2008. Polo on the Rise-from Mitotic Entry to Cytokinesis with Plk1. Dev Cell.

15. **Meitinger F, Palani S, Pereira G.** 2012. The power of MEN in cytokinesis. Cell Cycle.

16. J**aspersen SL, Charles JF, Tinker-Kulberg RL, Morgan DO.** 1998. A late mitotic regulatory network controlling cyclin destruction in Saccharomyces cerevisiae. Mol Biol Cell **9**:2803–2817.

17. **Visintin R, Craig K, Hwang ES, Prinz S, Tyers M, Amon A.** 1998. The phosphatase Cdc14 triggers mitotic exit by reversal of Cdk-dependent phosphorylation. Mol Cell **2**:709–718.

18. **Merlini L, Piatti S.** 2011. The mother-bud neck as a signaling platform for the coordination between spindle position and cytokinesis in budding yeast, p. 805–812. *In* Biological Chemistry.

19. **Bembenek J, Yu H.** 2001. Regulation of the Anaphase-promoting Complex by the Dual Specificity Phosphatase Human Cdc14a. J Biol Chem **276**:48237–48242.

20. **Kaiser BK, Nachury M V., Gardner BE, Jackson PK.** 2004. Xenopus Cdc14??/?? are localized to the nucleolus and centrosome and are required for embryonic cell division. BMC Cell Biol **5**.

21. **Satterwhite LL, Lohka MJ, Wilson KL, Scherson TY, Cisek LJ, Corden JL, Pollard TD.** 1992. Phosphorylation of myosin-II regulatory light chain by cyclin-p34(cdc2): A mechanism for the timing of cytokinesis. J Cell Biol **118**:595–605.

22. **Sellers JR.** 2000. Myosins: A diverse superfamily. Biochim Biophys Acta - Mol Cell Res.

23. **Meitinger F, Palani S.** 2016. Actomyosin ring driven cytokinesis in budding yeast. Semin Cell Dev Biol.

24. **Aboobakar EF, Wang X, Heitman J, Kozubowski L.** 2011. The C2 domain protein Cts1 functions in the calcineurin signaling circuit during high-temperature stress responses in Cryptococcus neoformans. Eukaryot Cell **10**:1714–1723.

25. **Kopecká M, Gabriel M, Takeo K, Yamaguchi M, Svoboda A, Ohkusu M, Hata K, Yoshida S.** 2001. Microtubules and actin cytoskeleton in Cryptococcus neoformans compared with ascomycetous budding and fission yeasts. Eur J Cell Biol **80**:303–311.

26. **Chang YC, Lamichhane AK, Kwon-Chung KJ.** 2012. Role of Actin-Bundling Protein Sac6 in Growth of Cryptococcus neoformans at Low Oxygen Concentration. Eukaryot Cell **11**:943–951.

27. **Kozubowski L, Heitman J.** 2010. Septins enforce morphogenetic events during sexual reproduction and contribute to virulence of Cryptococcus neoformans. Mol Microbiol **75**:658–675.

28. **Walther A, Wendland J.** 2003. Septation and cytokinesis in fungi. Fungal Genet Biol.

29. **Rincon SA, Paoletti A.** 2016. Molecular control of fission yeast cytokinesis. Semin Cell Dev Biol.

30. **Proctor SA, Minc N, Boudaoud A, Chang F.** 2012. Contributions of turgor pressure, the contractile ring, and septum assembly to forces in cytokinesis in fission yeast. Curr Biol **22**:1601–1608.

31. **Vallen EA, Caviston J, Bi E.** 2000. Roles of Hof1p, Bni1p, Bnr1p, and Myo1p in Cytokinesis in Saccharomyces cerevisiae. Mol Biol Cell **11**:593–611.

32. **Schmidt M, Bowers B, Varma A, Roh D-H, Cabib E.** 2002. In budding yeast, contraction of the actomyosin ring and formation of the primary septum at cytokinesis depend on each other. J Cell Sci **115**:293–302.

33. **VerPlank L, Li R.** 2005. Cell cycle-regulated trafficking of Chs2 controls actomyosin ring stability during cytokinesis. Mol Biol Cell **16**:2529–2543.

34. **Fang X, Luo J, Nishihama R, Wloka C, Dravis C, Travaglia M, Iwase M, Vallen EA, Bi E.** 2016. Correction to: Biphasic targeting and cleavage furrow ingression directed by the tail of a myosin II [JCB 191, 7, December **27**, (2010) (1333-1350)]. J Cell Biol.

35. **Adams DJ.** 2004. Fungal cell wall chitinases and glucanases. Microbiology.

36. **Maerz S, Seiler S.** 2010. Tales of RAM and MOR: NDR kinase signaling in fungal morphogenesis. Curr Opin Microbiol.

37. **Weiss EL.** 2012. Mitotic exit and separation of mother and daughter cells. Genetics **192**:1165–1202.

38. **Banks IR, Specht CA, Donlin MJ, Gerik KJ, Levitz SM, Lodge JK.** 2005. A chitin synthase and its regulator protein are critical for chitosan production and growth of the fungal pathogen Cryptococcus neoformans. Eukaryot Cell **4**:1902–1912.

39. **Baker LG, Specht CA, Lodge JK.** 2009. Chitinases are essential for sexual development but not vegetative growth in cryptococcus neoformans. Eukaryot Cell **8**:1692–1705.

40. **Rajasingham R, Smith RM, Park BJ, Jarvis JN, Govender NP, Chiller TM, Denning DW, Loyse A, Boulware DR.** 2017. Global burden of disease of HIV-associated cryptococcal meningitis: an updated analysis. Lancet Infect Dis **17**:873–881.

41. **May RC, Stone NRH, Wiesner DL, Bicanic T, Nielsen K.** 2016. Cryptococcus: From environmental saprophyte to global pathogen. Nat Rev Microbiol.

42. **Nosanchuk JD, Shoham S, Fries BC, Shapiro DS, Levitz SM, Casadevall A.** 2000. Evidence of zoonotic transmission of Cryptococcus neoformans from a pet cockatoo to an immunocompromised patient. Ann Intern Med **132**:205–208.

43. **Rohatgi S, Pirofski L-A.** 2015. Host immunity to Cryptococcus neoformans. Future Microbiol **10**:565–81.

44. **Gibson JF, Johnston SA.** 2015. Immunity to Cryptococcus neoformans and C. gattii during cryptococcosis. Fungal Genet Biol **78**:76–86.

45. **Shao X, Mednick A, Alvarez M, van Rooijen N, Casadevall A, Goldman DL.** 2005. An Innate Immune System Cell Is a Major Determinant of Species-Related Susceptibility Differences to Fungal Pneumonia. J Immunol **175**:3244–3251.

46. **Osterholzer JJ, Milam JE, Chen GH, Toews GB, Huffnagle GB, Olszewski MA.** 2009. Role of dendritic cells and alveolar macrophages in regulating early host defense against pulmonary infection with Cryptococcus neoformans. Infect Immun **77**:3749–3755.

47. **Perfect JR.** 2005. Cryptococcus neoformans: A sugar-coated killer with designer genes. FEMS Immunol Med Microbiol.

48. **Chang YC, Kwon-Chung KJ.** 1994. Complementation of a capsule-deficient mutation of Cryptococcus neoformans restores its virulence. Mol Cell Biol **14**:4912–9.

49. **Del Poeta M.** 2004. Role of phagocytosis in the virulence of Cryptococcus neoformans. Eukaryot Cell.

50. **Casadevall A, Rosas AL, Nosanchuk JD.** 2000. Melanin and virulence in Cryptococcus neoformans. Curr Opin Microbiol.

51. **Wang Y, Aisen P, Casadevall A.** 1995. Cryptococcus neoformans melanin and virulence: Mechanism of action. Infect Immun **63**:3131–3136.

52. **McFadden DC, Casadevall A.** 2001. Capsule and melanin synthesis in Cryptococcus neoformans. Med Mycol 39 Suppl **1**:19–30.

53. **Reese AJ, Doering TL.** 2003. Cell wall ??-1,3-glucan is required to anchor the Cryptococcus neoformans capsule. Mol Microbiol 50:1401–1409.

54. **Alspaugh JA.** 2015. Virulence mechanisms and Cryptococcus neoformans pathogenesis. Fungal Genet Biol **78**:55–58.

55. **Zaragoza O, Rodrigues ML, De Jesus M, Frases S, Dadachova E, Casadevall A.** 2009. The capsule of the fungal pathogen Cryptococcus neoformans. Adv Appl Microbiol **68**:133–216.

56. **Morrow CA, Fraser JA.** 2013. Ploidy variation as an adaptive mechanism in human pathogenic fungi. Semin Cell Dev Biol.

57. **Sionov E, Lee H, Chang YC, Kwon-Chung KJ.** 2010. Cryptococcus neoformans Overcomes Stress of Azole Drugs by Formation of Disomy in Specific Multiple Chromosomes. PLoS Pathog **6**:e1000848.

58. **Sionov E, Chang YC, Kwon-Chung KJ.** 2013. Azole heteroresistance in Cryptococcus neoformans: Emergence of resistant clones with chromosomal disomy in the mouse brain during fluconazole treatment. Antimicrob Agents Chemother **57**:5127–5130.

59. **Okagaki LH, Nielsen K.** 2012. Titan cells confer protection from phagocytosis in Cryptococcus neoformans infections. Eukaryot Cell **11**:820–826.

60. **Wiesner DL, Specht CA, Lee CK, Smith KD, Mukaremera L, Lee ST, Lee CG, Elias JA, Nielsen JN, Boulware DR, Bohjanen PR, Jenkins MK, Levitz SM, Nielsen K.** 2015. Chitin Recognition via Chitotriosidase Promotes Pathologic Type-2 Helper T Cell Responses to Cryptococcal Infection. PLoS Pathog **11**:1–28.

61. **Zaragoza O, Rocío GR, Nosanchuk JD, Cuenca-Estrella M, Rodríguez-Tudela JL, Casadevall A.** 2010. Fungal cell gigantism during mammalian infection. PLoS Pathog **6**.

62. **Gerstein AC, Fu MS, Mukaremera L, Li Z, Ormerod KL, Fraser JA, Berman J, Nielsen K.** 2015. Polyploid titan cells produce haploid and aneuploid progeny to promote stress adaptation. MBio **6**.

63. **Perfect JR, Bicanic T.** 2015. Cryptococcosis diagnosis and treatment: What do we know now. Fungal Genet Biol **78**:49–54.

64. **Babady NE, Bestrom JE, Jespersen DJ, Jones MF, Beito EM, Binnicker MJ, Wengenack NL.** 2009. Evaluation of three commercial latex agglutination kits and a commercial enzyme immunoassay for the detection of cryptococcal antigen. Med Mycol **47**:336–338.

65. **Boulware DR, Rolfes MA, Rajasingham R, von Hohenberg M, Qin Z, Taseera K, Schutz C, Kwizera R, Butler EK, Meintjes G, Muzoora C, Bischof JC, Meya DB.** 2014. Multisite validation of cryptococcal antigen lateral flow assay and quantification by laser thermal contrast. Emerg Infect Dis **20**:45–53.

66. **Tang MW, Clemons K V., Katzenstein DA, Stevens DA.** 2016. The cryptococcal antigen lateral flow assay: A point-of-care diagnostic at an opportune time. Crit Rev Microbiol.

67. **Bossche H Vanden, Lauwers W, Willemsens G, Marichal P, Cornelissen F, Cools W.** 1984. Molecular basis for the antimycotic and antibacterial activity of N???substituted imidazoles and triazoles: The inhibition of isoprenoid biosynthesis. Pestic Sci **15**:188–198.

68. **Santos JRA, Ribeiro NQ, Bastos RW, Holanda RA, Silva LC, Queiroz ER, Santos DA.** 2017. High-dose fluconazole in combination with amphotericin B is more efficient than monotherapy in murine model of cryptococcosis. Sci Rep **7**.

69. **Anderson TM, Clay MC, Cioffi AG, Diaz KA, Hisao GS, Tuttle MD, Nieuwkoop AJ, Comellas G, Maryum N, Wang S, Uno BE, Wildeman EL, Gonen T, Rienstra CM, Burke MD.** 2014. Amphotericin forms an extramembranous and fungicidal sterol sponge. Nat Chem Biol **10**:400–406.

70. **Vermes A.** 2000. Flucytosine: a review of its pharmacology, clinical indications, pharmacokinetics, toxicity and drug interactions. J Antimicrob Chemother **46**:171–179.

71. **Loyse A, Dromer F, Day J, Lortholary O, Harrison TS.** 2013. Flucytosine and cryptococcosis: Time to urgently address the worldwide accessibility of a 50-year-old antifungal. J Antimicrob Chemother **68**:2435–2444.

72. **Ssekitoleko R, Kamya MR, Reingold AL.** 2013. Primary prophylaxis for cryptococcal meningitis and impact on mortality in HIV: a systematic review and meta-analysis. Future Virol **8**:1–25.

73. **Mdodo RM.** 2010. Prevalence and susceptibility of Cryptococcus neoformans to fluconazole in HIV patients in Kenya. Diss Abstr Int Sect B Sci Eng.

74. **Bartizal K, Gill CJ, Abruzzo GK, Flattery AM, Kong L, Scott PM, Smith JG, Leighton CE, Bouffard A, Dropinski JF, Balkovec J.** 1997. In vitro preclinical evaluation studies with the echinocandin antifungal MK-0991 (L-743,872). Antimicrob Agents Chemother **41**:2326–2332.

75. **Franzot SP, Casadevall A.** 1997. Pneumocandin L-743,872 enhances the activities of amphotericin B and fluconazole against Cryptococcus neoformans in vitro. Antimicrob Agents Chemother **41**:331–336.

76. **Abruzzo GK, Flattery AM, Gill CJ, Kong L, Smith JG, Pikounis VB, Balkovec JM, Bouffard AF, Dropinski JF, Rosen H, Kropp H, Bartizal K.** 1997. Evaluation of the echinocandin antifungal MK-0991 (L-743,872): Efficacies in mouse models of disseminated aspergillosis, candidiasis, and cryptococcosis. Antimicrob Agents Chemother **41**:2333–2338.

77. **Mukaremera L, Lee KK, Wagener J, Wiesner DL, Gow NAR, Nielsen K.** 2018. Titan cell production in Cryptococcus neoformans reshapes the cell wall and capsule composition during infection. Cell Surf **1**:15–24.

78. **Mourad A, Perfect JR.** 2018. Tolerability profile of the current antifungal armoury. J Antimicrob Chemother **73**:i26–i32.

79. **Heese-Peck A.** 2002. Multiple Functions of Sterols in Yeast Endocytosis. Mol Biol Cell **13**:2664–2680.

80. **Ghannoum MA, Rice LB.** 1999. Antifungal agents: mode of action, mechanisms of resistance, and correlation of these mechanisms with bacterial resistance. ClinMicrobiolRev **12**:501–517.

81. **Zhang YQ, Gamarra S, Garcia-Effron G, Park S, Perlin DS, Rao R.** 2010. Requirement for ergosterol in V-ATPase function underlies antifungal activity of azole drugs. PLoS Pathog **6**.

82. **Watson PF, Rose ME, Ellis SW, England H, Kelly SL.** 1989. Defective sterol C5-6 desaturation and azole resistance: A new hypothesis for the mode of action of azole antifungals. Biochem Biophys Res Commun **164**:1170–1175.

83. **Abe F, Usui K, Hiraki T.** 2009. Fluconazole modulates membrane rigidity, heterogeneity, and water penetration into the plasma membrane in Saccharomyces cerevisiae. Biochemistry **48**:8494–8504.

84. **Kobayashi D, Kondo K, Uehara N, Otokozawa S, Tsuji N, Yagihashi A, Watanabe N.** 2002. Endogenous reactive oxygen species is an important mediator of miconazole antifungal effect. Antimicrob Agents Chemother **46**:3113–3117.

85. **Sorgo AG, Heilmann CJ, Dekker HL, Bekker M, Brul S, de Koster CG, de Koning LJ, Klis FM.** 2011. Effects of fluconazole on the secretome, the wall proteome, and wall integrity of the clinical fungus candida albicans. Eukaryot Cell **10**:1071–1081.

86. **Alvarez FJ, Douglas LM, Konopka JB.** 2007. Sterol-rich plasma membrane domains in fungi. Eukaryot Cell.

87. **Harrison BD, Hashemi J, Bibi M, Pulver R, Bavli D, Nahmias Y, Wellington M, Sapiro G, Berman J.** 2014. A Tetraploid Intermediate Precedes Aneuploid Formation in Yeasts Exposed to Fluconazole. PLoS Biol **12**.

88. **Berkow EL, Lockhart SR.** 2017. Fluconazole resistance in Candida species: A current perspective. Infect Drug Resist **10**:237–245.

89. **Selmecki AM, Dulmage K, Cowen LE, Anderson JB, Berman J.** 2009. Acquisition of aneuploidy provides increased fitness during the evolution of antifungal drug resistance. PLoS Genet **5**.

90. **Selmecki A, Forche A, Berman J.** 2010. Genomic plasticity of the human fungal pathogen Candida albicans. Eukaryot Cell.

91. **Selmecki A, Forche A, Berman J.** 2006. Aneuploidy and isochromosome formation in drug-resistant Candida albicans. Science (80-) **313**:367–370.

92. **Selmecki A, Gerami-Nejad M, Paulson C, Forche A, Berman J.** 2008. An isochromosome confers drug resistance in vivo by amplification of two genes, ERG11 and TAC1. Mol Microbiol **68**:624–641.

93. **Kwon-Chung KJ, Chang YC.** 2012. Aneuploidy and Drug Resistance in Pathogenic Fungi. PLoS Pathog **8**.

94. **Ngamskulrungroj P, Chang Y, Hansen B, Bugge C, Fischer E, Kwon-Chung KJ.** 2012. Characterization of the chromosome 4 genes that affect fluconazole-induced disomy formation in cryptococcus neoformans. PLoS One **7**.

95. **Malmanche N, Maia A, Sunkel CE.** 2006. The spindle assembly checkpoint: Preventing chromosome mis-segregation during mitosis and meiosis. FEBS Lett.

96. **Siegel JJ, Amon A.** 2012. New Insights into the Troubles of Aneuploidy. Annu Rev Cell Dev Biol **28**:189–214.

97. **Hartwell LH, Dutcher SK, Wood JS, Garvik B.** 1982. The fidelity of mitotic chromosome reproduction. Recent Adv Yeast Mol Biol **1**:28–38.

98. **Chen G, Rubinstein B, Li R.** 2012. Whole chromosome aneuploidy: Big mutations drive adaptation by phenotypic leap. BioEssays **34**:893–900.

99. **Orr B, Godek KM, Compton D.** 2015. Aneuploidy. Curr Biol **25**:R538–R542.

100. **Mondon P, Petter R, Amalfitano G, Luzzati R, Concia E, Polacheck I, Kwon-Chung KJ.** 1999. Heteroresistance to fluconazole and voriconazole in Cryptococcus neoformans. Antimicrob Agents Chemother **43**:1856–1861.

101. **Sionov E, Chang YC, Garraffo HM, Kwon-Chung KJ.** 2009. Heteroresistance to fluconazole in Cryptococcus neoformans is intrinsic and associated with virulence. Antimicrob Agents Chemother **53**:2804–2815.

102. **Levy SF, Ziv N, Siegal ML.** 2012. Bet hedging in yeast by heterogeneous, age-correlated expression of a stress protectant. PLoS Biol **10**.

103. **Ben-Ami R, Zimmerman O, Finn T, Amit S, Novikov A, Wertheimer N, Lurie-Weinberger M, Berman J.** 2016. Heteroresistance to fluconazole is a continuously distributed phenotype among candida glabrata clinical strains associated with in vivo persistence. MBio **7**.

104. **Avery S V.** 2006. Microbial cell individuality and the underlying sources of heterogeneity. Nat Rev Microbiol.

105. **Dhar N, McKinney JD.** 2007. Microbial phenotypic heterogeneity and antibiotic tolerance. Curr Opin Microbiol.

106. **Bigger JW.** 1944. Treatment of Staphylococcal infections with penicillin by intermittent sterilisation. Lancet **244**:497–500.

107. **Brauner A, Fridman O, Gefen O, Balaban NQ.** 2016. Distinguishing between resistance, tolerance and persistence to antibiotic treatment. Nat Rev Microbiol.

108. **Levin-Reisman I, Ronin I, Gefen O, Braniss I, Shoresh N, Balaban NQ.** 2017. Antibiotic tolerance facilitates the evolution of resistance. Science (80-) **355**:826–830.

109. **Cohen NR, Lobritz MA, Collins JJ.** 2013. Microbial persistence and the road to drug resistance. Cell Host Microbe.

110. **Sumner ER, Avery AM, Houghton JE, Robins RA, Avery S V.** 2003. Cell cycle- and age-dependent activation of Sod1p drives the formation of stress resistant cell subpopulations within clonal yeast cultures. Mol Microbiol **50**:857–870.

111. **Holland SL, Reader T, Dyer PS, Avery S V.** 2014. Phenotypic heterogeneity is a selected trait in natural yeast populations subject to environmental stress. Environ Microbiol **16**:1729–1740.

112. **Newman JRS, Ghaemmaghami S, Ihmels J, Breslow DK, Noble M, DeRisi JL, Weissman JS.** 2006. Single-cell proteomic analysis of S. cerevisiae reveals the architecture of biological noise. Nature **441**:840–846.

113. **Stewart EJ, Madden R, Paul G, Taddei F.** 2005. Aging and death in an organism that reproduces by morphologically symmetric division. PLoS Biol **3**:0295–0300.

114. **Vallen EA, Scherson TY, Roberts T, van Zee K, Rose MD.** 1992. Asymmetric mitotic segregation of the yeast spindle pole body. Cell **69**:505–515.

115. **Garcia-Hermoso D, Janbon G, Dromer F.** 1999. Epidemiological evidence for dormant Cryptococcus neoformans infection. J Clin Microbiol **37**:3204–3209.

116. **Alanio A, Vernel-Pauillac F, Sturny-Leclère A, Dromer F.** 2015. Cryptococcus neoformans host adaptation: Toward biological evidence of dormancy. MBio **6**.

117. **Bouklas T, Pechuan X, Goldman DL, Edelman B, Bergman A, Fries BC.** 2013. Old Cryptococcus neoformans cells contribute to virulence in chronic cryptococcosis. MBio **4**.

118. **Pettit RK, Repp KK, Hazen KC.** 2010. Temperature affects the susceptibility of Cryptococcus neoformans biofilms to antifungal agents. Med Mycol **48**:421–426.

CHAPTER TWO

FLUCONAZOLE-INDUCED PLOIDY CHANGE IN *CRYPTOCOCCUS NEOFORMANS* RESULTS FROM THE UNCOUPLING OF CELL GROWTH AND NUCLEAR DIVISION

Sophie Altamirano[1], Diana Fang[1], Charles Simmons[1], Shreyas Sridhar[2], Peipei Wu[1], Kaustuv Sanyal[2], Lukasz Kozubowski[1]

1) Department of Genetics and Biochemistry, Clemson University, Clemson, South Carolina, USA 2) Molecular Mycology Laboratory, Molecular Biology and Genetics Unit, Jawaharlal Nehru Centre for Advanced Scientific Research, Bangalore 560064, India

Published – mSphere, 2017

ABSTRACT

Cryptococcus neoformans is a pathogenic yeast that causes lethal cryptococcal meningitis in immunocompromised patients. One of the challenges in treating cryptococcosis is the development of resistance to azole antifungals. Previous studies linked azole resistance to elevated copies of critical resistance genes in aneuploid cells. However, how aneuploidy is formed in the presence of azole drugs remains unclear. This study found that treatment with inhibitory concentrations of an azole drug, fluconazole (FLC), led to a significant population of cells with increased DNA content, through the following defects: inhibition of budding, premature mitosis, and inhibition of cytokinesis followed by replication in the mother cell. Inhibition and/or a delay in cytokinesis led to the formation of cells with more than one daughter attached (multimeric cells). To investigate which part of cytokinesis fails in the presence of FLC, the dynamics of the actomyosin ring (AMR), septins, and Cts1, a protein involved in cell separation, were analyzed with time-lapse microscopy. Following the constriction of the AMR, septins assembled, and the septum was formed between the mother and daughter cells. However, a final degradation of the septum was affected. Enlarged cells with aberrant morphology including multimeric cells exhibited increased potential to proliferate in the presence of FLC. These findings suggest that pleiotropic effects of FLC on growth and mitotic division lead to an increase in DNA content resulting in cells less sensitive to the drug. Cells with increased DNA content continue to proliferate and therefore increase the chance of forming resistant populations.

INTRODUCTION

Genomic integrity is a crucial attribute of all living forms yet in some circumstances transient abnormalities in chromosomal number and composition are beneficial for the cell population (3, 4). For instance, development of aneuploidy is a common survival mechanism for cells under selective pressure of adverse environmental conditions (4). Aneuploidy is typical for malignant cells that strive to proliferate despite nutrient limitation and inhibitory effects of anticancer drugs (5). Aneuploidy occurs frequently in pathogenic organisms that encounter harsh inhibitory conditions within the host and battle against therapeutic regimens; prominent examples include the protozoan *Leishmania*, an ascomycetous yeast *Candida albicans* and a basidiomycetous yeast *Cryptococcus neoformans*, the most common causal agent of fungal meningitis in AIDS and transplant patients (1, 6-9). How can changes in chromosomal composition lead to an improved survival? The key to this process is the selection favoring cells with elevated copies of specific genes that provide growth advantage in particular inhibitory conditions. In most cases retention of an entire additional chromosome or addition of an arm of a specific chromosome occurs in selected population of cells. Importantly, the environmental inhibitory effects not only select for organisms with specifically altered chromosomal composition, those effects often induce genomic changes by mechanisms that remain ill-defined (3). The resulting pool of cells with various karyotypes increases the chances of survival; individuals with beneficial chromosomal compositions are selectively favored under the inhibitory pressure

(3). Prominent examples of fungal pathogens developing resistance to azole antifungal treatments are those observed in *C. albicans* and *C. neoformans*. The fungistatic azole drug fluconazole (FLC) targets lanosterol 14α-demethylase, Erg11, which is responsible for converting lanosterol to ergosterol in the ergosterol biosynthesis pathway (10). Ergosterol is known to be an essential component for cell membrane permeability and fluidity, but the exact inhibitory consequences of ergosterol diminishment remain elusive (11).

Specific genes that confer resistance to FLC and thus determine the selection of a particular chromosomal configuration in *C. albicans* and *C. neoformans* are well established (1, 8). On the other hand, mechanisms through which FLC potentially leads to changes in chromosomal composition in these human pathogens of significance remain poorly characterized. In a diploid yeast, *C. albicans*, treatment with FLC leads to growth inhibition, premature nuclear and spindle cycles, and a failure in cytokinesis resulting in a formation of multimeric cells containing tetraploid nuclei (12). Tetraploid cells give raise to aneuploid populations of which most fit individuals are selected under the FLC inhibitory pressure and lead to FLC resistance (12). The exact mechanism through which FLC inhibits cytokinesis in *C. albicans* remains unknown.

It is well established that the *in vitro* FLC-triggered drug resistance in *C. neoformans* called heteroresistance is a relatively rare occurrence and is based primarily on the formation of aneuploids (<1% of the FLC-treated population) (9). However, the initial effects of FLC on the population of *C. neoformans* have not

been characterized and the mechanisms by which FLC triggers changes in chromosome number in *C. neoformans* remain unclear. Recent studies reveal several differences in mitosis between *C. neoformans* and *S. cerevisiae*, which may suggest that FLC dependent aneuploidy formation in *C. neoformans* may differ from previously described mechanisms in hemiascomycetous yeasts including *C. albicans* (13).

Here we investigated mechanisms through which FLC affects ploidy in *C. neoformans*. Our data suggest that exposure to inhibitory concentrations of FLC leads to a progressive diminishment of the ability to initiate budding and subsequent growth while permitting nuclear events. In addition, FLC inhibits cytokinesis, most likely by imposing a delay or a permanent block in the degradation of the primary septum. The resulting populations of cells with an increase in DNA content grow better under the inhibitory concentration of FLC, hypothetically increasing the chance of forming aneuploids out of which the most adapted cells are selected giving rise to fully resistant populations.

RESULTS

FLC treatment results in an increase in DNA content in a significant fraction of cells.

At the concentration of FLC that is equal to the heteroresistance level, resistant colonies are aneuploids, initially with disomic chromosome 1 (9). FLC could potentially act solely as a selection agent to allow growth of only a small fraction

of pre-existing aneuploids that may be naturally present in a population. Alternatively, FLC may act as a driving force, stimulating the formation of aneuploids from which a small proportion is selected for proliferation under the inhibitory concentration of the drug, similarly to the recently proposed mechanism in *C. albicans* and as hypothesized in studies that involved *C. neoformans* (9, 12). Based on the fact that *C. neoformans* is predominantly haploid, development of aneuploidy could proceed through formation of diploid cells, analogous to the aneuploid formation based on a tetraploid intermediate described for *C. albicans* (12). To test if FLC has an effect on DNA content of *C. neoformans* during initial exposure to the drug, cells treated with FLC were fixed, stained with propidium iodide (PI), and examined using fluorescence flow cytometry. Strikingly, treatment of cells with 32 μg/ml FLC at 24°C for 12 and 14 hours resulted in 20% and 88%, respectively, of the cell population with ploidy levels at or above 4n (Figure 2.1). The significant increase of the cell number with ploidy level at or above 4n between 12 and 14 hours (Figure 2.1) was not consistent from experiment to experiment as in some cases maximum ploidy was present at around 9 hours with no significant further change in later time points (data not shown). The longest incubation time tested was 18 hours, which did not show further significant increase in ploidy level (data not shown). The maximum ploidy level in a significant population of cells observed at any of the test conditions was approximately 4n, although a smaller fraction of cells with ploidy levels beyond 4n was also present at inhibitory concentrations of FLC (Figure 2.1). The fraction of cells with increased DNA

content was proportional to the concentration of FLC. Altogether, these data suggest that FLC treatment at inhibitory concentrations leads to an increase in ploidy beyond 2n.

Treatment with FLC causes inhibition of budding.

We tested whether FLC treatment resulted in any of the following cellular defects that may individually or collectively result in increased DNA content: 1. Inhibition of growth coupled with re-replication. 2. A defect in cytokinesis. 3. Unequal chromosomal segregation during mitosis.

The inhibitory effect of FLC, similar to other azole antifungals, has been associated with the depletion of ergosterol from the plasma membrane (14). The minimum level of ergosterol needed to sustain cellular growth is not clear. Doubling time of *C. neoformans* under unperturbed growth conditions in the laboratory is approximately 2 hours (15). Therefore, during the initial period of FLC treatment, we expect the growth of cells to be relatively normal, as the depletion of ergosterol from the membranes may take more than a doubling time. Consistent with this prediction, we found that treatment of cells with 32 μg/ml FLC for 3 hours resulted in only ~20% reduction in new bud formation relative to the control (Figure 2.2). However, treatment for 6 hours resulted in a more significant inhibition of budding (~50% reduction as compared to the control, Figure 2.2). These data suggest that the effect of FLC on growth is delayed, presumably due to the relatively slow exchange rate of ergosterol within the plasma membrane. If this were the case, we

would expect that further slowdown in the exchange rate may lead to even longer delay in the effect of FLC on bud initiation. Consistent with this possibility, the addition of actin depolymerizing agent latrunculin B (LatB) during the pretreatment of unbudded cells with FLC leads to a further delay in time needed to significantly inhibit bud initiation; the effective inhibition by FLC when combined with the LatB was achieved by 14 hours (Figure 2.3). Cells treated with LatB for 18 hours initiated budding when released into drug free media indicated that prolonged exposure to LatB did not have any significant adverse permanent effects on cell growth (Figure 2.3). Taken together, these data suggest that FLC treatment leads to inhibition of bud initiation and subsequent growth. However, the effect is delayed. We speculate that levels of plasma membrane ergosterol reach a critical minimum after longer incubation with FLC, resulting in significant inhibitions in the initiation of budding and further bud growth.

FLC treatment leads to a defect in cytokinesis.

Hypothetically, the fraction of cells with increased DNA content may result from a debilitating effect of FLC on cytokinesis. To test this hypothesis, we assessed the morphology of FLC-treated cells. To differentiate between cells with normal and increased DNA content, we fixed the cells, stained the DNA with PI, and subsequently fractionated using a FACS (fluorescence assisted cell sorting) instrument. Fractions of cells with increased ploidy were collected, and the morphology was scored under the microscope. Cells with ploidy level close to 1n

were predominantly unbudded or contained a single usually small bud (Figure 2.4). Fractions with higher ploidy were enriched in cells characterized by the presence of more than one daughter cell (multimeric cells). These multimeric cells were either trimeras, with two daughter cells born from the mother cell, or contained an additional daughter (a granddaughter) born from one of the daughters (Figure 2.4). The fraction with ploidy above 4n contained ~44% of multimeric cells. These results suggest that treatment with FLC leads to failure in cytokinesis. To rule out the possibility that multimeric cells result from cell fusion events, we mixed two strains, one that expressed histone H4 tagged with GFP and the other expressing H4 tagged with mCherry and subjected the mixed cell culture to FLC. While multimeric cells expressing either of the two fluorescent chimeras were frequent after longer incubations with FLC, we could not find multimeric cells that expressed both GFP and mCherry (data not shown). This is consistent with our expectation that multimeric cells are a result of cell division failure rather than cell fusion events.

FLC treatment leads to uncoupling of growth from the cell cycle.

Interestingly the fraction of cells with the highest ploidy also contained significant amount of cells with a single bud (45%) and unbudded cells (11%) suggesting that re-replication has taken place as a result of FLC treatment (Figure 2.4). A delay or complete block in cell separation during FLC treatment potentially leads to an increase in DNA content in unseparated cells if the cell cycle continues and results in subsequent rounds of replication. We tested this hypothesis further by subjecting

a population of pre-selected unbudded cells to FLC and assessing DNA content based on PI fluorescence using flow cytometry. Importantly, we examined cells after 3 and 6 hours of treatment with 32 µg/ml FLC, which are times when no multimeric cells are detected in the population. Strikingly, after 6 hours of FLC treatment ~50% of cells indicated DNA content above 2n, with a predominant population (visible as a peak) that corresponded to cells with 3n DNA content (Figure 2.5A). These results suggest that upon FLC treatment, cells exhibit a failure or a delay in cytokinesis with a concomitant new round of replication in the mother cell. An alternative, non-exclusive possibility is that FLC treatment may result in a failure to transition the chromatin to the daughter cell prior to metaphase, an event that normally occurs in *C. neoformans* (13). Hypothetically, failure to translocate the chromatin to the daughter cell may be followed by spindle formation and subsequent nuclear division in the mother cell leading to increased ploidy. To address this possibility, we analyzed the localization of the mitotic spindle in cells treated with 32 µg/ml FLC for 22 hours, based on a strain that expressed GFP-tagged ß-tubulin. Consistent with previous studies, in the control sample the spindle was detected exclusively within daughter cells (Figure 2.5B). In contrast, ~ 16% (n = 33) of FLC-treated cells that had a detectable spindle were either unbudded or contained extremely small buds and the spindle was positioned within the mother cell (Figure 5B). Consistently, we found that when the spindle was visible, the size of the daughter cells in the control was relatively uniform ($\bar{x} = 3.2$,

SD = 0.31). However, the FLC-treated cells exhibited a broader range of sizes of daughter cells when spindle was detected ($\bar{x}$ = 3.5, SD = 0.84 μm) (Figure 2.5C).

To further assess the uncoupling of growth from the mitotic cycle, we monitored clustering of centromeres in FLC treated cells. In *C. neoformans*, centromeres are not clustered in interphase cells and cells with small buds, but they cluster in medium budded cells in preparation for mitosis (13). To visualize centromeres, we utilized a strain that expressed a centromeric histone variant Cse4 expressed from an endogenous promoter and tagged with mCherry and a component of the nuclear envelope, Ndc1, tagged with GFP. Strikingly, when cells were treated with 32 μg/ml FLC for 13 and 15 hours, 50% and 35% of unbudded cells, respectively, had already clustered centromeres (Figure 2.6, panel 3). In addition, 3% (13 hours, n = 65) and 9% (15 hours, n = 75) of budded cells contained 2 nuclei in the mother cell (Figure 6, panel 3). Moreover, 3% (13 hours, n = 65) and 4% (15 hours, n = 75) of budded cells showed some centromeres in the bud neck area (Figure 2.6, panels 1 and 4). Occasionally, we also observed cells with a portion of centromeres that localized outside of the nuclear area marked by the Ndc1 (Figure 2.6, panels 2 and 5). These data suggest that upon treatment with FLC, the mitotic cycle is less inhibited as compared to growth and budding. This leads to clustering of centromeres, spindle assembly, and nuclear division in the mother cell, resulting in cells with increased DNA content and potentially aberrant chromosomal composition.

Analysis of the mitotic defects resulting from FLC treatment.

We investigated what specific defects accounted for the inability of cells to separate during FLC treatment. Defects in cell separation in basidiomycetous yeasts may result from a lack of actomyosin ring (AMR) constriction, failure in septum deposition, or inadequate degradation of the primary septum toward the end of cytokinesis (16). To monitor constriction of the AMR, we performed time-lapse microscopy based on a strain of *C. neoformans* that expressed a component of the AMR, myosin heavy chain, Myo1, tagged with mCherry and a nucleoporin, Nup107, tagged with GFP (to monitor the stage of mitosis). Cells with single daughters in both the control and FLC treated samples, exhibited normal AMR constriction (Figure 2.8A and data not shown). However, FLC-treated cells with only a single daughter may be already partially resistant to FLC. Therefore, we focused on multimeric cells, as they represented the fraction of cells for which cell separation has failed. In all examined multimeras (n = 7), AMR constricted between the mother cell and the daughters (Figure 2.8A; Figure 2.7). Interestingly, the dynamics of the constriction varied significantly as compared to control cells. Specifically, while the time of constriction for the DMSO-treated control was estimated to take between 10 to 25 minutes (n = 9), assessed times of constriction in 5 multimeras that resulted from FLC treatment were 10, 20, 30, 35, and 50 minutes. Our results indicate that FLC does not inhibit AMR assembly, but FLC does cause a delay in AMR constriction.

Septin proteins in *C. neoformans* are essential for cytokinesis under stress conditions (17). Therefore, incomplete cytokinesis upon FLC treatment may stem from the inability of cells to assemble a robust septin complex at the site of cytokinesis. However, we did not observe marked defects in septin localization or organization upon FLC treatment (Figure 2.8B). The septins, Cdc3 and Cdc12, are essential for the assembly of the septin complex at the mother-bud neck, yet *cdc3*Δor *cdc12*Δ mutant strains exhibit largely normal cytokinesis in non-stress conditions (24°C), albeit having partially abnormal primary septa (17). Strikingly, *cdc3*Δand *cdc12*Δ strains exhibited hypersensitivity to FLC with a clear defect in cytokinesis at 24°C (Figure 2.8C, D). Synthetic interaction between septin deletions and FLC further suggests that FLC-mediated inhibition of cytokinesis is not directly related to septin function.

Calcineurin high temperature suppressor 1, Cts1, has been implicated in the cell separation pathway in *C. neoformans*. Cts1 is thought to contribute to the primary septum formation (18). GFP-Cts1 localizes to the mother-bud neck and follows the constriction of the AMR during cytokinesis (19). FLC treatment did not affect localization and dynamics of GFP-Cts1, a finding consistent with the septum being formed during FLC treatment (Figure 2.9A and B).

To assess septum formation, we stained FLC-treated cells with calcofluor white to visualize chitin deposition. We noted that in the control cells, the calcofluor fluorescence was visible at the mother bud neck in small, medium, and large budded cells (data not shown). This implies that chitin may be deposited at the bud

neck prior to mitosis in addition to the primary septum formation, similar to *S. cerevisiae* (20). Importantly, we did not find a significant diminishment of the calcofluor fluorescence at the mother-bud neck of cells treated with FLC including the multimeric cells, indicating that FLC does not prevent septum formation (Figure 2.9C). In support of this conclusion, we observed a dark line at the bud neck between the mother and the daughters in the trimeric cells when imaged in the bright field (Figure 2.8; Figure 2.7). In addition, cytoplasm between the mother and the daughter cells was discontinuous in multimeric cells when the dark line became visible at the mother-bud neck (Figure 2.7B, C)

Taken together, our data suggest that FLC inhibits final separation of cells undergoing cytokinesis, but this defect is not resulting from a lack of AMR constriction or septum formation or lack of Cts1 localization and constriction. Instead, the defect is in the failure of the final degradation of the primary septum.

Chromosomal loss is not the predominant mechanism responsible for generating FLC-resistant cells.

Harrison et al. have proposed that a diploid *C. albicans* becomes aneuploid under FLC treatment through generation of an intermediate tetraploid stage (12). Extrapolating from this scenario, we could envision a haploid *C. neoformans* becoming a diploid in the presence of FLC, which subsequently becomes an aneuploid through concerted loss of chromosomes. Hypothetically, a diploid strain of *C. neoformans* would possess a much higher potential to become aneuploid by

FLC triggered chromosomal loss and, therefore, the likelihood of a diploid to become resistant to FLC should be higher. To test this hypothesis, we artificially generated a diploid *C. neoformans* strain and compared it to two parent haploid strains with respect to early response to FLC and the ability to form FLC-resistant colonies. When grown on 32 μg/ml of FLC media, the diploid produced visible colonies after 72 hours whereas the two haploid parent strains produced no visible colonies at that time (data not shown). However, diploid cells grown in the presence of FLC reached an octoploid (8n) state after 14 hours in an analogous way to the DNA increase observed in the haploid strain (Figure 2.10). Morphological examination of the diploid cells grown in FLC showed multibudded cells, indicative of cytokinesis failure, similar to that observed in haploid cells (data not shown). These findings imply that diploid *C. neoformans* cells, while potentially less sensitive to FLC as compared to haploids, in an analogous way to the haploid cells, fail to undergo cytokinesis and double the ploidy level upon FLC treatment. This suggests that chromosomal loss is not sufficient and not the predominant mechanism of aneuploidy formation in response to FLC. Furthermore, these data indicate that a diploid state is not sufficient to render cells resistant to a concentration of FLC that is inhibitory to the isogenic haploid.

FLC treatment leads to unequal distribution of chromatin between the mother and the daughter cells.

We utilized a strain of *C. neoformans* that expressed histone H4 tagged with mCherry as a proxy to estimate distribution of chromatin during mitosis in cells treated with FLC. The strain expressing H4-mCherry exhibited similar sensitivity to FLC as the wild type strain, indicating that introducing the mCherry to the C terminus of the histone H4 did not change the way FLC affected cell division (data not shown). In DMSO-treated control cells, the chromatin was equally distributed between the daughter and the mother cell, as the ratio of the H4-mCherry fluorescence between the daughter and mother cells was nearly 1 ($\bar{x}$ = 1.13, SD: 028, n = 19). In contrast, some multimeric cells that were treated with FLC exhibited markedly unequal distributions of the H4-mCherry signal between the mother and the daughter cells (Figure 2.11). Interestingly, there was no consistency as to whether more H4-mCherry signal was in the mother or in any of the daughters; although, the predominant fraction of multimeras contained relatively more chromatin in the mother than in either of the daughters (Figure 2.11). These data suggest that FLC treatment results in aberrant chromosomal distribution leading to cells with relatively higher chromatin content.

FLC-treated cells that are enlarged and/or fail to separate are less sensitive to FLC

Our data suggest that FLC has a pleiotropic effect on cell growth, including inhibition of budding, cell separation, and mis-segregation of chromatin during mitosis. Collectively, these effects result in cells that are increased in size, have

higher DNA content, and are multibudded. Indeed, based on fluorescence microscopy profile of the cells treated with 32 μg/ml FLC for 14 hours, we found a significant correlation between the cell size and complexity and the DNA content (Figure 2.1 and data not shown). We hypothesized that enlarged cells are less sensitive to FLC. To test this, cells that were treated with 32 μg/ml FLC for 14 hours were fractionated using FACS based on the size and complexity of their morphology. Two fractions were collected, one with relatively small cells that were either unbudded or contained a single bud, and a second fraction that contained unbudded or budded cells that were enlarged or multimeric (Figure 2.12). A third (control) sample consisted of cells that were not fractionated, yet were processed the same way including passing through the FACS sorter. All three samples were plated on media containing 32 μg/ml of FLC and incubated at 24°C. Significantly, the fraction of cells containing multimeras exhibited relatively higher resistance to FLC as compared to the “small” cell fraction (Figure 2.12). Cells that were not subject to fractionation exhibited an intermediate ability to grow in the presence of FLC as compared to the other two samples. These findings indicate that cells that are enlarged and/or have changed morphologically upon treatment with FLC, possess a higher potential to grow in the presence of the drug.

These findings (Figure 2.12) coupled with our initial FACS data showing the morphology of cells with increased DNA content (Figure 2.4) highlight the role of multimeric cells as a contributing factor to the increase in ploidy and subsequent survival in the presence of FLC. Additionally, it also emphasizes enlarged,

unbudded cells as another potential factor contributing to survival. In order to better understand the role of enlarged morphology, cells were streaked in the middle of a plate containing 24 μg/ml FLC medium. After 9 hours, before the emergence of multimeras, 20 enlarged unbudded or budded cells were picked using a micromanipulator and placed on the same plate in known spots. 20 normal sized cells were also placed as controls. Six out of 20 of the enlarged cells progressed into colonies, while 0 out of 20 of the normal sized controls grew. These data are not surprising; the cells that showed an increase in survival were able to grow or enlarge during the initial insult of FLC, whereas the non-survivors were unable to handle the stress imposed by FLC. The microcolonies formed by the six enlarged cells at 24 hours were dissected and the morphology and subsequent mitotic divisions were monitored for the succeeding 24 hours. Cells that were already multimeras by 24 h exhibited the greatest chance for survival in the presence of FLC (formed microcolonies); ~89% of multimeras underwent further growth (Figure 2.13). In contrast, ~50% of budded cells and ~30% of unbudded cells formed microcolonies. The heterogeneity of the population to FLC is intriguing. It will be of interest to further explore the basis and the importance of the heterogeneity of the initial response to FLC.

DISCUSSION

Our data suggest that FLC results in an increase in the DNA content in a significant fraction of cells, but the effect is delayed. What is most likely to account

for the delay is the rate at which ergosterol is depleted in individual cells, however other reasons cannot be excluded. For instance, a relatively slow accumulation of a toxic byproduct of the FLC-mediated inhibition of ergosterol synthesis may also be responsible for the delay (11). Significant inhibition of budding when cells are treated with 32 μg/mL of FLC occurs at 6 hours, a time when no significant increase of DNA content is yet observed in a heterogeneous population. However, it only required ~3 hours for a significant population of cells corresponding to 3n to appear when the initial population was composed of unbudded cells. Thus, an initial increase in DNA content is likely to occur due to a lack of cell separation coupled with subsequent replication in the mother cell.

FLC inhibits cytokinesis in *C. albicans*, but the actual mechanism of cytokinesis failure has not been explored (12). While we also find that FLC causes inhibition of cell separation in *C. neoformans,* two main differences as compared to *C. albicans* are apparent. First, the *C. albicans* multimeric cells resulting from FLC treatment consist of mother cell and the daughters that remain connected via common cytoplasm (12). The authors speculate that the cytoplasmic signaling connection between individual cells within the multimera is important for the formation of the tetraploid intermediate (12). In contrast, we observe that multimeric *C. neoformans* cells are formed based on a failure of the final cell separation despite septa being formed. Therefore, the mother cell and the first daughter do not share a common cytoplasm when the second daughter is formed, which is consistent with images of multimeras with the discontinuous fluorescent

cytoplasmic signal between the attached cells (Figure 2.7). A second clear distinction is that the multimeric cells in *C. albicans* are chains of cells resulting from growth of the second daughter cell (a granddaughter) out of the first daughter cell, while in *C. neoformans*, both daughter cells grow consecutively from a single mother. We speculate that retention of the cytoplasmic connection in *C. albicans* and a lack thereof in *C. neoformans* account for this difference. Specifically, in *C. albicans*, cell cycle signaling that normally triggers the next round of budding in the mother is acting within the first daughter, which results in a granddaughter. In *C. neoformans*, the mother cell of the multimera is isolated from the unattached daughter and the signaling triggers second bud formation within the mother. Indeed, we observe multimeras with two daughters attached to the mother and a single granddaughter, indicating a later time at which one of the daughters is "ready" to initiate budding (Figure 2.4, purple arrow). It is interesting that in *C. neoformans* FLC treatment does not prevent septation in contrast to *C. albicans*. This may indicate that either the physical process of AMR constriction and/or septum formation differ in these species, or alternatively, the differences in signaling that triggers these events account for various effects of FLC in these species. Given that both species produce aneuploid progeny presumably based on multimeric cells, the question remains whether aneuploidy formation proceeds through distinct mechanisms in these unrelated yeasts. Alternatively, at least in *C. neoformans*, these multimeric cells may not constitute a critical prerequisite to truly resistant aneuploids, but rather a byproduct of FLC inhibition that nonetheless

increases the survival of cells in the presence of the drug. Answering these questions will require further investigation.

Fernandez C. et al. has demonstrated that mammalian equivalent of ergosterol, cholesterol, is required for cytokinesis in human HL-60 cell line and that sustained cholesterol starvation leads to the formation of polyploid, multinucleated cells with mitotic aberrations (21). The authors hypothesize that cell cycle perturbations and polyploidization observed in cholesterol-deficient cells are due to reduced Cdk1 activity. Furthermore, affected cells were able to partially traverse mitosis and to re-replicate DNA, which led to polyploidy (21). Thus, it is likely that the cell separation defect that we observed in *C. neoformans* is due to depletion of ergosterol. Our data suggest that FLC prevents cell separation in *C. neoformans* most likely via inhibition of the final degradation of the primary septum, as the primary septum was formed and the two other main events of cytokinesis, AMR constriction and septin assembly were not largely affected. Surprisingly, none of the endochitinases encoded by the *C. neoformans* genome are necessary for the final cell separation (22, 23). *C. neoformans* may not have an enzyme that specifically hydrolyzes chitosan, a constituent of the primary septum. Therefore, daughter cell separation may proceed based on the increased flexibility and solubility of the chitosan (22). It is plausible that FLC disrupts the relative content of chitosan leading to defects in cell separation. Alternatively, a delay in AMR constriction or other indirect effects of FLC may cause an interruption of a

conserved RAM (regulation of Ace2 and morphogenesis) pathway that signals final cell separation (24).

Several abnormal morphologies resulting from FLC treatment reflect its diverse effects on cell physiology. We propose that the variability in morphological defects result from the heterogeneity that exists in the population of cells that is initially exposed to the drug. In its simplest form, the heterogeneity may reflect cells that are at various stages of the cell cycle when they are initially exposed to the drug (Figure 2.14A). FLC leads to a gradual depletion of ergosterol and accumulation of toxic metabolic products. Consequently, cells will be affected in various ways depending on when ergosterol levels reach the critical minimum with respect to the stage of the cell cycle (Figure 2.14A). Interestingly, populations of cells exposed to FLC exhibit variability in the initial response to the drug (Figure 2.13). It will be of interest to investigate the basis for this heterogeneous response.

Cells that fail to separate, yet undergo DNA replication and subsequent initiation of budding and then proceed through additional rounds of mitosis (multimeric cells), are most likely a major group that accounts for the increased DNA content as detected via PI staining and flow cytometry (Figure 2.14B). The fact that the mother cells undergo replication despite the failure in daughter cell separation is consistent with previous findings demonstrating that timing of replication in *C. neoformans* is flexible with respect to timing of the bud initiation (15). Therefore, we speculate that inhibition of cell separation by FLC may be sufficient to result in next round of replication in those mother cells. Consistent

with multimeras contributing to the fraction of cells with increased ploidy as detected by flow cytometry, we find multimeric cells with increased and unequally distributed chromatin as judged by the fluorescence of H4-mCherry. Presently, the mechanism through which FLC leads to unequal distribution of histone H4 is unclear. This defect is likely associated with missegregation of chromosomes, as we also observe aberrant segregation of centromeres between mother and daughter cells (Figure 2.6). In *S. cerevisiae*, increase in ploidy is associated with chromosomal instability (25, 26). Hypothetically, missegregation of chromosomes may be a direct mechanism through which aneuploids are derived. A non-exclusive alternative is that cells with increased ploidy may undergo stepwise chromosomal loss leading to aneuploidy. FLC causes inhibition of budding, which when coupled with subsequent replication would lead to an increase in DNA content. In addition, we observe premature mitosis occurring within mother cells, which is consistent with unbudded cells present in the fraction with increased ploidy. Thus, FLC leads to an increase in DNA content by affecting cellular growth and division via multiple mechanisms. The central question is whether cells with increased DNA content that are formed in the presence of FLC give rise to a population of aneuploids that increases the chance for producing resistant populations. Our study shows that cells with increased size and aberrant morphology grow better in the presence of FLC consistent with this possibility.

While increased ploidy due to FLC treatment may not be sufficient to generate truly resistant aneuploids in the host, cells with increased DNA content

may increase the chance for survival in the presence of the drug and hypothetically lead to more persistent infections. Recent studies showed a *C. neoformans* morphological variant with vastly increased ploidy and size called the titan cell (27). Titan cells are found during infection and are more resistant to stress and FLC. Additionally, they produce populations of more resistant aneuploids (28). FLC is not sufficient to produce titan cells, and the mechanism through which FLC increases DNA content *in vitro* appears different from the ploidy increase seen in titan cells during infection. However, FLC treated mice infected with *C. albicans* show morphologically changed yeast cells that likely stem from an inability to undergo cytokinesis (12). Isolates of *C. neoformans* obtained from clinical samples exhibit significant variation in susceptibility to FLC, and resistant clones with chromosomal disomy have been detected in brains of mice treated with FLC (29, 30). Thus, our *in vitro* data suggest that during infection with *C. neoformans,* treatment with FLC may lead to an increase in DNA content in yeast cells through pleiotropic effects on cell division. Cells with increased DNA content would support microevolution of populations with an augmented potential to survive in the host environment.

As discussed by Cheong and McCormack, several studies demonstrate conflicting results regarding the correlation between the MIC values for FLC *in vitro* and the clinical outcomes (31). The authors demonstrate that 30% of patients with cryptococcosis who have never been exposed to FLC provided evidence of reduced susceptibility to this antifungal (31). Desnos-Ollivier et al. have recovered

genetically related haploid and diploid strains from the same patients and demonstrated through experimental infections and quantitative PCR that ploidy changes can result from endoreplication and that switching between haploid and diploid states can occur, consistent with microevolution within the host (32). Therefore, it is plausible that stress conditions in the host stimulate an increase in DNA content through inhibition of cellular division similar to the effects of FLC *in vitro* described herein. Several genes have been described in *S. cerevisiae* that are essential for viability of polyploid cells (26). It would be of interest to test if homologues of these genes in *C. neoformans* are essential for viability of FLC-derived polyploids and formation of FLC-resistant populations.

MATERIALS AND METHODS

Growth Conditions

Strains used in this study are listed in Table 2.1. Unless otherwise stated, cells were grown in liquid YPD overnight at 24°C and refreshed next day to optical density at 600 nm (OD_{600}) of 0.2 before treatment. For FLC-treated cultures, 50 mg/ml FLC stock solution (Sigma, St. Louis, MO, or Alfa Aesar, Haverhill, MA) was prepared in DMSO. Spot assays were performed using a 10-fold serial dilution starting with 10,000 cells per 5 µL and ending with 10 cells per 5 µL. Cells were spotted on semi-solid YPD media or YPD media containing indicated concentration of FLC, incubated at room temperature, and imaged after three days.

Strain constructions

All transformations were performed using biolistics transformation (33). The diploid, DSA3, was generated by mating a strain expressing nucleoporin Nup107 tagged with GFP, LK315, (constructed as described earlier based on plasmid pCN19, (17)), with a strain expressing an endogenous histone H4 tagged with mCherry, CNV121 (34). The two strains were mixed on the mating MS agar medium and after 2 days cells were plated on double selection (NAT, HYG) media from which diploids were recovered. Diploid generation was confirmed using fluorescence microscopy and flow cytometry. Strain LC4 was generated by transforming LK315 with the plasmid LKB77 (19). Strain LK126, expressing GFP-tagged beta tubulin (CNAG_01840) was generated by transforming strain H99 with the plasmid LKB37 (a pCN19-based plasmid expressing GFP-tagged beta tubulin from a constitutive histone H3 promoter). Strain LK65 (*cdc3*Δ) is identical to previously published LK64 (17).

Flow cytometry

Cells were harvested before exceeding OD_{600} ~0.8, spun down, washed with sterile water, suspended in 100 µl distilled water, and fixed with 70% EtOH (in a drop wise manner while vortexing). Cells were then incubated at 24°C for 1 hour and transferred to 4°C overnight. Next day, cells were washed with RNAse A buffer (0.2M Tris pH 7.5, 20 mM EDTA), suspended in 100 µl of RNAse A buffer with 1 µl RNAse A (from 10 mg/ml stock), and incubated for 4 hours at 37°C. Cells were

then washed twice with 1 ml phosphate-buffered saline (PBS), suspended in 900 µl of PBS, and incubated at 4°C overnight. Cells were stained with propidium iodide (PI) by adding 100 µl of 0.005 µg/ml PI stock and incubated in the dark for 30 minutes. Immediately before analysis, cells were sonicated at 20% amplitude for 5 sec. to avoid clumping.

For ploidy analysis, the PI fluorescence was collected from 10,000 cells using FL3 (488 nm laser) on BD Accuri C6 flow cytometer. To assess the morphology of cells according to ploidy levels, cell sorting was performed using a Biorad S3E cell sorter. At least 500,000 cells were sorted into each fraction based on PI fluorescence and morphology of cells was assessed using the following categories: unbudded, normal budded, abnormal (wide neck) budded, and multimera.

To assess FLC susceptibility of cell populations according to cell sizes, cell sorting based on size and complexity was performed using a Biorad S3E cell sorter. Cells from each fraction (R1, R2, and DMSO control) were scored based on morphology using the following categories: unbudded, budded, and multimera. Cells from each fraction were then plated on semi-solid YPD media containing 32 µg/ml FLC and grown at 24°C for 6 days. After 6 days, plates were imaged and areas of random 100 colonies were measured using ImageJ (35).

For analysis of re-replication, unbudded cells were selected via modified centrifugation method based on a procedure described by Ayscough et al. (36). Cells were treated for 3 h with 32 µg/ml FLC or equivalent DMSO then pelleted

and suspended in 50% sorbitol (1M) and 50% YPD. Cells were spun at 2000 rpm for 5 min. The supernatant was transferred to a new tube and spun at 1500 rpm for 5 min. Again, the supernatant was transferred to a new tube and spun at 4000 rpm for 10 min. The morphology of the pelleted cells was then assessed under the microscope to ensure the majority of the population was unbudded. Cells were released into DMSO or 32 µg/ml FLC. At various time points the morphology was checked to ensure that no multimera cells were present and the cells were fixed and stained with the PI for ploidy assessment using flow cytometry.

Microscopy

Bright field and fluorescence images were captured using the 100x objective with a Zeiss Axiovert 200 inverted microscope (Carl Zeiss, Thornwood, NY) interfaced with AxioVision Rel 4.8 software (Carl Zeiss, Thornwood, NY). Micromanipulation was performed using SporePlay dissection microscope (Singer Instruments, UK). Unless otherwise stated, images were processed in Adobe Photoshop (Adobe Systems Incorporated, San Jose, CA). Zen Blue (Carl Zeiss, Thornwood, NY) was used to measure the diameter of the bud of mitotic spindle containing cells. ImageJ (35) was used to measure H4-mCherry nuclear fluorescence. This was done by flattening the Z-sections to project the maximum intensities from each section and outlining the fluorescence of the nucleus. To account for DNA compaction, the pixel value of the outlined area was multiplied by the area. To establish a criterion based on which to group cells according to relative H4-mCherry fluorescence, we

first measured variation of the fluorescent signal in control cells (not exposed to FLC). Specifically, we found that the ratio of the fluorescent signal between the daughter and mother cell ranges between 0.7 and 1.6. Based on this variation, we decided a ratio of less than 0.7 and more than 1.6 to define less and more chromatin in the daughter as compared to the mother cell, respectively.

For time-lapse analysis of components of cytokinesis, cells were pre-treated with 24 μg/mL FLC in YPD or yeast-nitrogen-base (YNB) medium with 2% glucose at 24°C for ~ 6 h. Subsequently, cells were transferred to YNB+2% glucose medium containing 24 μg/mL FLC (300 μl of 1.00 x 10^6 cells/mL cell suspension) and placed in a chamber of a borosilicate 8-chamber-slide (Bio-Tek, Winooski, VT). At each time-point, 5 Z-sections spaced 1.20 μm apart were taken.

To visualize chitin, calcofluor white staining was performed. H99 cells were grown in YPD and treated with either 24 μg/ml or 32 μg/ml FLC for 9 hours. Cells were then harvested, washed with YNB, and fixed with 3.7% formaldehyde for 1 hour while culture was aerated. Cells were washed with PBS and permeabilized with 1% Trition-X (Sigma-Aldrich, St. Louis, MO) for 10 minutes. Finally, cells were incubated for 30 minutes after the addition of 1 μg/mL of calcofluor white (Sigma-Aldrich, St. Louis, MO), washed, resuspended in YNB and visualized with the Zeiss Axiovert 200 inverted microscope.

For evaluation of budding, cell surface was biotinylated using EZ-Link Sulfo-NHS-LC-Biotin (ThermoScientific) and stained with ExtraAvidin (TM) tetramethylrhodamine (TRITC) (Sigma, St. Louis, MO). Cells were washed three

times with PBS and suspended to a density of 5x10^7 cells/ml. Subsequently, 4 mg/ml of Sulfo-NHS-LC-Biotin reagent was added. Cells were incubated at 24°C for 30 minutes. Cells were washed three times with YPD. Biotinylated cells were released into 2 ml of YPD with DMSO or 32 μg/ml FLC and after three hours the cells were washed three times with PBS and incubated in the dark with TRITC (1:200) for 10 min. Cells were washed three times with PBS and imaged. The total number of cells was counted using the bright field. Then the number of new buds (buds that were not stained) were counted using the Rhodamine channel.

To assess the effect of ergosterol exchange rate on budding inhibition, unbudded cells were selected via centrifugation (36). Cells were then incubated with either 100 μm LatB (Enzo Life Sciences, Inc., Farmingdale, NY) or 100 μm LatB + 32 μg/ml FLC for various time points. Cells were then washed and incubated for 3 additional hours in DMSO or 32 μg/ml FLC. The percentage of budded cells was then estimated based on Bright field microscopy.

ACKNOWLEDGEMENTS

We thank Julie Nelson, from Flow Cytometry Core Facility, Center for Tropical and Emerging Global Disease, University of Georgia, and Justin Scott from Clemson University Light Imaging Facility (CLIF), for providing invaluable help with cell sorting using FACS. CLIF is supported, in part, by the Clemson University Division of Research, NIH EPIC COBRE Award #P20GM109094, and NIH SCBiocraft COBRE Award #5P20RR021949-03. The BioRad S3e cell sorter

purchase was also supported in part with funds from the Air Force Office of Scientific Research (Award #FA9550-16-1-027007). The content of this material and any opinions, findings, conclusions, or recommendations expressed in this material is solely the responsibility of the author(s) and does not necessarily represent the official views of the National Institutes of Health or the United States Air Force. We thank Logan Crowe for constructing the LC4 strain. This work was supported by the NIH (grant 1R15 AI119801-01).

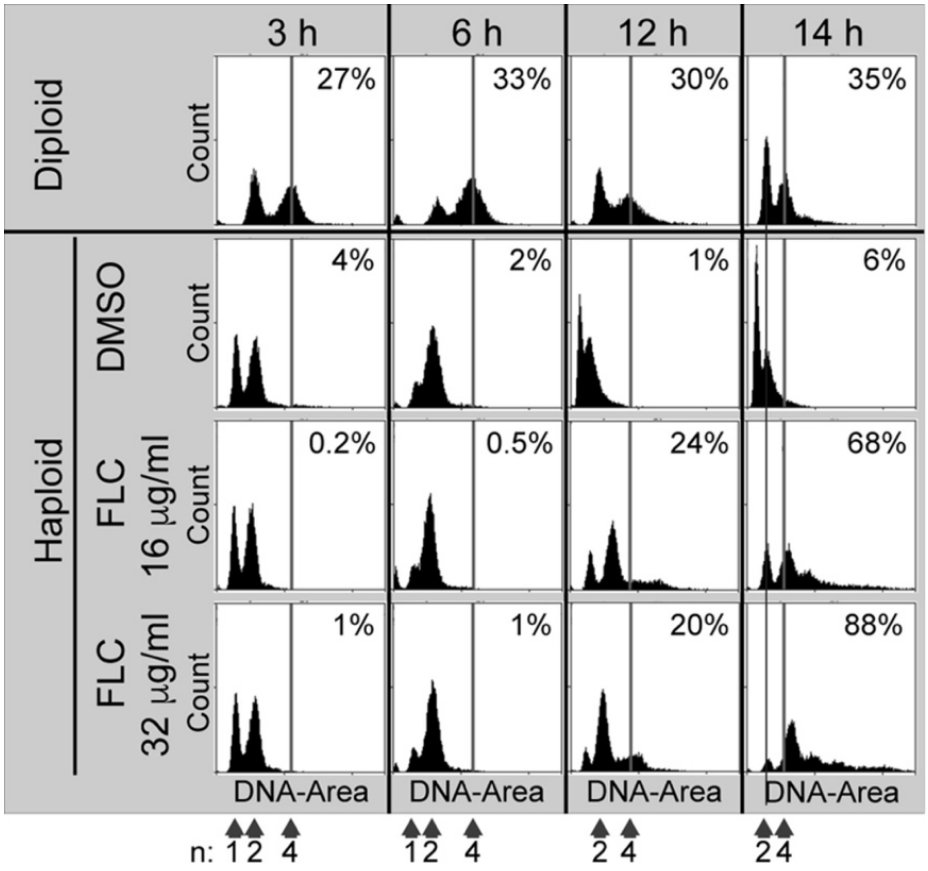

Figure 2.1. FLC treatment results in an increase in ploidy in a significant fraction of cells. *C. neoformans* cells treated with FLC were fixed, stained with propidium iodide (PI) and examined using fluorescence flow cytometry. Treatment of cells with 32 μg/ml FLC at 24°C for 12 and 14 hours resulted in ~20% and 88%, respectively, of the cell population with ploidy levels at or above 4n, as indicated by vertical line.

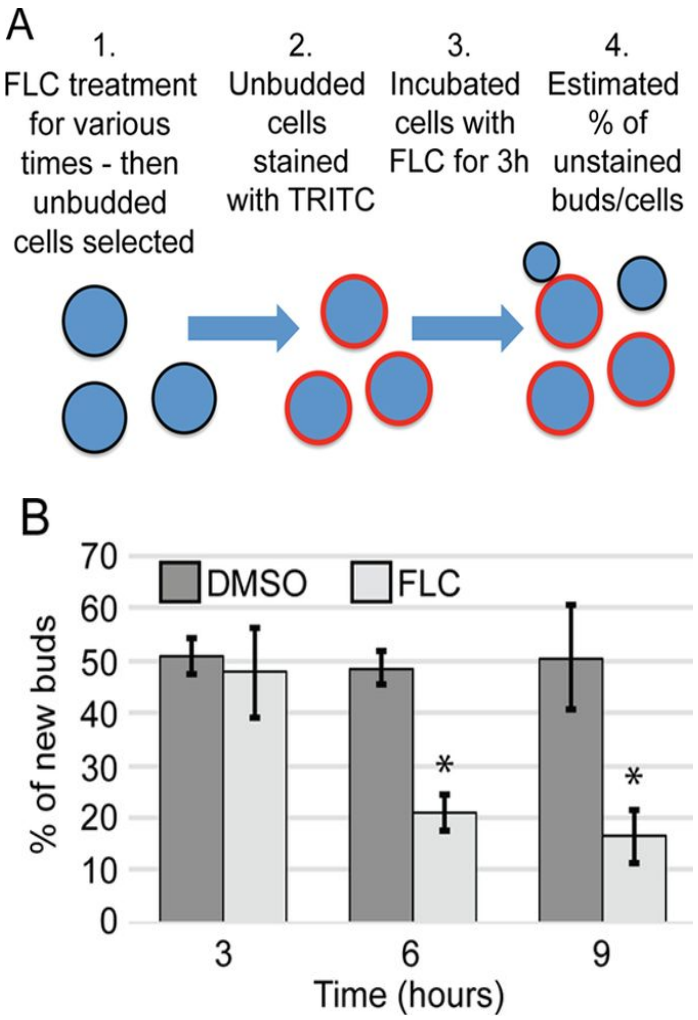

Figure 2.2. Treatment with FLC causes inhibition of budding. A) Schematic showing experimental procedure. After FLC treatment cell surface was stained with tetramethylrhodamine (TRITC). Stained cells were released into DMSO-containing control medium or 32 μg/ml FLC medium and after three hours the cells were imaged. The total number of cells was counted using the bright field channel and the number of new buds (buds that were not stained) were counted using the Rhodamine channel. B) Analysis of new buds showed that after 6 and 9 hours of FLC treatment budding was significantly inhibited ($p = 0.01$).

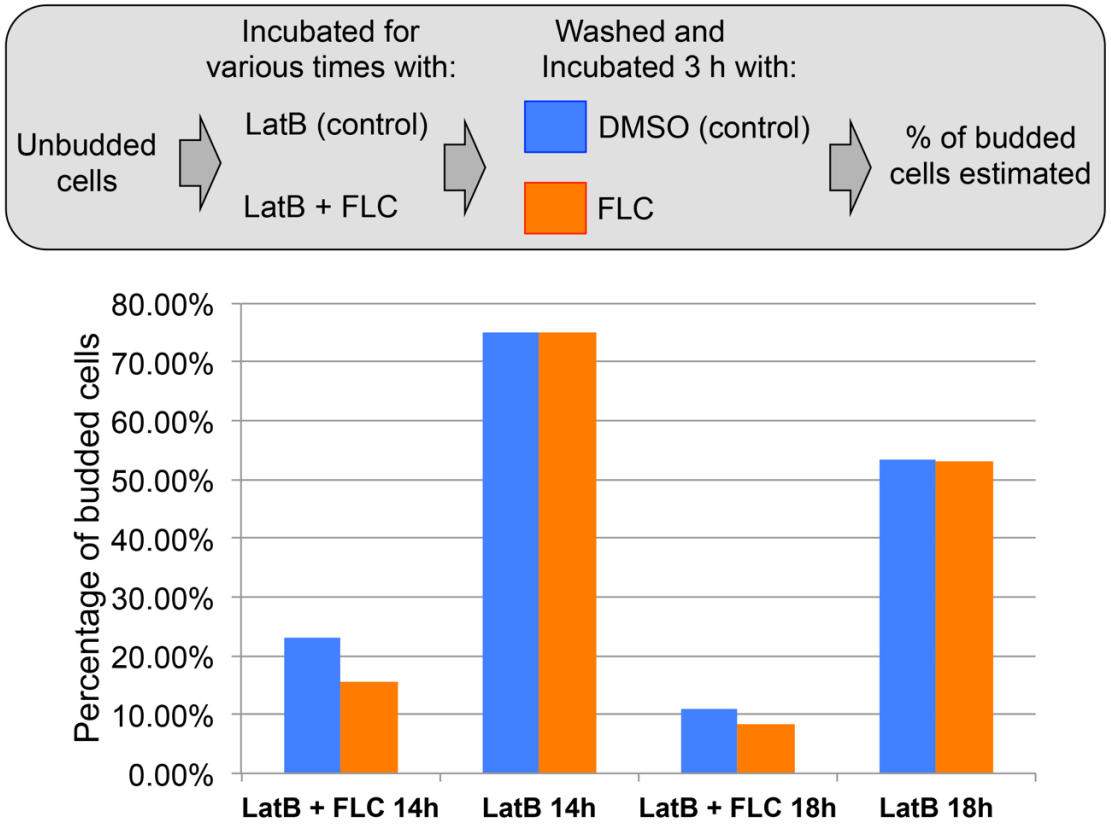

Figure 2.3. Pretreatment of cells with FLC and actin inhibitor Latrunculin B leads to a delayed inhibition of budding by FLC. Schematic of methodology explains the experimental procedure. Unbudded cells were selected and then treated with either LatB or LatB+FLC. Cells were then washed and released into DMSO or 32 µg/ml FLC and budding was assessed. Treatment with LatB was used to assess the effect of the rate of ergosterol exchange on budding inhibition. Inhibition of budding was delayed during LatB + FLC treatment; unbudded cells that were treated with LatB + FLC took 14 hours for budding to be significantly inhibited.

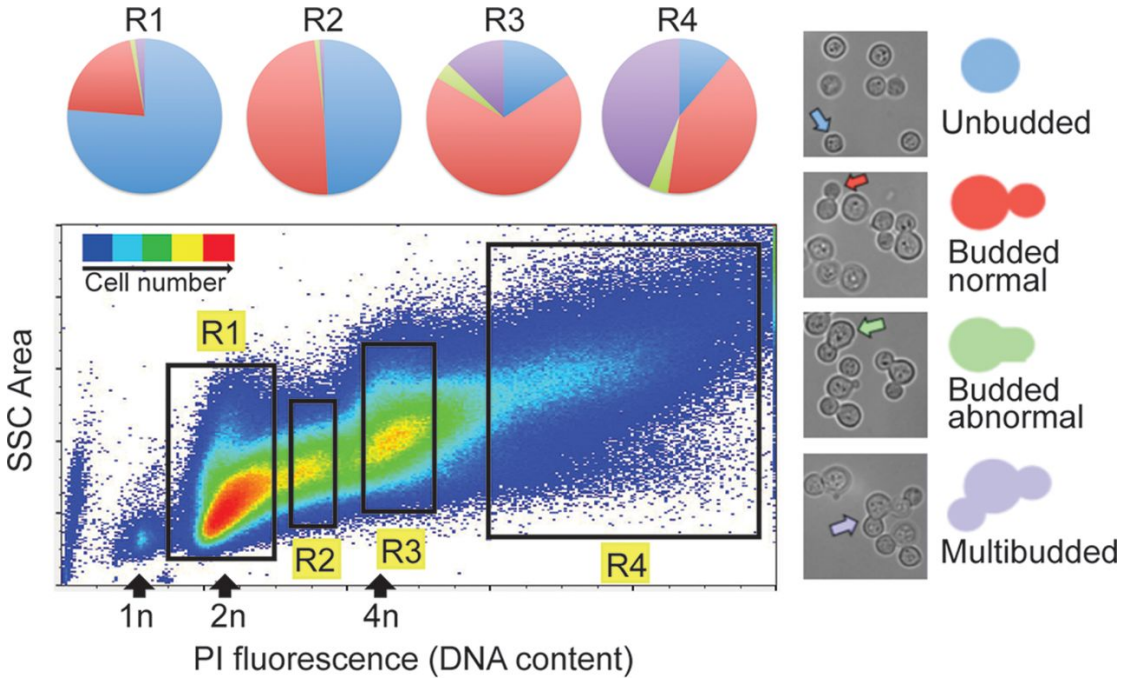

Figure 2.4. FLC treatment leads to a defect in cell separation. Cells were treated with 32 µg/ml FLC for 10 hours, fixed and the DNA was stained with PI. Subsequently, cells were fractionated using a fluorescence assisted cell sorting (FACS) instrument. Fractions of cells with increasing ploidy were collected and morphology scored under the microscope. Fractions of cells with highest ploidy level were enriched in multimeric cells. Multimeric cells (purple) were either trimeras, with two daughter cells formed out of the mother cell, or contained an additional daughter (a granddaughter) grown out of one of the daughters (purple arrow).

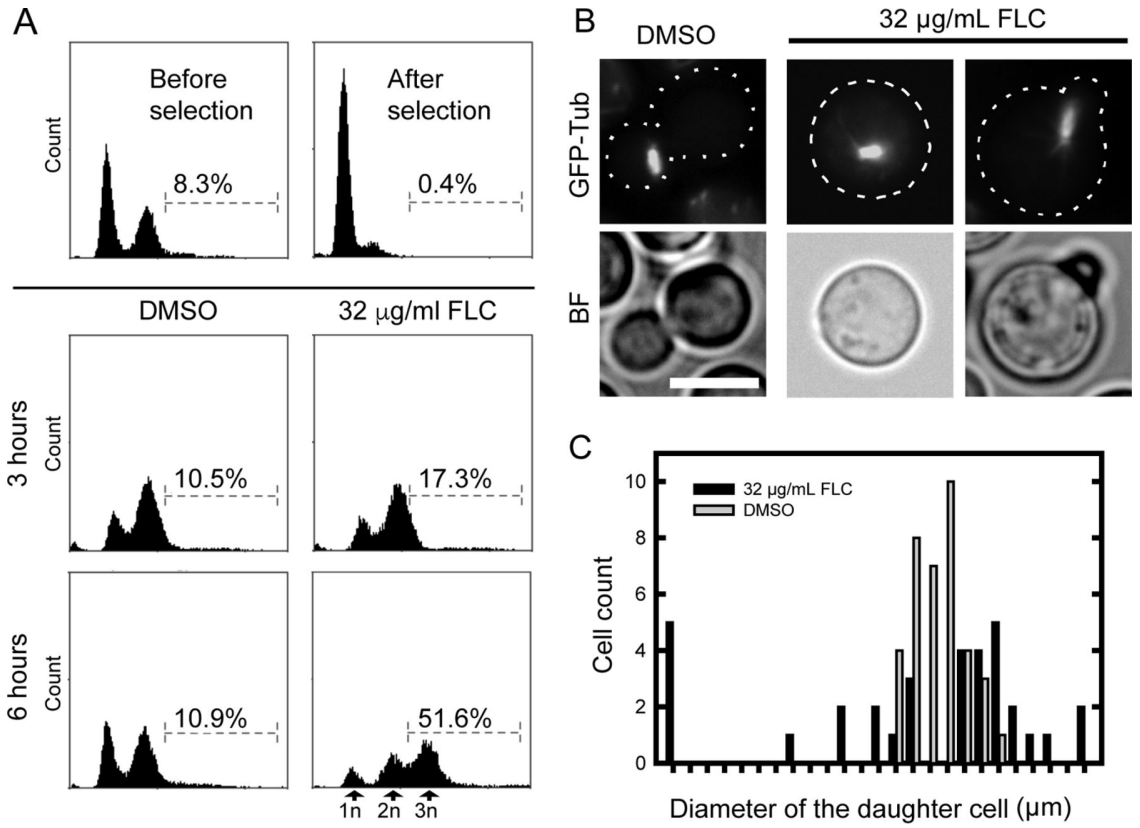

Figure 2.5. A delay or complete block in cell separation during FLC treatment may lead to an increase in DNA content in unseparated cells. A) A population of pre-selected unbudded cells was incubated with 32 μg/ml FLC for 3 or 6 hours (times when no multimeric cells were formed) and the DNA content based on the PI staining was assessed using flow cytometry. After 6 hours of FLC treatment ~50% of cells indicated DNA content above 2n with a predominant population (visible as a peak) that corresponded to cells with 3n DNA content. B) FLC treatment results in aberrant dynamics of the mitotic spindle. Localization of mitotic spindle in cells treated with 32 μg/ml FLC for 22 hours was analyzed based on a strain that expressed GFP-tagged beta tubulin (LK126). In control sample (DMSO), spindle was detected exclusively within daughter cells. In contrast, FLC-treated

cells that had detectable spindle were either unbudded or contained extremely small buds (C). The size of the daughter cell when spindle was visible was relatively uniform for the control treatment (DMSO), while the FLC-treated cells exhibited a broader range of sizes of daughter cells when spindle was visible (C). Bar represents 5 microns.

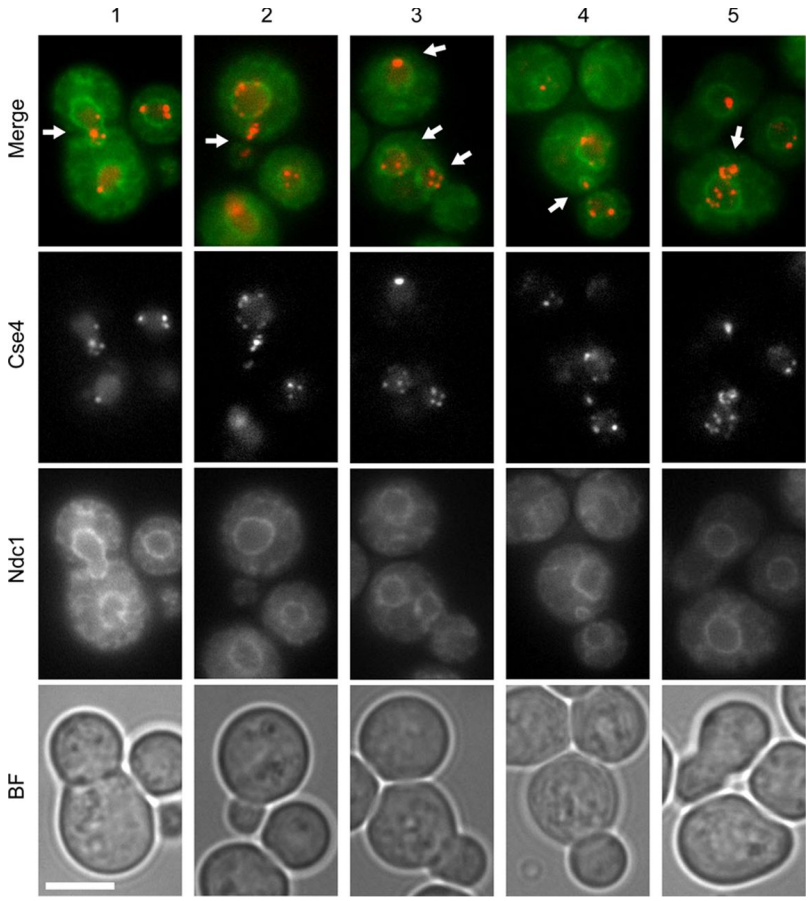

Figure 2.6. Analysis of centromere dynamics in FLC treated cells. A strain that expressed fluorescently-tagged centromeric histone variant, mCherry-Cse4, and a component of the nuclear envelope, GFP-Ndc1 (CNV111), was subject to treatment with 32 μg/ml FLC for 13 and 15 hours prior to imaging. Panels 1-5 depict representative types of aberrations in Cse4 dynamics, including centromeres positioned at the mother bud neck (panels 1 and 4, arrows), clustered centromeres in unbudded cells or cells with small daughters (panels 2 and 3), two nuclei present in one mother cell (panel 3), and centromeres that appear outside of the nuclear area (panels 2 and 5). Bar represents 5 microns.

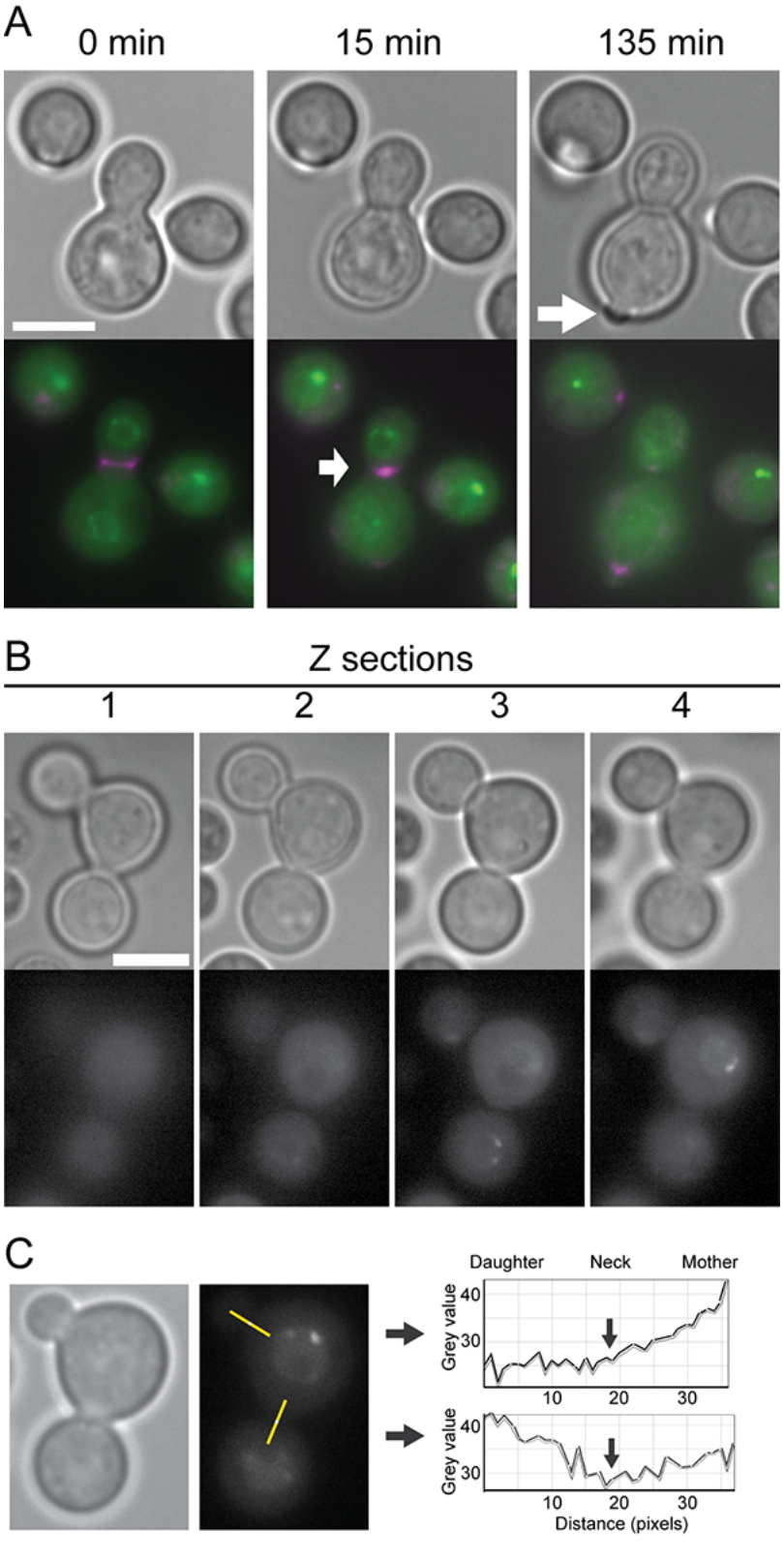
A
0 min
15 min
135 min
B
Z sections
1
2
3
4
C
Daughter
Neck
Mother
Grey value
40
30
10
20
30
Grey value
40
30
10
20
30
Distance (pixels)

Figure 2.7. FLC does not significantly inhibit AMR assembly and constriction. A) Time-lapse microscopy was performed with strain LC4 expressing GFP-Nup107 (to visualize the nuclear envelope, shown in green) and mCherry-Myo1 (to visualize the AMR, shown in magenta) after 6 hours of pre-incubation with FLC. In the example shown, by 15 min of subsequent FLC treatment the AMR constricts (white arrowhead), and by 135 min a new bud starts to emerge (white arrow) with no detachment of the first daughter cell. B) A multimeric cell treated as in (A) was imaged and individual focal planes (Z-sections) are shown to illustrate a lack of cytoplasmic connection (based on the cytoplasmic signal of the GFP-Nup107). In this cell, both of the daughter cells possess the septa separating them from the mother cell. C) Cell from (B) was imaged at an earlier time point when the second daughter has not developed a septum and therefore its cytoplasm is not yet separated from the mother. To assess separation of the cytoplasmic signal pixel brightness along a line perpendicular to the mother daughter axis was plotted for both daughters as shown. While the second daughter (top graph) shows a steady increase of fluorescence along the line drawn, the first daughter shows diminishment of the fluorescence in the area corresponding to the mother-bud neck suggesting discontinuous cytoplasm between the two cells. Bars represent 5 microns

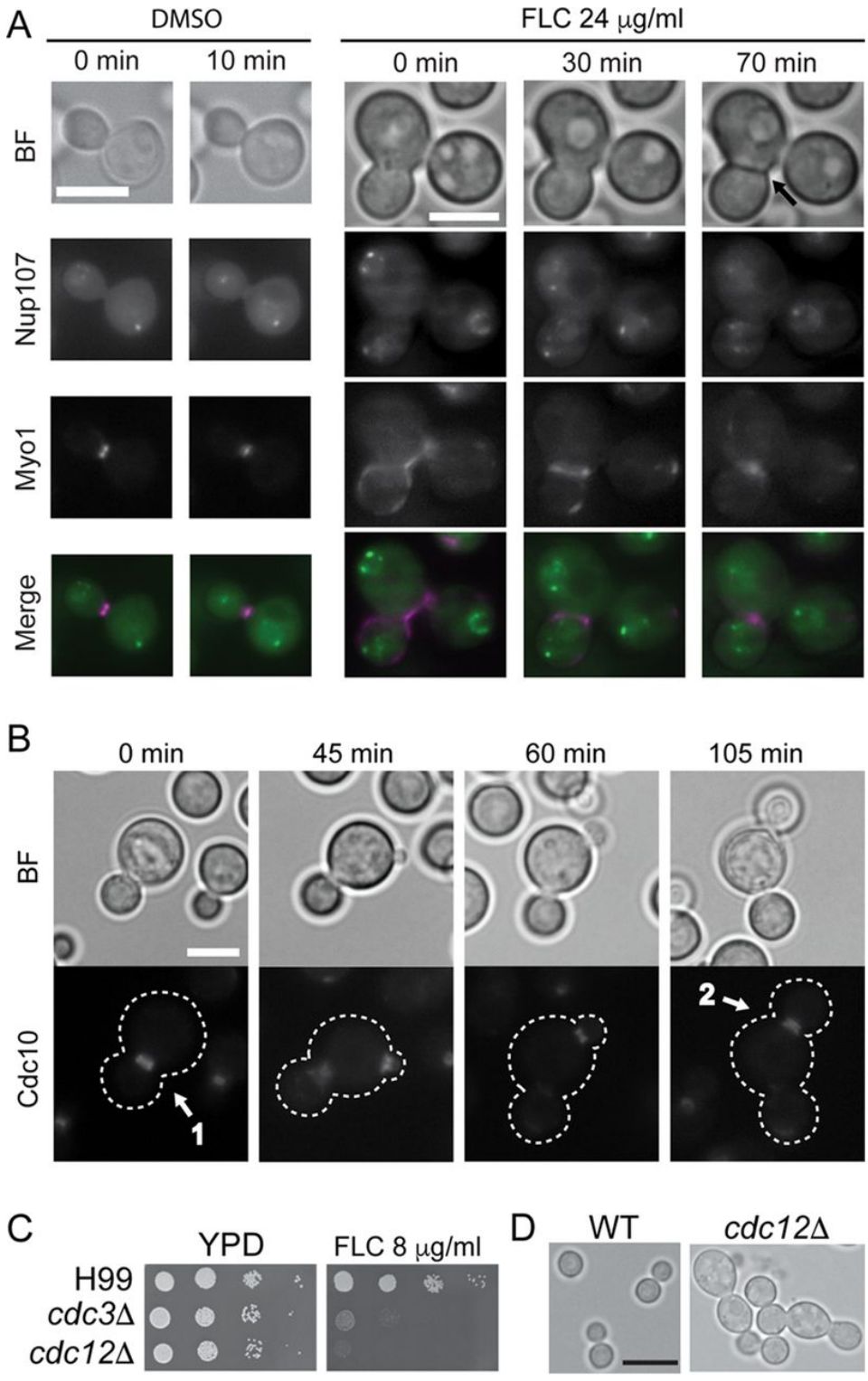
A
DMSO
FLC 24 μg/ml
0 min
10 min
0 min
30 min
70 min
BF
Nup107
Myo1
Merge
B
0 min
45 min
60 min
105 min
BF
Cdc10
1
2
C
YPD
FLC 8 μg/ml
H99
cdc3Δ
cdc12Δ
D
WT
cdc12Δ

Figure 2.8. FLC does not significantly inhibit AMR assembly and constriction and septin localization. A) To monitor constriction of the AMR, time-lapse microscopy was performed using a strain that expressed a component of the AMR, myosin heavy chain, Myo1, tagged with mCherry and a nucleoporin Nup107, tagged with GFP (to monitor the stage of mitosis, LC4). Cells from the control treatment (DMSO) have constricted the AMR. FLC-treated cells that formed multimeras also constricted the AMR, although the dynamics of the constriction varied significantly as compared to non-treated control cells. The arrow at 70 min indicates a dark line that likely corresponds to septum formed after the AMR has constricted. Bars represent 5 microns. B) Cells expressing septin Cdc10-mCherry (LK62) were pre-treated with 24 μg/ml FLC for 6 hours and the localization of Cdc10-mcherry was analyzed by time-lapse microscopy while the cells were continually exposed to FLC (time indicates progression of the time-lapse). Cdc10-mCherry formed a collar and a double ring between the mother and the first daughter (arrow 1) and when the second daughter was formed (arrow 2). C) Cells deleted for Cdc3 or Cdc12-encoding genes (LK65, LK162) exhibited hypersensitivity to FLC with a clear defect in cytokinesis at 24°C (D). Bars represent 5 microns in A and B and 10 microns in D.

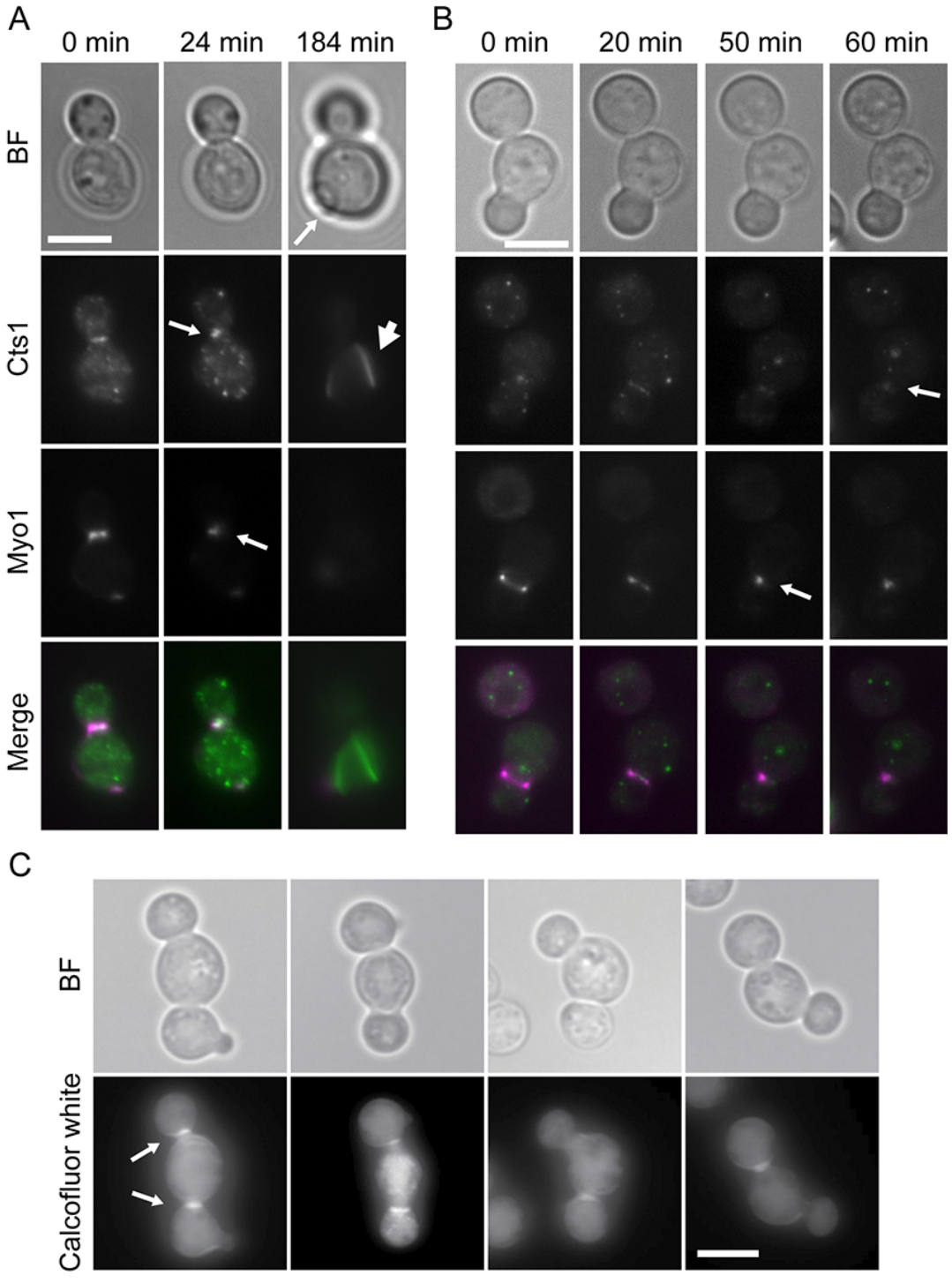
A
0 min
24 min
184 min
BF
Cts1
Myo1
Merge
B
0 min
20 min
50 min
60 min
C
BF
Calcofluor white

Figure 2.9. Analysis of the dynamics of Cts1 and deposition of the chitin in FLC treated cells. (A) and (B) depict cells expressing GFP-Cts1 and mCherry-Myo1 (LK274) treated with 24 μg/mL FLC and imaged using time-lapse microscopy. A) Constriction of the actomyosin and Cts1 rings occur within 24 minutes in the bud neck between the first daughter and mother cells (arrows). The first daughter cell fails to separate while a new bud emerges after 184 minutes (BF panel, arrow). Microtubule resembling structures of cts1 were seen (arrowhead). B) Formation of the cts1 ring follows that of the actomyosin ring. Constriction of the AMR takes place at 50 minutes while the constriction of the Cts1 ring follows 10 minutes later. C) Cells treated with FLC for 9 hours were stained with calcofluor white and show the presence of chitin at the mother-bud neck of multimeric cells. Bars represent 5 microns.

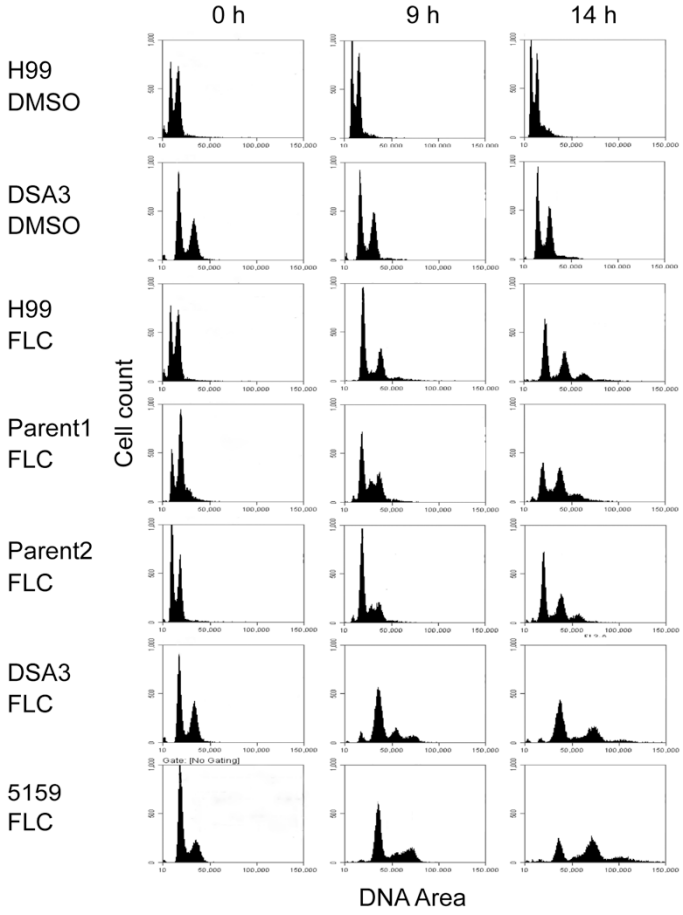

Figure 2.10. FLC treatment results in an increase in ploidy in a significant fraction of diploid cells. Two haploid strains (Parent 1 – LK315 and Parent 2 – CNV121) and two diploids, a diploid derived from the two haploids (DSA3) and a reference diploid (Bt163), were treated with 32 µg/ml FLC, fixed, stained with PI, and passed through a fluorescence flow cytometer to assess ploidy. Both diploids underwent increase in ploidy analogous to the haploid strains (parents of derived diploid and wildtype), suggesting that 32 µg/ml of FLC imposes similar inhibitory effects on both haploids and diploids. Therefore, diploid is not significantly resistant to FLC as compared to the isogenic haploids.

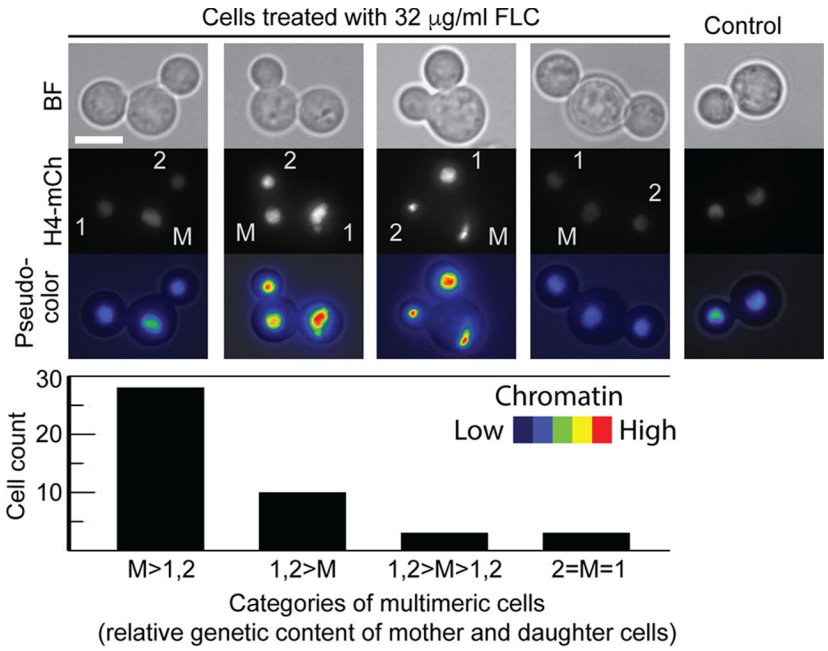

Figure 2.11. FLC treatment leads to unequal distribution of chromatin between the mother and the daughter cells. Cells expressing histone H4-mCherry from the endogenous promoter (CNV121) were treated with 32 μg/ml FLC for 12 hours and imaged using Z-section fluorescence microscopy. A total of 44 multimeric cells were evaluated for the H4-mCherry signal in each of the cells constituting a trimera (M-mother, 1-first daughter, 2-second daughter). Cells were grouped depending on the relative amount of H4-mCherry fluorescence in each of the three cells as described in detail in materials and methods. The number of cells belonging to each category was counted as indicated. The meaning of each category is as follows: M >1,2 (more signal in the mother than in either of the daughter cells); 1,2 >M (more signal in either of the daughter cells than in the mother); 1,2>M>1,2 (one daughter with more and one with less signal than in the mother); 2=M=1 (all three cells with equal signal). Bar represents 5 microns.

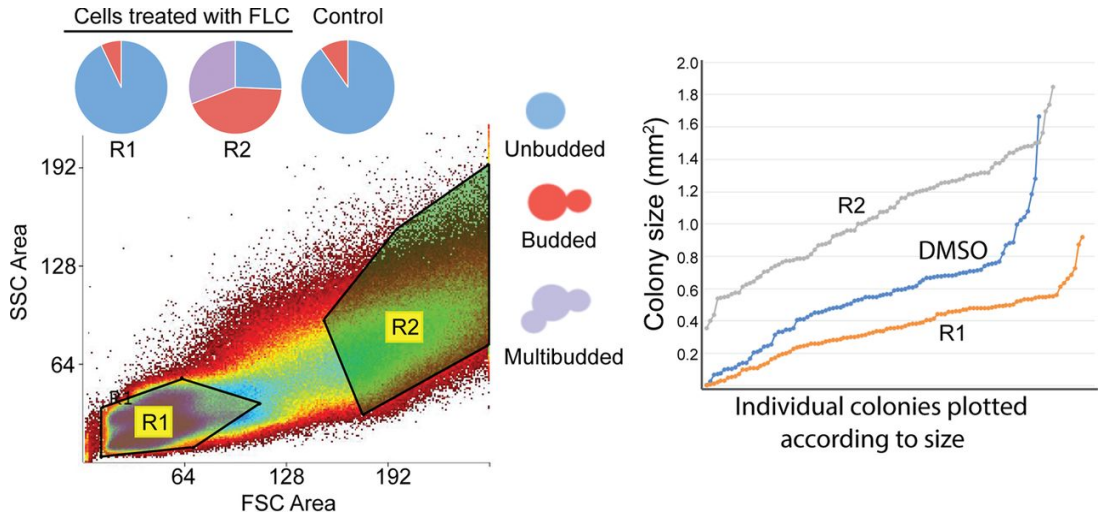

Figure 2.12. FLC-treated cells that are enlarged and/or fail to separate are less sensitive to FLC. Cells were treated with 32 μg/ml FLC for 14 hours. Two separate fractions were obtained based on size and complexity of morphology using FACS (fraction R1, R2). The morphology of each fraction was assessed. Fraction R1 consisted of predominantly unbudded cells with a smaller fraction of budded cells. Fraction R2 consisted of approximately equal amounts of unbudded cells, budded cells, and multibudded cells. Cells were then plated on media containing 32 μg/ml FLC, and the areas of colonies were measured after 3 days. Fraction R1 did not produce as many large colonies as fraction R2, suggesting the enlarged and/or multibudded cells are relatively less sensitive to FLC.

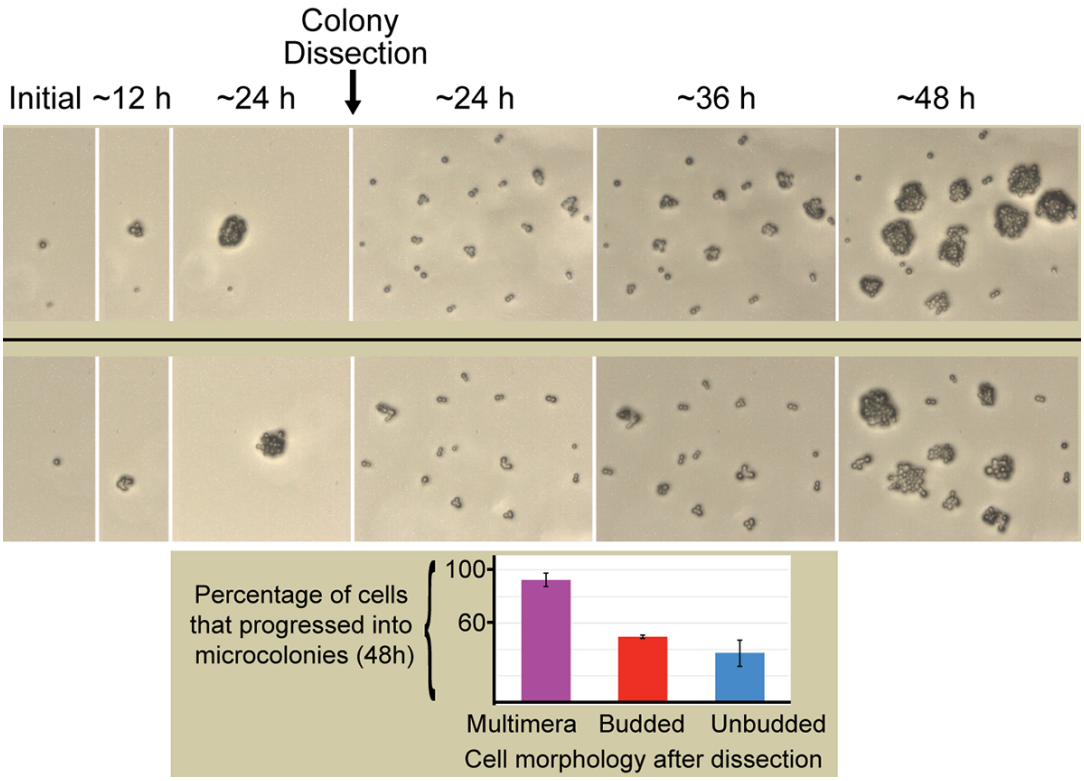

Figure 2.13. Microdissection of colonies grown on FLC media. Slightly enlarged budded or unbudded cells were placed on specific regions of a 32 µg/ml FLC plate using a micromanipulator. After 24 hours, 6 microcolonies derived from the enlarged cells were dissected separating each of the cells within a colony (2 representative dissections are shown). The morphology of each cell at this point was assessed. Cells were then imaged at 36 and 48 hours time points and the number of resulting microcolonies was scored. Quantification of the 6 microcolonies at 48 hours with respect to the initial morphologies of the cells at 24 hours (after dissection) was performed as shown in the graph. Multimeric cells developed into significantly more microcolonies as compared to single-budded or unbudded cells.

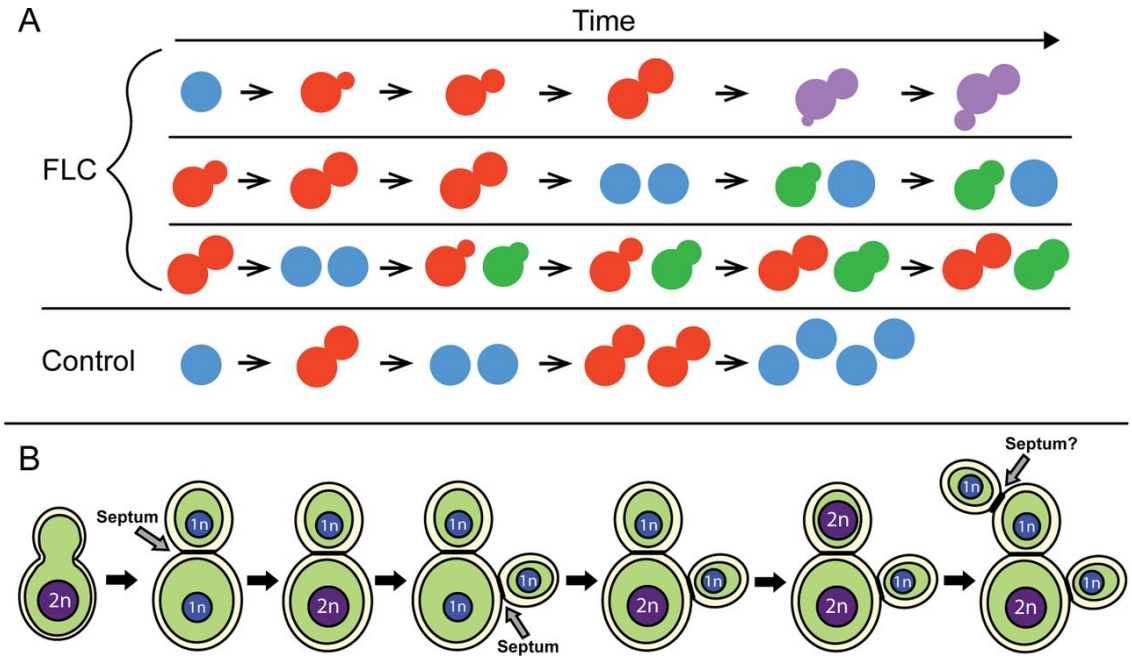

Figure 2.14. A) Model illustrating the effects of FLC on cell growth, cell cycle progression and cytokinesis that result in cells with increased ploidy including single cells, multimeric cells, and cells with abnormal buds. According to this model, the resulting morphological defect for a given cell depends on the cell cycle stage when the cell was exposed to FLC initially. **B) Model** depicting progression of events that lead to formation of a multimeric cell during exposure to FLC. In this model, a multimera with equally distributed chromatin may transition to a stage when more chromatin is present in the mother cell as compared to daughters. While this seems to be the most prevalent type of multimeric cell, cells with other chromatin distribution and mother cells with two nuclei were also found (Figures 5 and 7).

.

Strain	Genotype	Source
H99	α WT	(37)
Bt163	**Diploid;** environmental isolate	(38)
CNV111	**a** *GFP-NDC1:NAT + mCherry-CSE4:NEO*	(13)
CNV121	**α** *H4-mCherry:NEO*	Sutradhar Sanyal ref
DSA3	**a/α** *H4-mCherry:NEO/H4 GFP-NUP107:NAT/NUP107*	This study
LC4	**a** *GFP-NUP1:NAT mCherry-MYO1:HYG*	This study
LK62	**a** *CDC10-mCherry:NEO*	(17)
LK65	**α** *CDC3::NAT*	(17)
LK162	**α** *CDC12::NEO*	(17)
LK274	**a** *GFP-CTS1:NAT mCherry-MYO1:HYG*	(19)
LK126	**α** *GFP-TUB:NAT*	This study
LK315	**a** *GFP-NUP107:NAT*	This study

Table 2.1. List of strains used in this study.

REFERENCES

1. **Kwon-Chung KJ, Chang YC.** 2012. Aneuploidy and drug resistance in pathogenic fungi. PLoS Pathog **8:**e1003022.

2. **Morschhauser J.** 2016. The development of fluconazole resistance in Candida albicans - an example of microevolution of a fungal pathogen. J Microbiol **54:**192-201.

3. **Berman J.** 2016. Ploidy plasticity: a rapid and reversible strategy for adaptation to stress. FEMS Yeast Res **16**.

4. **Gerstein AC, Berman J.** 2015. Shift and adapt: the costs and benefits of karyotype variations. Curr Opin Microbiol **26:**130-136.

5. **Weaver BA, Cleveland DW.** 2006. Does aneuploidy cause cancer? Curr Opin Cell Biol **18:**658-667.

6. **Morrow CA, Fraser JA.** 2013. Ploidy variation as an adaptive mechanism in human pathogenic fungi. Semin Cell Dev Biol **24:**339-346.

7. **Lachaud L, Bourgeois N, Kuk N, Morelle C, Crobu L, Merlin G, Bastien P, Pages M, Sterkers Y.** 2014. Constitutive mosaic aneuploidy is a unique genetic feature widespread in the Leishmania genus. Microbes Infect **16:**61-66.

8. **Selmecki A, Forche A, Berman J.** 2010. Genomic plasticity of the human fungal pathogen Candida albicans. Eukaryot Cell **9:**991-1008.

9. **Sionov E, Lee H, Chang YC, Kwon-Chung KJ.** 2010. Cryptococcus neoformans overcomes stress of azole drugs by formation of disomy in specific multiple chromosomes. PLoS Pathog **6:**e1000848.

10. **Morrow JD.** 1991. Fluconazole: a new triazole antifungal agent. Am J Med Sci **302:**129-132.

11. **Zhang YQ, Gamarra S, Garcia-Effron G, Park S, Perlin DS, Rao R.** 2010. Requirement for ergosterol in V-ATPase function underlies antifungal activity of azole drugs. PLoS Pathog **6:**e1000939.

12. **Harrison BD, Hashemi J, Bibi M, Pulver R, Bavli D, Nahmias Y, Wellington M, Sapiro G, Berman J.** 2014. A tetraploid intermediate precedes aneuploid formation in yeasts exposed to fluconazole. PLoS Biol **12:**e1001815.

13. **Kozubowski L, Yadav V, Chatterjee G, Sridhar S, Yamaguchi M, Kawamoto S, Bose I, Heitman J, Sanyal K.** 2013. Ordered kinetochore assembly in the human-pathogenic basidiomycetous yeast Cryptococcus neoformans. MBio **4:**e00614-00613.

14. **Yoshida Y.** 1988. Cytochrome P450 of fungi: primary target for azole antifungal agents. Curr Top Med Mycol **2:**388-418.

15. **Yamaguchi M, Ohkusu M, Biswas SK, Kawamoto S.** 2007. Cytological study of cell cycle of the pathogenic yeast Cryptococcus neoformans. Nihon Ishinkin Gakkai Zasshi **48:**147-152.

16. **Altamirano S. CS, Kozubowski L.** 2017. Mechanisms of cytokinesis in basidiomycetous yeasts. Fungal Biology Reviews.

17. **Kozubowski L, Heitman J.** 2009. Septins Enforce Morphogenetic Events during Sexual Reproduction and Contribute to Virulence of Cryptococcus neoformans. Mol Microbiol.

18. **Fox DS, Cox GM, Heitman J.** 2003. Phospholipid-binding protein Cts1 controls septation and functions coordinately with calcineurin in Cryptococcus neoformans. Eukaryot Cell **2:**1025-1035.

19. **Aboobakar EF, Wang X, Heitman J, Kozubowski L.** 2011. The C2 domain protein Cts1 functions in the calcineurin signaling circuit during high-temperature stress responses in Cryptococcus neoformans. Eukaryot Cell **10:**1714-1723.

20. **Orlean P.** 2012. Architecture and biosynthesis of the Saccharomyces cerevisiae cell wall. Genetics **192:**775-818.

21. **Fernandez C, Lobo Md Mdel V, Gomez-Coronado D, Lasuncion MA.** 2004. Cholesterol is essential for mitosis progression and its deficiency induces polyploid cell formation. Exp Cell Res **300:**109-120.

22. **Baker LG, Specht CA, Lodge JK.** 2009. Chitinases are essential for sexual development but not vegetative growth in Cryptococcus neoformans. Eukaryot Cell **8:**1692-1705.

23. **Banks IR, Specht CA, Donlin MJ, Gerik KJ, Levitz SM, Lodge JK.** 2005. A chitin synthase and its regulator protein are critical for chitosan production and growth of the fungal pathogen Cryptococcus neoformans. Eukaryot Cell **4:**1902-1912.

24. **Walton FJ, Heitman J, Idnurm A.** 2006. Conserved elements of the RAM signaling pathway establish cell polarity in the basidiomycete Cryptococcus neoformans in a divergent fashion from other fungi. Mol Biol Cell **17:**3768-3780.

25. **Mayer VW, Aguilera A.** 1990. High levels of chromosome instability in polyploids of Saccharomyces cerevisiae. Mutat Res **231:**177-186.

26. **Storchova Z, Breneman A, Cande J, Dunn J, Burbank K, O'Toole E, Pellman D.** 2006. Genome-wide genetic analysis of polyploidy in yeast. Nature **443:**541-547.

27. **Okagaki LH, Strain AK, Nielsen JN, Charlier C, Baltes NJ, Chretien F, Heitman J, Dromer F, Nielsen K.** 2010. Cryptococcal cell morphology affects host cell interactions and pathogenicity. PLoS Pathog **6:**e1000953.

28. **Gerstein AC, Fu MS, Mukaremera L, Li Z, Ormerod KL, Fraser JA, Berman J, Nielsen K.** 2015. Polyploid titan cells produce haploid and aneuploid progeny to promote stress adaptation. MBio **6:**e01340-01315.

29. **Venkateswarlu K, Taylor M, Manning NJ, Rinaldi MG, Kelly SL.** 1997. Fluconazole tolerance in clinical isolates of Cryptococcus neoformans. Antimicrob Agents Chemother **41:**748-751.

30. **Sionov E, Chang YC, Kwon-Chung KJ.** 2013. Azole heteroresistance in Cryptococcus neoformans: emergence of resistant clones with chromosomal disomy in the mouse brain during fluconazole treatment. Antimicrob Agents Chemother **57:**5127-5130.

31. **Cheong JW, McCormack J.** 2013. Fluconazole resistance in cryptococcal disease: emerging or intrinsic? Med Mycol **51:**261-269.

32. **Desnos-Ollivier M, Patel S, Spaulding AR, Charlier C, Garcia-Hermoso D, Nielsen K, Dromer F.** 2010. Mixed infections and In Vivo evolution in the human fungal pathogen Cryptococcus neoformans. MBio **1**.

33. **Davidson RC, Cruz MC, Sia RA, Allen B, Alspaugh JA, Heitman J.** 2000. Gene disruption by biolistic transformation in serotype D strains of Cryptococcus neoformans. Fungal Genet Biol **29:**38-48.

34. **Sutradhar S, Yadav V, Sridhar S, Sreekumar L, Bhattacharyya D, Ghosh SK, Paul R, Sanyal K.** 2015. A comprehensive model to predict mitotic division in budding yeasts. Mol Biol Cell **26:**3954-3965.

35. **Schindelin J, Rueden CT, Hiner MC, Eliceiri KW.** 2015. The ImageJ ecosystem: An open platform for biomedical image analysis. Mol Reprod Dev **82:**518-529.

36. **Ayscough KR, Stryker J, Pokala N, Sanders M, Crews P, Drubin DG.** 1997. High rates of actin filament turnover in budding yeast and roles for actin in establishment and maintenance of cell polarity revealed using the actin inhibitor latrunculin-A. J Cell Biol **137:**399-416.

37. **Perfect JR, Ketabchi N, Cox GM, Ingram CW, Beiser CL.** 1993. Karyotyping of Cryptococcus neoformans as an epidemiological tool. J Clin Microbiol **31:**3305-3309.

38. **Lin X, Patel S, Litvintseva AP, Floyd A, Mitchell TG, Heitman J.** 2009. Diploids in the Cryptococcus neoformans serotype a population homozygous for the alpha mating type originate via unisexual mating. PLoS Pathog **5:**e1000283.

CHAPTER THREE

SINGLE CELL AND COLONY LEVEL ANALYSIS OF THE HETEROGENEOUS RESPONSE OF *CRYPTOCOCCUS NEOFORMANS* TO FLUCONAZOLE

Sophie Altamirano, Charles Simmons, Lukasz Kozubowski

Department of Genetics and Biochemistry, Clemson University, Clemson, South Carolina, USA

ABSTRACT

Cryptococcus neoformans is a human fungal pathogen that can cause fatal meningitis in immunocompromised individuals. Fluconazole (FLC) is a fungistatic drug administered to treat cryptococcosis. When exposed to the inhibitory concentration of FLC, *C. neoformans* exhibits heteroresistance where a small subpopulation of cells develops into FLC-resistant colonies. FLC-resistant cells are aneuploids with regard to specific beneficial chromosomal regions. Factors underlying the potential for only certain *C. neoformans* cells in a genetically isogenic population to become FLC-resistant are unknown. In this study, we systematically examine the heterogeneous response of *C. neoformans* to FLC at a colony and individual cell level. We find that the heterogeneity in response to FLC is reflected by variable diminishment of the ergosterol at the plasma membrane. A population of *C. neoformans* spread on a semi-solid medium displays two types of outcomes following FLC exposure. The first outcome is colonies consisting of non-resistant cells (survivors). The size of colonies consisting of survivors ranges from a few cells to visible colonies, which reflects intrinsic phenotypic heterogeneity of the *C. neoformans* population. The second outcome is FLC-resistant cells forming colonies of sizes significantly larger as compared to colonies made of survivors. We propose a model that describes how a distribution of these types of cellular responses within a population changes depending on FLC concentration and factors that influence the rate of cellular growth including temperature, media type, growth phase, and the age of cells. Our

findings highlight a complex nature of the response to a fungistatic drug and provide insights that may help to optimize FLC therapy.

INTRODUCTION

Single-cell clonal populations are made up of genetically homogeneous cells, but genetic identity does not necessarily translate to phenotypic similarity. Phenotypic heterogeneity has been shown to provide diversity among genetically clonal populations, allowing for adaptation to the environment without permanently locking the cells into a particular fate. It can be defined with respect to multiple aspects with various underlying physiological occurrences (1-4). Of particular importance is the heterogeneous response of pathogens to drug treatment, especially in the context of the development of drug resistance as it constitutes a major barrier to effective therapy.

Drug therapies that aim at eliminating a certain cell type (i.e. microbial pathogens, cancer cells) often overlook the phenotypic heterogeneity that exists within the targeted cell population and its potential to promote survival during treatment. For example, one distinct challenge to antimicrobial therapy is the occurrence of “persister” subpopulations of slow growing cells, which contribute to recurrent infections (5). Persisters are thought to remain throughout infection; they do not make up the population of truly resistant cells, but may contribute to the formation of resistant cells through the ability to survive in the presence of the drug. Although more commonly studied in bacterial populations, the presence of

persisters has been characterized in several eukaryotic pathogens and cancer cells (5). An important question to consider when aiming at identifying a drug therapy that does not allow for resistance or recurrence is: Why are some genetically identical cells able to proliferate when challenged with a drug while others are inhibited? A better understanding of the intrinsic, phenotypic heterogeneity of cell populations is crucial to improve our current therapeutic approaches.

In this study, we addressed the intrinsic heterogeneity within the population of *Cryptococcus neoformans*, a human fungal pathogen, in the context of the response to an azole drug, fluconazole (FLC) (6). FLC inhibits lanosterol 14α-demethylase, Erg11p, which is an essential enzyme for the synthesis of ergosterol, an important sterol present in the cellular membranes and enriched in the plasma membrane (7). Previous studies have defined a phenomenon of heteroresistance in *C. neoformans* as an intrinsic ability to develop a small subpopulation of aneuploid, FLC-resistant cells, when exposed to the inhibitory concentrations of FLC (8-10). Specific genes that confer resistance to FLC in *C. neoformans* are well established (11, 12). On the other hand, mechanisms through which FLC potentially contributes to the development of resistance remain poorly characterized. Former studies have demonstrated that the response of *C. neoformans* to FLC is heterogeneous (8, 9). A plasticity of gene duplication patterns at the single colony level was observed, which suggested that the process of multiple chromosome duplication vary among individual cells (9). These findings

suggested that *C. neoformans* exhibits an inherent, non-genetic heterogeneity that influences the response to the drug. However, the nature of the heterogeneous response of *C. neoformans* to FLC has not been thoroughly investigated.

We characterized the response of *C. neoformans* to FLC using colony and single-cell level analyses. We provide evidence that individual cells in the population exhibit variable diminishment of ergosterol within the plasma membrane during the initial exposure to FLC. This heterogeneity is reflected by the variable sizes of colonies that arise on a semi-solid medium supplemented with FLC. The resulting colonies can be divided into two groups: colonies that consist of non-resistant cells (survivors) and colonies that contain primarily resistant cells. Growth conditions that promote higher growth rate, including high nutrient content or higher temperature, lead to a diminishment of size of the colonies consisting of survivors and a decrease in number of resistant colonies in the presence of FLC. Conversely, conditions that lead to a slower growth rate, including nutrient poor media, lower temperature, and stationary phase of growth result in a more successful proliferation of survivors in the presence of FLC. Consistent with these results, relatively young cells form smaller colonies upon FLC exposure, as compared to the remaining population. Analysis of cell morphology indicates that conditions that promote slower growth may lead to a delay in daughter cell separation, which may contribute to a better survival in the presence of FLC. Based on our data, we propose a model, which describes how FLC concentration and temperature modulate distribution of colonies that contain non-resistant and

resistant *C. neoformans* cells. Our study provides insights that may help to improve *in vitro* drug susceptibility testing and augment treatments of cryptococcal infections.

RESULTS

Population of cells treated with fluconazole exhibits variable diminishment of ergosterol.

The inhibitory effect of FLC has been associated with the depletion of ergosterol from the plasma membrane (13). Two non-exclusive possibilities may explain the heterogeneity of the response to FLC: 1) The degree of FLC-triggered depletion of ergosterol may vary from cell to cell or 2) The degree to which a cell is affected by a specific diminishment of ergosterol may vary from cell to cell. To test the first possibility, we utilized filipin as a proxy to estimate ergosterol levels in the plasma membrane of individual *C. neoformans* cells (14). As filipin exhibits high sensitivity to light and oxygen, imaging the samples separately could potentially lead to false interpretations of the data. To resolve this issue, we employed two strains, a wild type (H99) strain and H99-derived strain that expressed histone H4 tagged with mCherry (15). One of the strains was treated with FLC and the other served as a control. Prior to imaging, cells of the two samples were mixed, and filipin fluorescence was visualized for the mixed population. Scoring was executed taking into account mCherry fluorescent signal to differentiate between the samples

(Figure 3.1A). For each evaluation, we conducted two reciprocal experiments to account for possible differences between the strains used (Figure 3.1A and E).

Untreated samples exhibited considerable variation in levels of filipin fluorescence between individual cells (Figure 3.1B, time 0). The variances for the two samples at time 0 were equal (at 0.05 significance level). A treatment with the inhibitory concentration of FLC (32 μg/ml) at 24°C caused an overall decrease of filipin fluorescence reaching an average fluorescence of ~56% of the control after 4 hours (Figure 3.1B). Strikingly, after 4 hours of FLC treatment the variance of filipin signal among cells increased significantly as compared to the untreated control (443 vs 91; these variances are unequal at 0.05 significance level), as some cells showed almost no detectable filipin fluorescence while others showed fluorescence levels close to those of the non-treated control (Figure 1B). We also noted that at 4 hours of incubation over 50% of cells treated with FLC exhibited a non-uniform (patchy) fluorescence signal within the plasma membrane whereas less than 5% of control cells exhibited such irregular filipin fluorescence (Figure 3.1C and D).

Contrary to our expectation, treatment with FLC for 12 hours or longer resulted in a less significant overall diminishment of the filipin fluorescence and also a smaller percentage of cells with non-uniform filipin fluorescence within the plasma membrane, as compared to the 4-hour incubation (Figure 3.1A and D). In addition, differences in variance between the treated and the control sample were not significant for longer incubations except for 12 hours where variance for treated

sample was significantly higher (675 vs 82). These data suggest that ergosterol levels vary from cell to cell in untreated population. Furthermore, FLC, at inhibitory concentrations, causes considerable diminishment of ergosterol from plasma membrane after 4 hours of treatment and the effect is unequal between individual cells. Moreover, at the level of an individual cell, the depletion of ergosterol is non-uniform within the plasma membrane with areas exhibiting more or less diminishment of ergosterol. Together, these results point to considerable variation of levels to which FLC affects individual cells in the population with respect to the ergosterol content.

A non-resistant subpopulation of cells forms colonies under inhibitory concentration of FLC without the fitness cost.

Our analysis of sterol content in plasma membrane of individual cells suggested that a cell population exhibits variable ergosterol content before drug exposure and unequal diminishment of ergosterol during response to the initial exposure to FLC. We would predict that variability in sterol content should be reflected by heterogeneity with respect to the growth rate in the presence of FLC. A simple way to probe for the heterogeneity of cell population with respect to growth rate is to analyze the sizes of individual colonies on a semi-solid medium. In order to analyze the heterogeneity in response to the drug, we applied FLC at 24 μg/ml, which is a concentration below the heteroresistance level of 32 μg/ml established for the strain we utilized (10).

An overnight culture plated on drug-free YPD rich semi-solid medium grew into colonies relatively uniform in size after 2-day incubation at 24°C (Figure 3.2, ON culture). An exposure of the same overnight culture to FLC at 24 μg/ml resulted in more variable colony sizes (Figure 3.2). After 5 days of incubation at 24°C, the effect of FLC ranged from a significant inhibition of proliferation (single cells or micro-colonies not visible by naked eye; data not shown) to growth retardation that resulted in visible colonies of various sizes (Figure 3.2).

Did all colonies that were visible after 5 days on FLC-supplemented media contain cells that were resistant to FLC? To address this question, we picked at random 4 relatively small, and 4 relatively large colonies and re-plated the cells on media containing 24 μg/ml of FLC at 24°C. In addition, the same samples were also plated on YPD drug-free media to test for potential growth retardation that would be expected if the cells were aneuploids (9). Cells from all 4 small colonies, when re-plated on FLC-containing media resulted in colonies of various sizes and single cells after 5 days, indicating a range of inhibition characteristic of a population that is not resistant to the drug, although the visible colonies were relatively larger as compared to the initial culture plated on FLC media (Figure 3.2 and data not shown). In contrast, cells from the large colonies grew significantly better on new FLC plates (Figure 3.2). Interestingly, when the distribution of colony sizes was assessed for the cells re-plated on the control YPD media, cells from three out of four large colonies grew relatively slower as compared to cells obtained from small colonies (Figure 3.2). Notably, cells from one large colony,

indicated as L3 in Figure 3.2, exhibited a fraction of colonies that were particularly large on FLC-supplemented media, while the majority of cells derived from this colony formed significantly smaller colonies on YPD-drug free media. Thus, for the cells derived from FLC-supplemented media, their ability to proliferate subsequently on new FLC-containing media correlates inversely with their proliferation rate on drug-free media. These results suggest that when the original overnight culture was spread on FLC-containing media only a fraction of colonies, likely the largest colonies, contained cells resistant to FLC used at concentration equal to 24 μg/ml, potentially through becoming aneuploids (as judged indirectly based on relatively slower growth on drug-free media). The remaining, smaller colonies represented cells that were not resistant to the drug yet managed to grow into visible colonies without a loss of fitness. We designate these non-resistant cells as survivors in contrast to cells that did not proliferate and truly resistant cells that formed relatively large colonies. Our data suggest that an asynchronous population of *C. neoformans* exhibits an intrinsic heterogeneity that is reflected by variable growth rate in the presence of FLC. Furthermore, upon exposure to a sub-inhibitory concentration of FLC a fraction of the cell population develops into colonies that are not resistant to the drug yet manage to grow at a rate that is slower than resistant cells.

C. neoformans cells display a normal distribution with respect to colony size on semi-solid, drug-free media.

What could account for the heterogeneity of response to FLC? Given that the variable response can be detected already after 4 hours of incubation with FLC (Figure 1), this heterogeneity is likely an intrinsic feature that characterizes the cell population prior to the drug exposure. Potentially such an intrinsic heterogeneity may be reflected by variable growth rates of individual cells even under unperturbed growth conditions. To examine this possibility, cells were spread on semi-solid rich YPD drug-free media, and the size distribution among randomly sampled ~100 micro-colonies detected under the microscope after 24 hours of incubation at 24°C was analyzed (Figure 3.3A). This analysis revealed that under drug-free conditions individual colonies of *C. neoformans* exhibit distribution of sizes that fits significantly to a normal distribution (R^2 = 0.95). Accordingly, the population of cells contained two small subpopulations characterized by opposite extreme behaviors with respect to growth rate; a small fraction grew significantly slower and a second small fraction grew significantly faster as compared to the majority of cells in the population. Such a distribution of growth rates among the cells may reflect how the cell population would respond to FLC treatment.

Rate of growth influences the response to FLC

We hypothesized that the size of the colony that a given cell develops into in the presence of FLC correlates inversely with the rate of growth of a colony that would develop from this cell in drug free conditions. For example, a fraction of cells that are most successful in proliferating during the initial exposure to the inhibitory

concentration of FLC would be cells that are predisposed to exhibit relatively slower growth in drug-free conditions. If that were the case, we would predict that introducing conditions that normally (without the drug) promote slower growth should lead to an overall improved survival in the presence of FLC.

Comparison of colony sizes indicated that cells incubated on drug-free semi-solid defined minimal media (YNB) proliferate significantly slower as compared to those cultured on rich YPD media (Figure 3.3A and B). Consistent with our hypothesis, plating cells on YNB minimal medium supplemented with 32 µg/ml of FLC (YNB+FLC) led to a significant increase in the number and size of colonies as compared to the YPD supplemented with the same amount of FLC (YPD+FLC) (Figure 3.4A). Randomly picked, relatively large colonies grown at 24^{o}C on YPD+FLC media contained mostly resistant cells, as majority of these cells formed robust colonies when re-plated and incubated under the same conditions (Figure 3.4B). In contrast colonies randomly obtained from YNB+FLC media incubated at 24^{o}C were not resistant to subsequent exposure to FLC in analogous conditions (Figure 3.4B). This suggests that the majority of colonies derived from the YNB+FLC plates are not resistant to FLC. Consistent with these findings, 4 out of 5 randomly picked large colonies from the YPD+FLC plates grew relatively slower when re-plated on the YPD drug-free media, whereas colonies obtained from the YNB+FLC plates contained cells that grew relatively better when spread on the YPD media (Figure 3.4B). These findings suggest that conditions

that promote slower growth lead to an increase in the number of colonies that contain non-resistant cells (survivors).

Another condition that results in an overall lower proliferation rate is nutrient deprivation and increased cell density when the culture approaches stationary phase of growth. We tested whether incubation of cells without refreshing the medium would influence subsequent growth on media containing FLC. Strikingly, prolonged incubation of cells in liquid rich YPD medium before plating on FLC-containing media led to an overall increase in colony number and size as compared to cells that were grown exponentially prior to FLC exposure (Figure 3.4C). The effect was already observed for cells incubated for 2 days (data not shown) in liquid YPD prior to FLC treatment and was more pronounced for longer incubation times (Figure 3.4C). This result suggests that in contrast to cells at the exponential phase of growth, cells derived from a nearly stationary phase culture are relatively less sensitive to FLC and more likely to develop into colonies.

Together our data suggest that external conditions that lead to an overall slower growth result in a better survival in the presence of FLC. We would predict that generating external conditions, which lead to an increased growth rate should elicit an opposite effect. One such condition is elevated temperature, which in case of *C. neoformans* results in increased proliferation rate. The intrinsic level of heteroresistance for the *C. neoformans* var. *grubii* (serotype A) strain H99 has been estimated at 32 μg/ml FLC at 30°C on semi-solid YPD media (10). We confirmed that when H99 cells were incubated with FLC under these conditions,

only a very small fraction developed into visible colonies (up to ~ 15 colonies were visible without magnification after 5 days on a plate on which ~ 10,000 cells were plated), in contrast to cells incubated at 24°C (Figure 3.4D compared to 3.4A). Consistent with previous reports, all of the visible colonies were resistant to the drug (most cells derived from a given colony grew upon subsequent plating on the same FLC concentration) and were likely aneuploids (most cells derived from a given colony grew slower on YPD drug-free media as compared to control cells, which were never exposed to the drug) (Figure 3.4E) (data not shown). These findings suggest that higher temperature leads to more susceptibility to FLC. Interestingly, cells derived from all randomly picked colonies that developed at 30°C on YNB 32 μg/ml FLC media were resistant to the drug (Figure 3.4E). Notably, while the effect of YNB at 30°C was significant (more colonies as compared to YPD 32 μg/ml at 30°C), the number of visible colonies was significantly smaller as compared to YNB 32 μg/ml FLC plates incubated at 24°C. This result suggests that the higher temperature resulted in an overall lower percentage and a decrease in colony size of “survivors”, while maintaining (or potentially increasing) the number of resistant colonies. Consistent with these findings, higher temperature incubation also led to a decrease in colony numbers of cells derived from nearly stationary culture (Figure 3.4F).

While 30°C has been established as a standard growth condition for drug susceptibility testing of *C. neoformans*, the temperature relevant to infection is at least 37°C (16). Therefore, we tested the effect of 37°C on colony growth in the

presence of FLC. When a culture that was maintained initially in drug-free liquid YPD media at 24°C was subsequently incubated on drug-containing YPD semi-solid media at 37°C, a complete inhibition of growth was observed at a FLC concentrations as low as 1 μg/ml with no occurrence of resistance to the drug (out of 10,000 cells plated, no colonies were observed after 5 days at 37°C). Such a high sensitivity to FLC could stem from a synergistic effect between FLC and a significant and sudden change in temperature (from 24°C to 37°C) and media type (liquid to semi-solid). Indeed, when cells were initially grown for 24 hours at 37°C in liquid YPD drug-free media and subsequently incubated at 37°C on semi-solid media containing FLC, the concentration of 1 μg/ml was no longer inhibitory (data not shown). However, under those conditions the level of heteroresistance was estimated at ~5 μg/ml FLC, which is significantly lower than 32 μg/ml established at 30°C (data not shown).

A previous study has suggested that already after ~ 10 hours of exposure, FLC leads to an increase in ploidy in a significant population of *C. neoformans* (17). Notably, we found that for a given concentration of FLC, the effect on ploidy was more significant with an increase in temperature (Figure 3.5). Together, these findings suggest that temperature is a critical factor that modulates the response of *C. neoformans* to FLC and influences the level of heteroresistance. These data are consistent with the important role of growth rate in the susceptibility to FLC.

Age of cells may be one of the intrinsic factors contributing to heterogeneity of the response to FLC.

A culture of *C. neoformans* contains cells with various life spans. Therefore, age may potentially be one of the factors contributing to the heterogeneity in response to FLC. To test this possibility, we labeled cell walls with the fluorescent probe, Fluorescein Isothiocyanate (FITC), washed away the staining reagent, and incubated the culture for 3.5 hours in drug-free media such that the newly grown and detached daughters were no longer labeled. Next, cells that were FITC-positive (a mix of cells with variable age) and FITC-negative (more homogenous with respect to age, relatively young cells) were separated using fluorescence-assisted cell sorter (FACS). Subsequently, the separated fractions were plated on 32 μg/ml FLC YPD semi-solid media and incubated at 30°C. Strikingly, in contrast to the mixed population, the “young” cells exhibited less heterogeneous response and were overall more sensitive to FLC as judged based on the distribution of colony sizes (Figure 3.6A). This finding suggests that the age of cells in the population is one of the factors contributing to the heterogeneous response to FLC.

Multimera morphology is contributing positively to the survival in the presence of FLC.

According to previous studies, *C. neoformans* cells that develop resistance to the initial inhibitory concentration of FLC are aneuploids typically with disomic chromosomes 1, and/or 4 (9). Studies in *Candida albicans* suggested that a

prerequisite to aneuploidy-derived resistance to FLC is the formation of aberrant multimeric cells that give rise to tetraploid populations, which subsequently undergo chromosomal loss (18). A recent study also demonstrates that FLC leads to cell separation defect followed by development of a second daughter cell, which results in formation of multimeric cells in *C. neoformans* (17). This study also reported that cells with increased ploidy and aberrant morphology exhibit overall improved growth in the presence of FLC (17). If the ability of *C. neoformans* to grow in the presence of FLC were dependent on the formation of multimeric cells, we would expect a correlation between the colony size and the presence of multimeric cells within a colony. In order to assess the response of individual cells to FLC, we plated cells on rich YPD media containing 32 μg/ml FLC, incubated at 30°C for ~ 6 days, and evaluated growth under the microscope. Out of 10,000 cells that were plated, 12 colonies were visible consistent with previously established heteroresistance level (10). Microscopic observation of the remaining cells present on the medium revealed single cells as well as micro-colonies of various sizes. To gain more insight into the morphology of the cells we scored or dissected 100 random cells or colonies, respectively, and analyzed cellular morphology of all the cells from each micro-colony (Figure 6B). Among 100 scored, we found four single cells suggesting that approximately 96% of cells that were originally plated have divided at least once within 6 days of incubation. These single cells exhibited normal morphology (were not multimeras). In contrast, microcolonies contained variable number of multimeric cells, which correlated with the colony size (Figure

3.6B; R^2 = 0.77). Thus, our data suggest that formation of multimeric cells may promote proliferation and reflect the heterogeneity of the response to FLC.

While the aneuploid state associated with the resistance is not stable, FLC-resistant aneuploid cells should persist under the selective pressure of the drug (9). This may potentially indicate that the cells at the edge of the visible resistant colony grown under selective pressure of FLC should exhibit wild type morphology. However, the analysis of the edge of resistant colonies (found on YPD media containing 32 µg/ml FLC and incubated at 30°C for ~ 6 days) contradicted this possibility as it showed the presence of multimeric cells (data not shown). This finding was further supported by the flow cytometry analysis of sizes and the complexity of morphology of the cells derived from YPD plates supplemented with 32 µg/ml FLC and incubated at 30°C. The results of this analysis suggest that both small (survivors) and large (resistant) colonies contain a significant fraction of enlarged and morphologically changed cells (data not shown). Thus, colonies consisting of resistant cells are morphologically heterogeneous suggesting that growth of the resistant colony involves a continual evolution of resistance based on formation of multimeric cells. While multimeric cells may not be sufficient for generation of FLC resistance, their formation may positively influence the survival of initially formed microcolonies in the presence of FLC.

If multimeric cells were indeed contributing to a better survival in the presence of FLC, we would predict that conditions that lead to a delay in daughter cell separation (a phenomenon that leads to multimeric state) may promote

improved proliferation in the presence of FLC. Interestingly, a culture grown in YNB medium without FLC consisted of a significant number of multimeras at both 24°C and 30°C (Figure 3.7). Therefore, the increased survival on YNB semi-solid media may be due to increased multimera formation and may be common to other conditions that promote slow proliferation and improve growth in the presence of FLC. Alternatively, multimera formation could be a side effect of slow growth rather than a factor contributing to better survival. For instance, cells derived from nearly stationary culture are not multimeras (data not shown). Additionally, colonies grown on YNB semi-solid media at 30°C appeared to grow at approximately the same rate as cells grown on YPD semi-solid media at 24°C, which did not promote multimera formation (Figure 3.3C and D). These results suggest that while conditions that promote slower proliferation generally improve survival in the presence of FLC, the mechanisms through which this occurs may vary depending on a specific condition.

DISCUSSION

Our data and previous studies indicate that *C. neoformans* genetically homogenous population consists of cells that differ in their potential to proliferate when first exposed to FLC (9). We propose that this potential depends, at least in part, on the ability to retain ergosterol at the plasma membrane during FLC exposure. Most studies have assessed the effects of FLC on ergosterol levels after an overnight treatment with FLC. Moreover, the actual dynamics of the depletion

of ergosterol has not been well established in any model organism. Furthermore, most studies assessed the total amount of ergosterol extracted from an entire cell population. The only study that describes ergosterol content at the level of an individual cell assessed ergosterol levels based on the fluorescence of the sterol-binding agent filipin in *Penicillium discolor* and *Saccharomyces cerevisiae* (14). Filipin staining utilized here as a proxy to assess the ergosterol content suggests an overall diminishment of plasma membrane ergosterol in FLC-treated populations that is non-uniform between individual cells. Interestingly, diminishment appeared also non-uniform within a single cell. Specifically, patches of higher fluorescence were distributed throughout the plasma membrane. This finding suggests that specific areas within the plasma membrane are more resistant to diminishment of ergosterol. One such area could be the sterol-rich lipid raft domains described previously in other cell types (19).

At 12 and 24 hours of incubation with FLC the overall diminishment of ergosterol was less significant as compared to 4-hour time-point. One potential explanation could be that longer incubations may lead to a compensatory synthesis and incorporation of alternative sterols into the plasma membrane and an overall change in sterol composition (20). An alternative and non-exclusive possibility is that longer incubations lead to re-establishment of ergosterol in cells that have gained the resistance potential to continue proliferating in the presence of the drug.

The degree to which FLC affects the levels of ergosterol may depend on multiple factors, each characterized by a specific distribution within the population. In addition, factors independent of ergosterol levels may be involved. For instance, our other studies suggest that FLC treatment leads to an increase in Reactive Oxygen Species (ROS), which contribute to the inhibition of growth. Upon FLC exposure, individual cells within the population may vary in the levels of ROS. Similar to the retention of ergosterol, levels of ROS may also depend on multiple factors. In addition, we cannot exclude the possibility that the levels of ergosterol and ROS are interdependent.

Based on our data and previous findings, we propose that each cell in the population is characterized by a net potential (derived from multiple factors) to proliferate in the presence of FLC. These potentials are specifically distributed among cells within the population. We postulate that the shape of this distribution will depend on intrinsic as well as extrinsic factors. Critical extrinsic factors that were characterized here include drug concentration, temperature, and the availability of nutrients. Our data suggest that an intrinsic factor that influences the response to FLC is replicative age of the cell. Specifically, a population consisting of mostly young cells exhibited a response that displayed relatively lower heterogeneity and an overall higher sensitivity to FLC. Interestingly, such a population still contains a small fraction of cells capable of becoming resistant to FLC. Consistent with our findings, it has been reported that *C. neoformans* cells that are old with respect to the replicative life span are more resistant to FLC (21).

As schematically depicted in Figure 3.8, at a given temperature, a population of cells that is treated with FLC is divided into those that do not grow into visible (by naked eye) colonies after ~ 5 days (significantly inhibited), those that form visible colonies consisting of non-resistant cells (survivors, depicted as green triangular line), and those that form colonies composed of mostly resistant cells (red line). As the concentration of FLC increases, the number and size of colonies consisting of survivors decrease until no visible colonies are observed even after ~5 days (FLC heteroresistance level, depicted as H). We postulate that colonies consisting of resistant cells appear only when the concentration of FLC is at a necessary minimum (depicted as R1). The number of resistant colonies reaches a maximum at the FLC concentration depicted as Rm. Based on our data, we propose that at concentration Rm, colonies of survivors are visible albeit their size is relatively smaller as compared to lower concentrations. According to this model, a minimum concentration of FLC at which survivors are no longer observed and resistant colonies are still present (depicted as H) is the heteroresistance level as described previously (10). Finally, at a concentration of FLC depicted as R2 no colonies are visible with a naked eye.

While, according to this model, the size of colonies consisting of survivors decreases with increasing FLC concentrations (depicted as the width of the green triangular line), the size of colonies consisting of resistant cells is relatively uniform (red line), consistent with the definition of the resistant state. While our model depicts linear relationships between colony numbers (or colony size for the

survivors) and concentration of FLC, in reality these relationships are likely non-linear. The exact function describing these relationships will depend on the nature of multiple factors (intrinsic and extrinsic) influencing cell growth in the presence of FLC.

Our findings suggest that temperature is one of the critical extrinsic factors impacting the distribution of the potential to proliferate in the presence of FLC. Previous findings suggested that the susceptibility of *C. neoformans* to FLC increases with the elevation of temperature. Pettit et al. noted that biofilms formed by *C. neoformans* were more susceptible to FLC and the MIC's of the planktonic yeast cultures were lower at 35°C as compared to 30°C (22). Mondon et al. demonstrated that a clinical isolate of *C. neoformans* fully resistant to 64 μg/ml FLC at 30°C forms a reduced number of colonies at 35°C, and no colonies at 37°C or 40°C (23). Our data suggest that the concentrations depicted in our model as R1, Rm, H, and R2 shift towards lower values as temperature of incubation increases (Figure 8). We propose that other factors will shift these concentration values in either of the two directions depending on the specific factor. Thus, these concentration values for a given population of cells under specific conditions would result from the net interaction between all factors.

One factor that is influenced by various conditions (extrinsic and intrinsic) is rate of proliferation. Three extrinsic factors we analyzed in this study are temperature, the type of growth media (rich medium versus minimal medium), and the phase of growth (exponential versus stationary), all of which influence the

proliferation rate. Specifically, lower temperatures, higher cell densities (cells at or approaching stationary phase) and growth in minimal media (as opposed to rich media) result in an increase in the number and size of colonies consisting of survivors and resistant cells. Thus, for all three extrinsic factors studied here, the conditions that result in shift of concentrations R1, Rm, H, and R2 towards higher values are all associated with slower growth rate in drug free media, suggesting that conditions which result in slower growth/metabolism promote survival in the presence of FLC.

Microbial pathogens may become less susceptible to an inhibition imposed by a drug through reducing the rate of the process that is the primary drug target (24). Such cells are not resistant to the drug, but they possess a better chance of survival during the initial exposure to the drug and therefore exhibit a higher chance to develop into drug resistant populations. While the effects of FLC are likely pleiotropic, a prominent result of FLC treatment in *C. neoformans* is inhibition of budding (17). It is therefore likely that conditions that promote slower growth result in less susceptibility to FLC. Alanio et al. showed that a subpopulation exhibiting slower growth rate, thought to be dormant cells, exist *in vitro* and *in vivo* in *C. neoformans* populations (25). These dormant cells could potentially promote survival during FLC treatment.

Our data based on microscopic examination suggest that at concentrations of FLC depicted in our model as between R1 and R2, a large fraction of cells (increasing as the concentration of FLC approaches R2) form micro-colonies (not

visible by naked eye after ~ 5 days). These micro-colonies typically consist of multimeric cells, but the presence of multimeric cells does not ensure resistance. In fact, most of the cells that form multimeric micro-colonies do not gain true fluconazole resistance. Our data suggest that formation of multimeric cells is not sufficient to form a resistant colony under the inhibitory concentration of FLC. This however does not exclude the possibility that the formation of multimeras is necessary for the subsequent development of resistance. For instance, multimeric cells may promote sufficient proliferation to increase the number of stochastic events of aneuploidy formation out of which only a small percentage provides sufficient growth advantage and resistance to the particular concentration of the drug. Moreover, multimeras may be necessary for the maintenance of the resistant state. This is supported by the observation that multimeras are present at edges of the resistant colonies. This finding also suggests that a colony consisting of resistant cells is heterogeneous and contains cells at various resistance levels. It is possible that as the resistant colony grows, a continual process of gaining and losing the resistance continues within the colony, and a distribution of cells with various levels of resistance characterizes the colony.

Recent findings suggest that in cancer cells exposed to an anticancer drug an epigenetic reprogramming takes place rendering a subpopulation of cells less sensitive to the drug (26). While our study suggests that a preexisting heterogeneity within the population of *C. neoformans* determines the response of individual cells to the drug, it is possible that in a population under specific growth

conditions and drug concentration, a subset of cells may possess the ability to divide and/or reprogram epigenetically, so that these cells lead to progeny able to acquire the resistant state subsequently.

Grossman and Casadevall highlighted that *C. neoformans* undergoes unique changes during infection compared to laboratory *in vitro* conditions, making *in vitro* analyses suboptimal in predicting outcomes in infection models (27). Our study highlights another barrier to effective therapeutic strategies based on standardized *in vitro* susceptibility testing. The variability of the response to FLC due to extrinsic and intrinsic factors reported here should help to better understand phenotypic heterogeneity in *C. neoformans* and its role during FLC treatment.

MATERIALS AND METHODS

Growth Conditions

Strains used in this study are *Cryptococcus neoformans* var. *grubii* wild type (H99) and an isogneic strain, in which a sequence encoding fluorescent protein mCherry was introduces to replace the STOP codon of the gene encoding histone H4 (28). Unless otherwise stated, cells were grown in liquid YPD overnight at 24°C and refreshed next day to 0.2 at 600 nm (OD_{600}) before treatment. For FLC treated cultures, FLC (Alfa Aesar, Haverhill, MA) was prepared to a final concentration from a 50 mg/ml stock in DMSO. For experiments at 30°C or 37°C, cells were pre-incubated in YPD overnight at 30°C or 37°C.

Flow cytometry

Cells were harvested before exceeding ~0.8 OD_{600}, spun down, washed with sterile water, suspended in 100µl distilled water, and fixed with 70% EtOH (in a dropwise manner while vortexing). Cells were then incubated at 24°C for 1 hour and transferred to 4°C overnight. Next day, cells were washed with RNAse A buffer (0.2M Tris pH 7.5, 20 mM EDTA), suspended in 100 µl of RNAse A buffer with 1 µl RNAse A (10 mg/ml), and incubated for 4 hours at 37°C. Cells were then washed twice with 1 ml phosphate-buffered saline (PBS), suspended in 900 µl of PBS, and incubated at 4°C overnight. Cells were stained with propidium iodide (PI) by adding 100 µl of 0.005 µg/ml PI stock and incubated in the dark for 30 minutes. Immediately before analysis, cells were sonicated at 20% amplitude for 5 sec. to avoid clumping. For ploidy analysis, the PI fluorescence was collected from 10,000 cells using FL3 (488nm laser) on BD Accuri C6 flow cytometer. Cell sorting was performed using Biorad S3E cell sorter. At least 500,000 cells were sorted into two fractions based on cells labelled or not labelled with FITC using FL1 (488 nm laser).

In order to separate young cells from the population, unbudded cells were selected via centrifugation. Cells were grown in 200ml for two days then pelleted and suspended in 50% sorbitol (1M) and 50% YPD. Cells were spun at 2000 rpm for 5 min. The supernatant was transferred to a new tube and spun at 1500 rpm for 5 min. Again, the supernatant was transferred to a new tube and spun at 4000 rpm for 10 min. The morphology of the pelleted cells was then assessed under the microscope to ensure the majority of the population was unbudded. Cells were

then biotinylated using EZ-Link Sulfo-NHS-LC-Biotin (ThermoScientific) and stained with fluorescein (FITC) (Sigma, St. Louis, MO). Cells were washed three times with PBS and suspended to a density of $5x10^7$ cells/ml. Subsequently, 4 mg/ml of Sulfo-NHS-LC-Biotin reagent was added. Cells were incubated at 24°C for 30 minutes then washed three times with YPD. Biotinylated cells were released into YPD for an additional four hours and then washed three times and stained with FITC (1:200) for 10 minutes. Cells were then washed and released into PBS to be sorted.

Microscopy

Bright field and fluorescence images were captured using the 100x objective with a Zeiss Axiovert 200 inverted microscope (Carl Zeiss, Thornwood, NY) interfaced with AxioVision Rel 4.8 software (Carl Zeiss, Thornwood, NY). Micromanipulation was performed using SporePlay dissection microscope (Singer Instruments, UK). Unless otherwise stated, images were processed in Adobe Photoshop (Adobe Systems Incorporated, San Jose, CA).

Ergosterol analysis at a single cell level

Cells were harvested from liquid YPD, washed, and suspended in 1 ml PBS. Cells were then rotated in the dark with 5 µg/ml filipin III (Cayman Chemical, Ann Arbor, MI) for 5 min. Cells were allowed to settle for 5 min in chamber slide prior to imaging. Importantly, the total time in filipin stain did not exceed 15 min. To ensure

uniform filipin stain and to allow for comparison of treatments, wild type cells (H99) and cells expressing histone H4 tagged with the mCherry were incubated in conditions tested, and subsequently mixed together, and stained with filipin. Images were processed using ImageJ (https://imagej.nih.gov/ij/). To measure the intensity of filipin fluorescence, the plasma membrane marked by the filipin fluorescence was traced by a line 1 pixel thick, excluding an area where the daughter cell originates, and the intensity of each pixel was recorder along the traced line. Filipin value for each cell was calculated as an average of the pixel intensities from the entire traced line. To assess uniformity of the filipin signal along the plasma membrane section, images were assessed by 3 independent evaluators (who had no knowledge which cell in an image was treated with FLC and which one was the control) and cells were classified as either patchy or having a smooth filipin signal. All three evaluations were consistent indicating that classification of “patchy” was indeed based on a true difference between cells.

ACKNOWLEDGEMENTS

We thank Dr. Mariusz Dylag and Jessica Zielinski for help with the editing. This work was supported by the NIH grant (1R15 AI119801-01). We also thank Justin Scott from Clemson Light Imaging Facility (CLIF) for help with cell sorting. The research reported in this publication was conducted using a BioRad S3e cell sorter, housed in CLIF. CLIF is supported, in part, by the Clemson University Division of Research, NIH EPIC COBRE Award #P20GM109094, and NIH

SCBiocraft COBRE Award #5P20RR021949-03. The BioRad S3e cell sorter purchase was also supported in part with funds from the Air Force Office of Scientific Research (Award #FA9550-16-1-027007). The content of this material and any opinions, findings, conclusions, or recommendations expressed in this material is solely the responsibility of the author(s) and does not necessarily represent the official views of the National Institutes of Health or the United States Air Force.

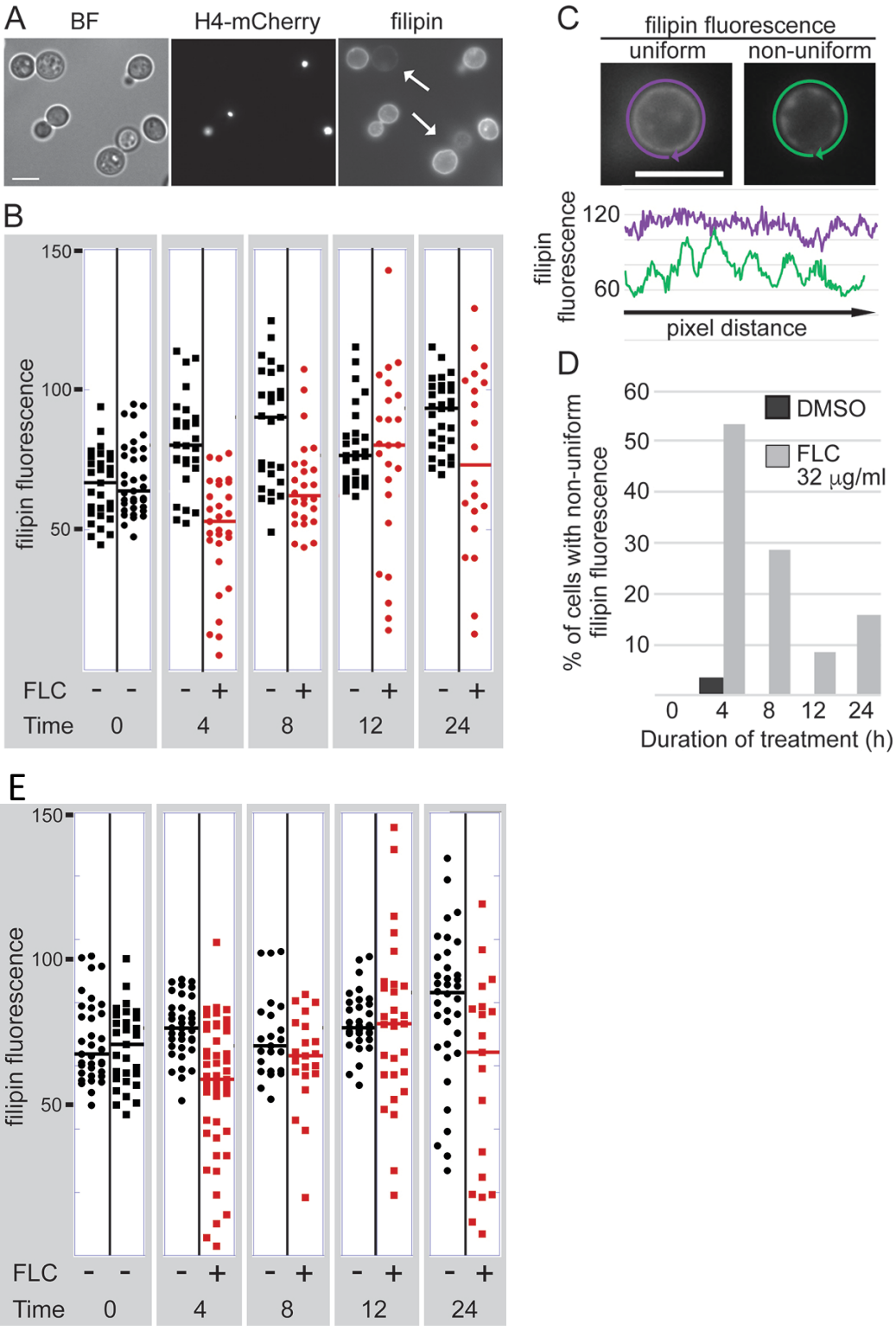
A
BF
H4-mCherry
filipin
B
filipin fluorescence
150
100
50
FLC - - - + - + - + - +
Time 0 4 8 12 24
C
filipin fluorescence
uniform
non-uniform
filipin fluorescence
120
60
pixel distance
D
% of cells with non-uniform filipin fluorescence
60
50
40
30
20
10
DMSO
FLC 32 μg/ml
0 4 8 12 24
Duration of treatment (h)
E
filipin fluorescence
150
100
50
FLC - - - + - + - + - +
Time 0 4 8 12 24

Figure 3.1. Unequal depletion of the plasma membrane ergosterol during FLC treatment. The fluorescent dye, filipin, served as a proxy to examine the effect of FLC on the ergosterol content in the plasma membrane at a single cell level. Cells were treated with 32 µg/ml FLC or DMSO as control for various hours, stained with filipin, and imaged immediately. A strain expressing histone H4-mCherry was treated with FLC, whereas a strain lacking nuclear fluorescence was treated with DMSO and served as a control. Prior to filipin staining the two strains were mixed in a 1:1 ratio. (A) Cells treated with FLC were recognized based on the H4-mCherry fluorescent signal (B) The average filipin fluorescence of cells treated with FLC exhibited increase in variability compared to DMSO treated cells. (C, D) FLC leads to a non-uniform depletion of sterol from the plasma membrane within a single cell. Filipin fluorescence was measured by tracing the fluorescent signal corresponding to the plasma membrane, and the intensity of the fluorescence of every pixel in the tracing path was plotted. Bar in A and C corresponds to 5 microns. (E) The reciprocal analysis showing the average filipin fluorescence when H4-mCherry cells were treated with 32 µg/ml FLC and wildtype cells were treated with DMSO.

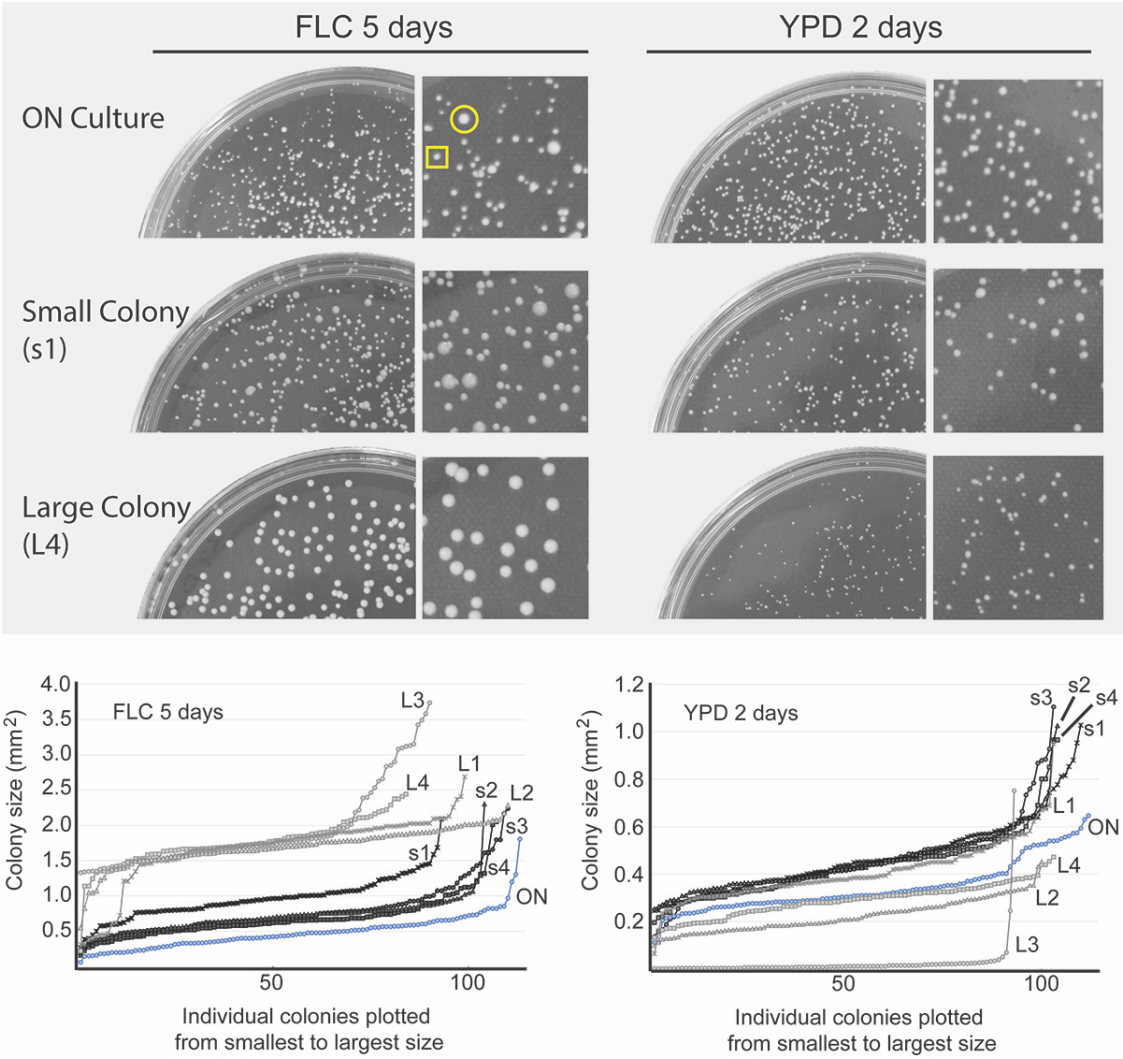

Figure 3.2. Heterogeneous response to FLC on a semisolid media. Cells from the overnight culture (ON culture) were spread on YPD semi-solid media and YPD media containing 24 µg/ml FLC and incubated at 24ºC. Cells incubated on FLC-containing media produced colonies that varied in size after 5 days, whereas cells incubated on YPD drug-free media formed colonies more uniform in size (top two plates). Four small colonies (representative indicated by yellow square) and four large colonies (representative indicated by yellow circle) were randomly picked

from the FLC-containing plate and spread on YPD control media or YPD media containing 24 μg/ml FLC. Plates were photographed (representative images are shown) and sizes of the resulting colonies from areas containing ~ 100 colonies were analyzed and plotted. Next to each plate a magnified area is shown. Cells obtained from the small colonies (black lines, s1-4) displayed similar colony size heterogeneity on FLC media compared to the initial population (ON) (left graph) and largely retained their ability to proliferate when grown on YPD (right graph). Cells derived from big colonies (grey lines, L1-4) displayed smaller colonies on YPD and larger, more homogenous colonies on FLC-containing media.

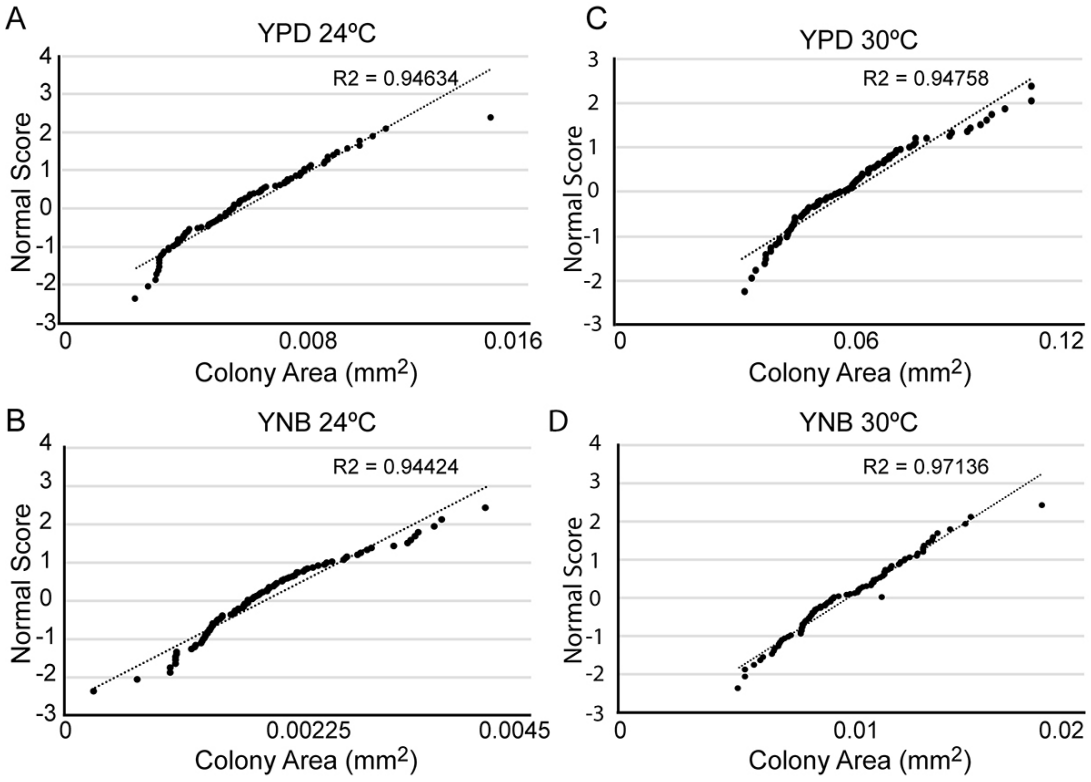

Figure 3.3. Cells not exposed to FLC exhibit a normal distribution of colony sizes. Cells were plated on YPD semi-solid media (A, C) or YNB semi-solid media (B, D) and incubated at either 24ºC (A, B) or 30ºC (C, D). The size of approximately 100 colonies was measured and plotted against a normal distribution of numbers (correlation coefficient R2 indicates correlation between distribution of colony sizes and the normal distribution). Cells grown on YPD exhibited relatively larger colonies as compared to cells grown on YNB, and 30ºC led to relatively larger colonies as compared to 24ºC.

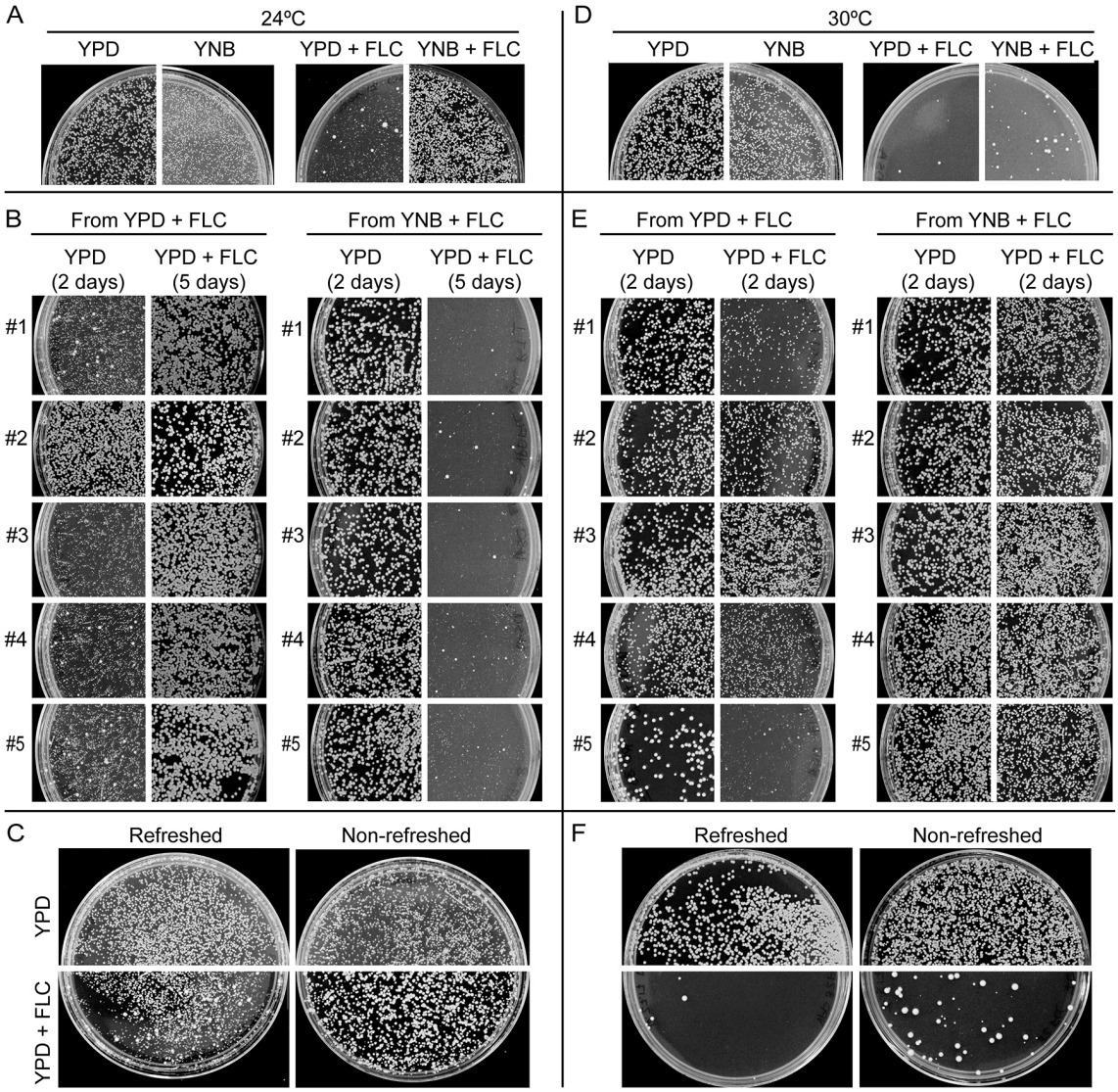

Figure 3.4. The response of FLC depends on temperature, media composition, and nutrient availability. (A, D) Incubation of cells on minimal medium YNB supplemented with 32 μg/ml FLC led to a significantly larger number of colonies at both 24ºC and 30ºC as compared to cells incubated on rich YPD media containing 32 μg/ml FLC. Incubation at 30ºC led to an increased FLC susceptibility on both YPD and YNB media as compared to 24ºC. (B, E) Five

relatively big colonies obtained from either YPD or YNB FLC-containing media (shown in A and D) were re-plated on YPD semi-solid media with and without 32 µg/ml FLC. (C, F) Cells that were grown for 7 days in YPD liquid media without refreshing the media exhibited more colonies when subsequently spread on semisolid media containing 32 µg/ml FLC as compared to cells that were at the exponential phase of growth prior to FLC exposure. This effect was significant at both 24ºC and 30ºC.

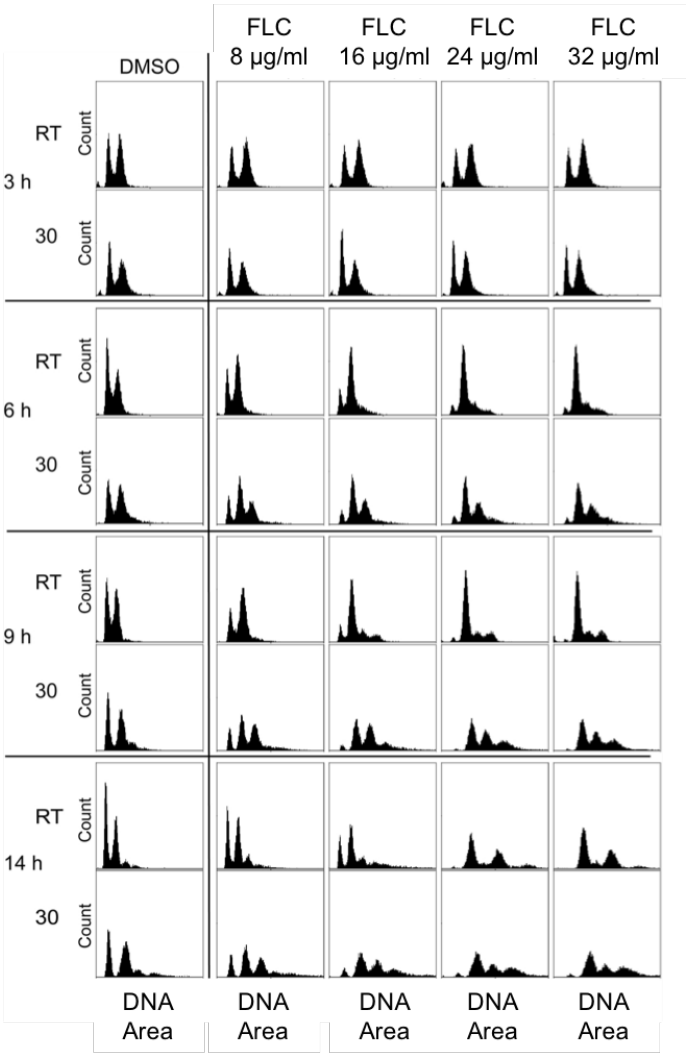

Figure 3.5. Ploidy increase during FLC treatment is more severe in higher temperatures. *C. neoformans* cells were treated with varying concentrations of FLC for various time points. They then were fixed, stained with propidium iodide (PI), and their DNA content was assessed using fluorescence flow cytometry. FLC treatment at 30ºC led to a more pronounced increase in ploidy compared to FLC treatment at 24ºC (RT).

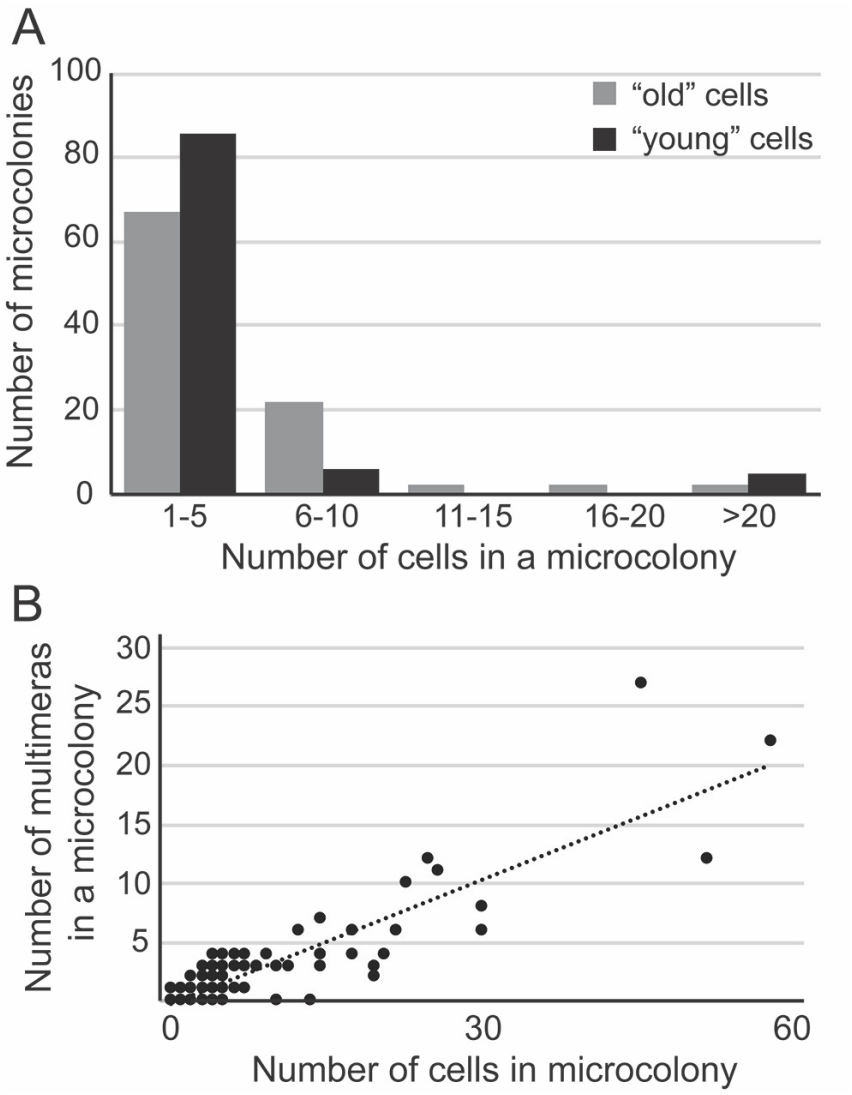

Figure 3.6. (A) "Young" cells display more sensitivity towards FLC. Pre-selected unbudded cells were biotinylated and released into YPD for four hours. Cells were then stained with streptavidin-conjugated FITC and sorted based on +FITC (older cells) or –FITC (young cells) signal. Young and older cells were spread on YPD media supplemented with 32µg/ml FLC, incubated at 30ºC, and after 6 days 100 colonies were dissected and number of cells in each colony was counted to assess degree of proliferation in the presence of FLC. The majority of

young cells display an overall higher sensitivity to FLC as compared to the mixed population. **(B) Multimera morphology is not sufficient, but may be essential for the development of resistance to FLC.** Cells were incubated on YPD media containing 32 µg/ml FLC at 30ºC for 6 days. 100 random colonies/cells were dissected and the number of normal and multimeric cells was counted in each micro-colony.

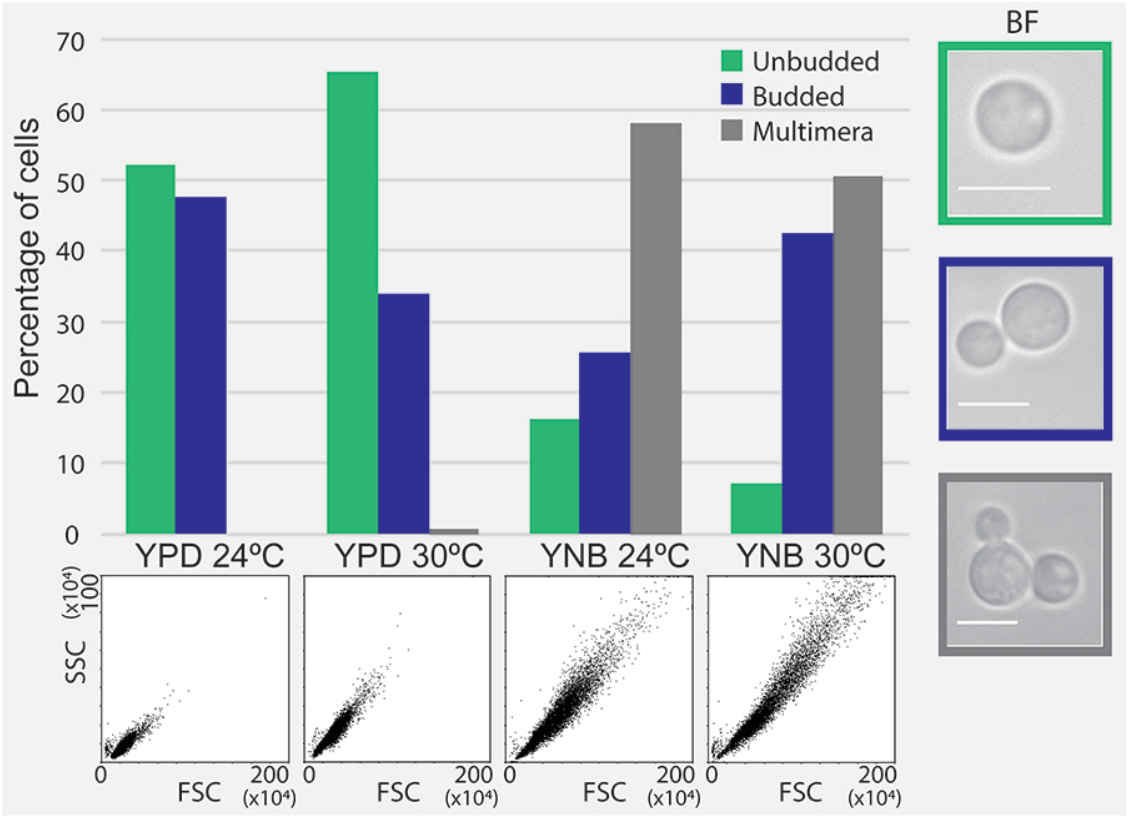

Figure 3.7. Incubation in minimal YNB media results in the formation of multimeric cells. Cells were incubated in YPD and YNB media at 24ºC and 30ºC and cellular morphology was assessed by flow cytometry and brightfield microscopy. A significant fraction of cells grown in YNB media exhibited multimera morphology, in contrast to cells incubated in YPD.

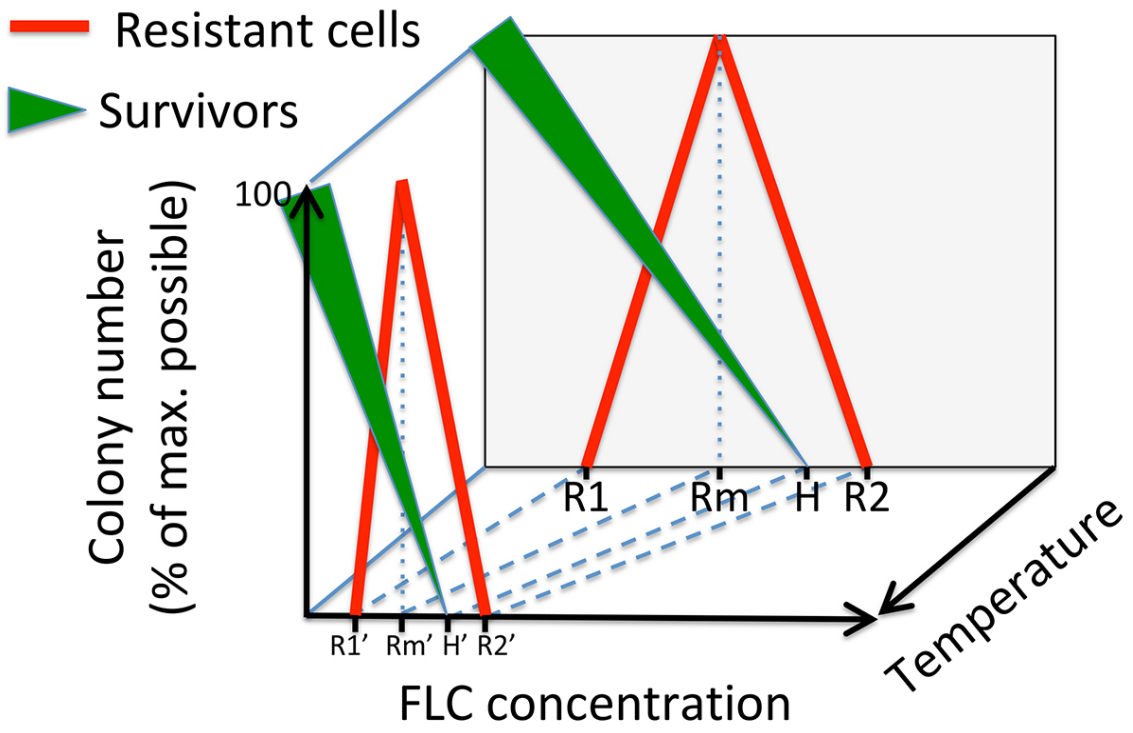

Figure 3.8. A model depicting the effects of the FLC concentration and the temperature on the distribution of two types of colonies of *C. neoformans* that are visible on semi-solid media. Green triangular lines illustrate colonies consisting of survivors, which are cells not resistant to FLC. Importantly, the thickness of the green line refers to the average colony size. The red line illustrates colonies consisting of mostly resistant cells. Specific concentrations of FLC included in the model are: R1 – minimum concentration at which resistant cells develop, Rm – concentration at which maximum resistant colonies develop, H – heteroresistance level (lowest concentration at which no survivors form visible colonies), R2 – lowest concentration at which no colonies are observed.

REFERENCES

1. **Huang S.** 2009. Non-genetic heterogeneity of cells in development: more than just noise. Development **136:**3853-3862.

2. **Avery SV.** 2006. Microbial cell individuality and the underlying sources of heterogeneity. Nat Rev Microbiol **4:**577-587.

3. **Sharma SV, Lee DY, Li B, Quinlan MP, Takahashi F, Maheswaran S, McDermott U, Azizian N, Zou L, Fischbach MA, Wong KK, Brandstetter K, Wittner B, Ramaswamy S, Classon M, Settleman J.** 2010. A chromatin-mediated reversible drug-tolerant state in cancer cell subpopulations. Cell **141:**69-80.

4. **van Dijk D, Dhar R, Missarova AM, Espinar L, Blevins WR, Lehner B, Carey LB.** 2015. Slow-growing cells within isogenic populations have increased RNA polymerase error rates and DNA damage. Nat Commun **6:**7972.

5. **Cohen NR, Lobritz MA, Collins JJ.** 2013. Microbial persistence and the road to drug resistance. Cell Host Microbe **13:**632-642.

6. **Perfect JR, Dismukes WE, Dromer F, Goldman DL, Graybill JR, Hamill RJ, Harrison TS, Larsen RA, Lortholary O, Nguyen MH, Pappas PG, Powderly WG, Singh N, Sobel JD, Sorrell TC.** Clinical Practice Guidelines for the Management of Cryptococcal Disease: 2010 Update by the Infectious Diseases Society of America. Clin Infect Dis.

7. **Zhang YQ, Gamarra S, Garcia-Effron G, Park S, Perlin DS, Rao R.** 2010. Requirement for ergosterol in V-ATPase function underlies antifungal activity of azole drugs. PLoS Pathog **6:**e1000939.

8. **Sionov E, Chang YC, Kwon-Chung KJ.** 2013. Azole heteroresistance in Cryptococcus neoformans: emergence of resistant clones with chromosomal disomy in the mouse brain during fluconazole treatment. Antimicrob Agents Chemother **57:**5127-5130.

9. **Sionov E, Lee H, Chang YC, Kwon-Chung KJ.** 2010. Cryptococcus neoformans overcomes stress of azole drugs by formation of disomy in specific multiple chromosomes. PLoS Pathog **6:**e1000848.

10. **Sionov E, Chang YC, Garraffo HM, Kwon-Chung KJ.** 2009. Heteroresistance to fluconazole in Cryptococcus neoformans is intrinsic and associated with virulence. Antimicrob Agents Chemother **53:**2804-2815.

11. **Selmecki A, Forche A, Berman J.** 2010. Genomic plasticity of the human fungal pathogen Candida albicans. Eukaryot Cell **9:**991-1008.

12. **Kwon-Chung KJ, Chang YC.** 2012. Aneuploidy and drug resistance in pathogenic fungi. PLoS Pathog **8:**e1003022.

13. **Yoshida Y.** 1988. Cytochrome P450 of fungi: primary target for azole antifungal agents. Curr Top Med Mycol **2:**388-418.

14. **Van Leeuwen MR, Smant W, de Boer W, Dijksterhuis J.** 2008. Filipin is a reliable in situ marker of ergosterol in the plasma membrane of germinating conidia (spores) of Penicillium discolor and stains intensively at the site of germ tube formation. J Microbiol Methods **74:**64-73.

15. **Sutradhar S, Yadav V, Sridhar S, Sreekumar L, Bhattacharyya D, Ghosh SK, Paul R, Sanyal K.** 2015. A comprehensive model to predict mitotic division in budding yeasts. Mol Biol Cell **26:**3954-3965.

16. **Archibald LK, Tuohy MJ, Wilson DA, Nwanyanwu O, Kazembe PN, Tansuphasawadikul S, Eampokalap B, Chaovavanich A, Reller LB, Jarvis WR, Hall GS, Procop GW.** 2004. Antifungal susceptibilities of Cryptococcus neoformans. Emerg Infect Dis **10:**143-145.

17. **Altamirano S, Fang D, Simmons C, Sridhar S, Wu P, Sanyal K, Kozubowski L.** 2017. Fluconazole-Induced Ploidy Change in Cryptococcus neoformans Results from the Uncoupling of Cell Growth and Nuclear Division. mSphere **2**.

18. **Harrison BD, Hashemi J, Bibi M, Pulver R, Bavli D, Nahmias Y, Wellington M, Sapiro G, Berman J.** 2014. A tetraploid intermediate precedes aneuploid formation in yeasts exposed to fluconazole. PLoS Biol **12:**e1001815.

19. **Alvarez FJ, Douglas LM, Konopka JB.** 2007. Sterol-rich plasma membrane domains in fungi. Eukaryot Cell **6:**755-763.

20. **Ghannoum MA, Spellberg BJ, Ibrahim AS, Ritchie JA, Currie B, Spitzer ED, Edwards JE, Jr., Casadevall A.** 1994. Sterol composition of Cryptococcus neoformans in the presence and absence of fluconazole. Antimicrob Agents Chemother **38:**2029-2033.

21. **Bouklas T, Pechuan X, Goldman DL, Edelman B, Bergman A, Fries BC.** 2013. Old Cryptococcus neoformans cells contribute to virulence in chronic cryptococcosis. MBio **4**.

22. **Pettit RK, Repp KK, Hazen KC.** 2010. Temperature affects the susceptibility of Cryptococcus neoformans biofilms to antifungal agents. Med Mycol **48:**421-426.

23. **Mondon P, Petter R, Amalfitano G, Luzzati R, Concia E, Polacheck I, Kwon-Chung KJ.** 1999. Heteroresistance to fluconazole and voriconazole in Cryptococcus neoformans. Antimicrob Agents Chemother **43:**1856-1861.

24. **Shan Y, Brown Gandt A, Rowe SE, Deisinger JP, Conlon BP, Lewis K.** 2017. ATP-Dependent Persister Formation in Escherichia coli. MBio **8**.

25. **Alanio A, Vernel-Pauillac F, Sturny-Leclere A, Dromer F.** 2015. Cryptococcus neoformans host adaptation: toward biological evidence of dormancy. MBio **6**.

26. **Shaffer SM, Dunagin MC, Torborg SR, Torre EA, Emert B, Krepler C, Beqiri M, Sproesser K, Brafford PA, Xiao M, Eggan E, Anastopoulos IN, Vargas-Garcia CA, Singh A, Nathanson KL, Herlyn M, Raj A.** 2017. Rare cell variability and drug-induced reprogramming as a mode of cancer drug resistance. Nature **546:**431-435.

27. **Grossman NT, Casadevall A.** 2017. Physiological Differences in Cryptococcus neoformans Strains In Vitro versus In Vivo and Their Effects on Antifungal Susceptibility. Antimicrob Agents Chemother **61**.

28. **Sutradhar S, Yadav V, Sridhar S, Sreekumar L, Bhattacharyya D, Ghosh SK, Paul R, Sanyal K.** 2015. A comprehensive model to predict mitotic division in budding yeasts. Mol Biol Cell **26**:3954–3965.

CHAPTER FOUR

CONCLUSIONS AND FUTURE DIRECTIONS

This work aims at defining the mechanisms of aneuploid formation in response to FLC and the underlying factors that play a role in the heterogeneous response to FLC in *C. neoformans*. The findings suggest that FLC treatment results in an initial increase in ploidy in a large percentage of cells. Based on our results, we hypothesize that FLC resistant aneuploids are selected from this population of cells exhibiting an overall increase in ploidy. This work also highlights several intrinsic and extrinsic factors that contribute to the heterogeneous response to FLC.

Our data presented in Chapter 2 suggest that initial exposure to FLC inhibits budding and cell separation, which leads to the formation of multimeras that appear to be better equipped to proliferate in the presence of FLC. A major unanswered question that arises from this study is: Do multimeras occur during FLC treatment *in vivo*? Given the increased survival of cells exhibiting the multimera morphology during FLC treatment *in vitro*, it would be interesting to further explore the role of multimeras in promoting infection during *in vivo* treatment. A previous study has shown that FLC heteroresistance and aneuploidy does occur in mouse models, but the morphology of the cells was never assessed (1). In addition to analyzing the morphology of cells during *in vivo* FLC treatment,

it would be intriguing to perform virulence testing on multimera cells to analyze their ability to promote infection and survive host environment and FLC treatment.

Another major conclusion from the data presented in Chapter 2 is the lack of coordination between nuclear division and cellular growth in *C. neoformans* cells during FLC treatment. The process of cell cycle regulation and mitotic checkpoints are largely unknown in *C. neoformans*. The spindle assembly checkpoint (SAC) is a major mitotic checkpoint shown to prevent chromosome missegregation. SAC defects have been shown to be a major cause of aneuploid formation in cancer (2). To further explore the effects of FLC on chromosome segregation, further studies could aim at characterizing the SAC pathway in *C. neoformans* and the potential effects of FLC on the SAC pathway.

Although the effects of FLC described in Chapter 2 may be largely associated with defects at the plasma membrane level, we cannot exclude the possibility that the integrity of the nuclear envelope is also compromised due to FLC treatment. Such defects could lead to chromosomal instability. Indeed, our data indicating mislocalization of the centromeres is consistent with such a possibility. Utilizing a strain expressing mCherry-Cse4, to visualize the centromeres, and GFP-Ndc-1, to visualize the nuclear envelope, we provide preliminary evidence that FLC treatment may lead to “nuclear spillage” of chromosomes. These effects of FLC on the nuclear envelope could be further studied. Further microscopy, including confocal and electron microscopy, would

be needed to further characterize the occurrence of nuclear spillage during FLC treatment.

In addition to the effects of FLC on the nuclear envelope, the indirect effects of FLC on chromosomal instability could also be further explored. Unpublished work from our lab suggests that FLC may indirectly increase DNA damage through upregulation of reactive oxygen species (ROS) and inhibition metallothionenin transcription. FLC treatment leads to DNA damage *in vitro* likely due to an increase of ROS in the presence of redox-active metals. Further studies assessing FLC potential to damage DNA *in vivo* could be further explored. Additionally, as previously seen in human cells, ROS accumulation may lead to SAC defects and subsequent aneuploid formation (3). Further analysis of the effects of ROS accumulation on the SAC pathway during FLC treatment would be of interest to explore.

In Chapter 3, we describe the heterogeneous response of *C. neoformans* to FLC. We show that cells that exhibit slower growth are able to produce a population of cells that can grow during FLC treatment without becoming aneuploid. The mechanisms underlying increased survival in slow growers could be evaluated. One potential explanation for the increased survival of slow-growers during FLC treatment could be due to the decreased ATP production and mitochondrial function in slow-growing cells, as has been seen during persistence in bacterial populations (4). Consistent with this possibility, a study in *Candida albicans* shows that ATP levels serve as a good predictor for FLC susceptibility.

Populations of cells exhibiting higher ATP levels had lower minimum inhibitory concentration levels of FLC (5). Additionally, another study in *C. neoformans* showed that cells treated with tetracycline, a mitochondrial translation inhibitor, were more resistant to FLC. The correlation between ATP levels of individual cells and their survival in FLC could be further studied using the fluorescent ATP assay previously described by Kretschmar et al. (5).

We show that extrinsic factors, such as: temperature, nutrient availability, and media composition affect the response of *C. neoformans* to FLC. We establish the initial rates of colony growth based on colony sizes fall under a normal distribution. It would be of interest to see how the rates of growth change during FLC treatment and how more physiological components contribute to FLC heterogeneity. A collaboration with a statistician to model population dynamics of FLC treated cells under various conditions would be critical for proper evaluation.

REFERENCES

1. **Sionov E, Chang YC, Kwon-Chung KJ.** 2013. Azole heteroresistance in Cryptococcus neoformans: Emergence of resistant clones with chromosomal disomy in the mouse brain during fluconazole treatment. Antimicrob Agents Chemother **57**:5127–5130.

2. **Li M, Zhang P.** 2009. Spindle assembly checkpoint, aneuploidy and tumorigenesis. Cell Cycle.

3. **D'Angiolella V, Santarpia C, Grieco D.** 2007. Oxidative stress overrides the spindle checkpoint. Cell Cycle **6**:576–579.

4. **Shan Y, Gandt AB, Rowe SE, Deisinger JP, Conlon BP, Lewis K.** 2017. ATP-Dependent persister formation in Escherichia coli. MBio **8**.

5. **Kretschmar M, Nichterlein T, Kuntz P, Hof H.** 1996. Rapid detection of susceptibility to fluconazole in Candida species by a bioluminescence assay of intracellular ATP. Diagn Microbiol Infect Dis **25**:117–121.